

# Small x physics

*Anna Staśto*

Penn State University



# Outline

---

## Lecture 1:

Introduction to Deep Inelastic Scattering  
Parton model  
Collinear framework: factorization  
DGLAP evolution equations  
Parton distribution functions from DGLAP  
Nuclear structure functions  
Nuclear PDFs  
EIC prospects for inclusive DIS and nPDFs

## Lecture 2:

Intro: Regge theory and Pomeron  
Outline of BFKL construction:  
    Effective Lipatov vertex  
    Gluon reggeization: trajectory  
BFKL equation  
Eigenvalue. Collinear structure  
Properties of the solution:  
    Diffusion  
    Increase with energy  
Small  $x$  anomalous dimension

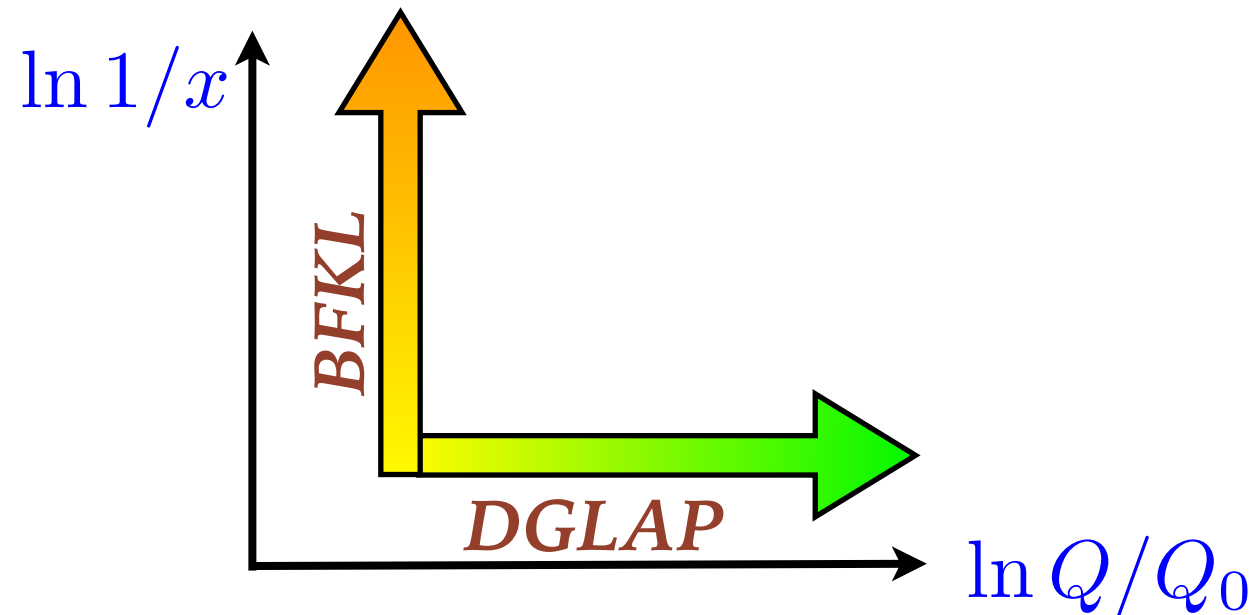
## Lecture 3:

BFKL at NLO: large correction  
Collinear limit of NLO BFKL  
Resummation:  
    Kinematical constraint, shifts of poles  
    DGLAP anomalous dimension  
Resummed result in Mellin space  
Resummed result in momentum space  
Improved small  $x$  splitting function  
Phenomenology examples

## Lecture 4:

Dipole model: GBW example  
BFKL revisited: Mueller dipole evolution  
Multiple rescattering: BK evolution  
Properties of solution to BK equation  
Saturation scale  
Impact parameter dependence  
Phenomenology examples: structure functions, diffraction, angular decorrelations

# DGLAP vs BFKL : brief summary



$$\left( \alpha_s \ln \frac{Q^2}{Q_0^2} \right)^n \quad \text{leading logs of scale } Q$$

$$\left( \alpha_s \ln \frac{1}{x} \right)^n \quad \text{leading logs of } x \text{ (or energy } s)$$

## Collinear framework

DGLAP evolution

$$Q^2 \frac{d}{dQ^2} g(x, Q^2) = \int_x^1 \frac{dz}{z} P(\alpha_s(Q^2), z) g\left(\frac{x}{z}, Q^2\right)$$

strong ordering in transverse momenta

solution  
(at small  $x$ )  $xg(x, Q^2) \sim \exp \left[ \sqrt{\frac{2C_A}{\pi\beta_0} \ln \frac{\alpha_s(Q_0^2)}{\alpha_s(Q^2)} \ln \frac{1}{x}} \right]$

## Small $x$ framework

BFKL evolution

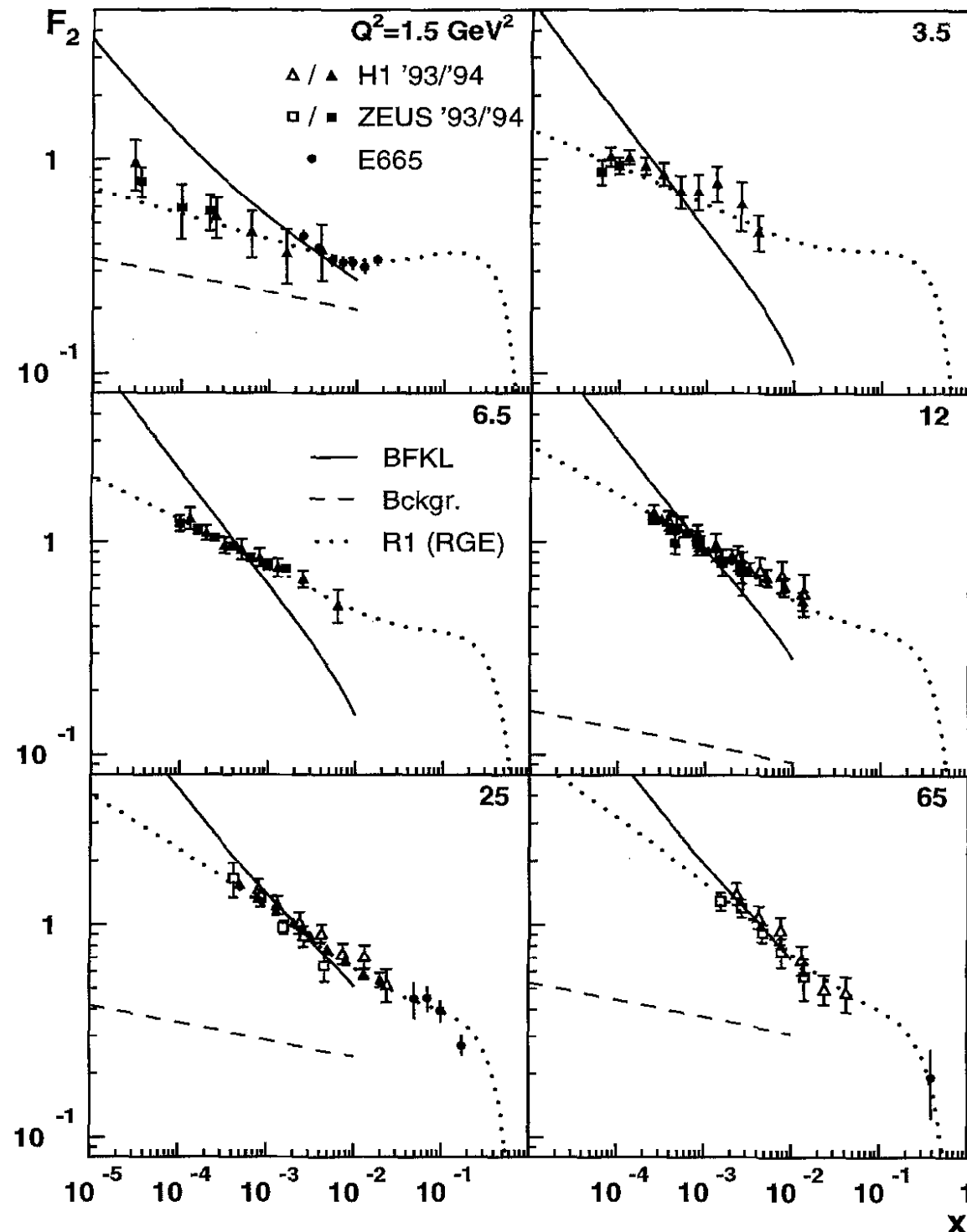
$$\frac{\partial}{\partial \ln 1/x} f(x, k^2) = \int d^2k \mathcal{K}(k, k'; \alpha_s) f(x, k'^2)$$

strong ordering in rapidities

solution  $f(x, k) \sim \frac{1}{kk_0} \left( \frac{1}{x} \right)^{\omega_0} \exp \left( - \frac{\ln^2(k^2/k_0^2)}{4\bar{\alpha}_s a^2 \ln 1/x} \right)$

# Example: BFKL at LL and HERA data

Bojak, Ernst



see also: Ball, Forte

- Rise with energy (or decreasing Bjorken  $x$ ) too steep for the phenomenology
- Cannot describe HERA data with LL BFKL

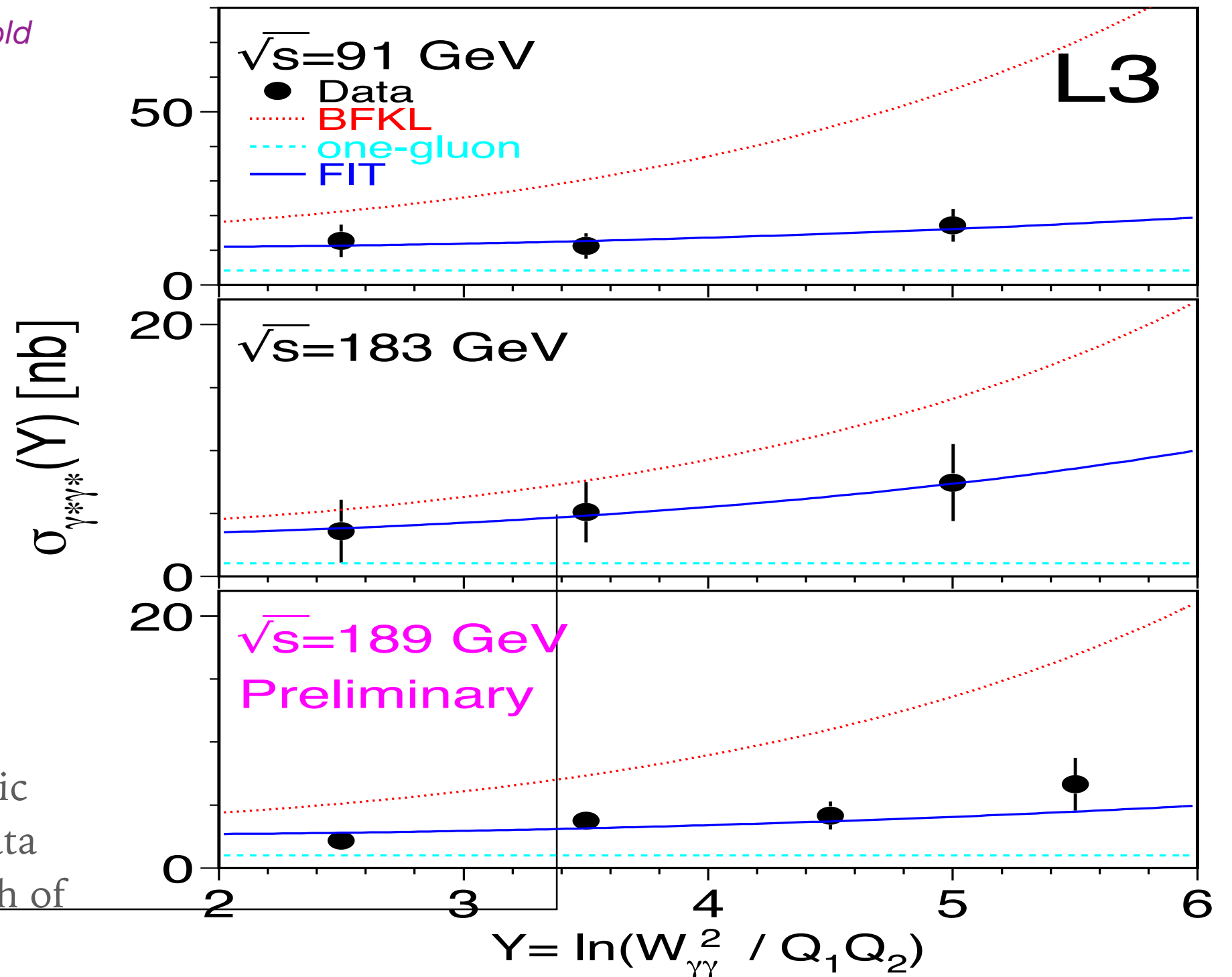
HERA:  $F_2 \sim x^{-(0.2 \sim 0.3)}$

BFKL:  $F_2 \sim x^{-0.5}$

- Need **higher order**, next-to-leading logarithmic, **NLL** terms.
- Powerlike growth eventually violates unitarity bounds for amplitudes. Will need to consider also other class of corrections: **saturation**.

# Example: application of LL BFKL to $\gamma^*\gamma^*$ scattering

*Donnachie, Soldner-Rembold*



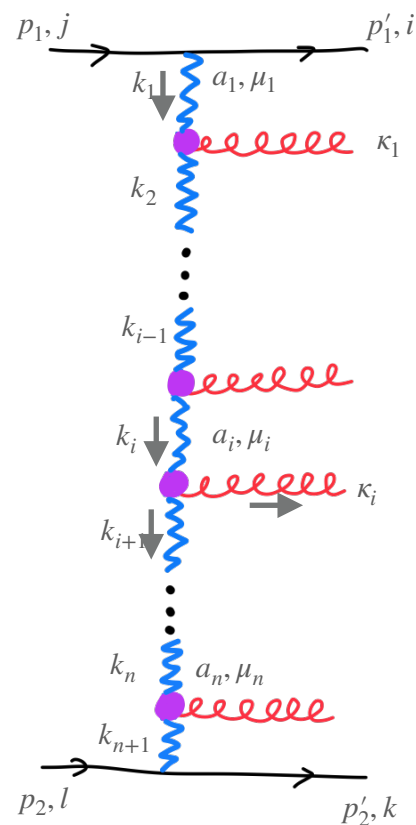
BFKL at leading logarithmic order overestimates the data and gives too steep growth of the cross section

# BFKL at NLL

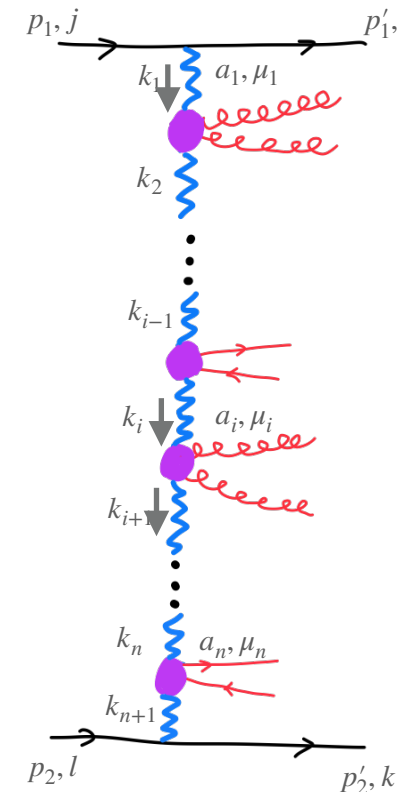
BFKL at NLL was computed by: *Fadin, Lipatov* and *Camici, Ciafaloni*

$$\alpha_s^n \ln^n \frac{s}{s_0} \rightarrow \alpha_s^{n+1} \ln^n \frac{s}{s_0}$$

One loop corrections to real emission in MRK kinematics (Reggeon-Reggeon-gluon vertex) and virtual corrections (trajectory). Also, production of pair of particles (two-gluon production and quark-antiquark) which are not widely separated in rapidity: **quasi-multi-Regge kinematics (QMRK)**



Particles strongly ordered in rapidity: **multi-Regge kinematics**



Clusters of particles ordered in rapidity: **quasi-multi-Regge kinematics**

# BFKL kernel at NLL

Kernel expansion up to NLL

$$\mathcal{K}(\mathbf{k}, \mathbf{k}') = \bar{\alpha}_s(\mu^2) \mathcal{K}_0 + \bar{\alpha}_s^2(\mu^2) \mathcal{K}_1 + \dots$$

(will consider integrated over angle now,  
so here  $k, k'$  are absolute values of 2-d  
transverse momenta)

$$\mathcal{K}(k, k') = \bar{\alpha}_s(\mu^2) \mathcal{K}_0 + \bar{\alpha}_s^2(\mu^2) \mathcal{K}_1 + \dots$$

Use Mellin representation

$$\bar{\alpha}_s \chi(\gamma) = \int dk'^2 \left( \frac{k'^2}{k^2} \right)^{\gamma-1} \mathcal{K}(k, k') = \bar{\alpha}_s(\mu^2) \chi_0(\gamma) + \bar{\alpha}_s^2(\mu^2) \chi_1(\gamma) + \dots$$

LLx kernel in Mellin space

$$\chi_0(\gamma) = 2\psi(1) - \psi(\gamma) - \psi(1 - \gamma)$$

## NLLx kernel in Mellin space

$$\begin{aligned} \chi_1(\gamma) = & -\frac{b}{2} [\chi_0^2(\gamma) + \chi_0'(\gamma)] - \frac{1}{4} \chi_0''(\gamma) - \frac{1}{4} \left( \frac{\pi}{\sin \pi \gamma} \right)^2 \frac{\cos \pi \gamma}{3(1-2\gamma)} \left( 11 + \frac{\gamma(1-\gamma)}{(1+2\gamma)(3-2\gamma)} \right) \\ & + \left( \frac{67}{36} - \frac{\pi^2}{12} \right) \chi_0(\gamma) + \frac{3}{2} \zeta(3) + \frac{\pi^3}{4 \sin \pi \gamma} \\ & - \sum_{n=0}^{\infty} (-1)^n \left[ \frac{\psi(n+1+\gamma) - \psi(1)}{(n+\gamma)^2} + \frac{\psi(n+2-\gamma) - \psi(1)}{(n+1-\gamma)^2} \right] \end{aligned}$$

(Note: technically functions  $(k^2)^\gamma$  are not eigenfunctions at NLL, however one can still perform Mellin transform and analyze properties)

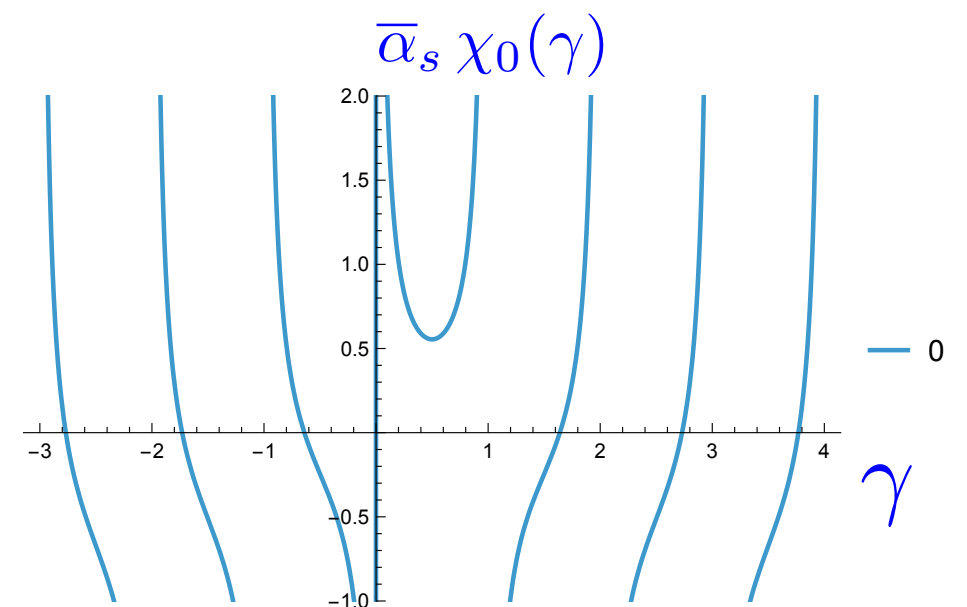
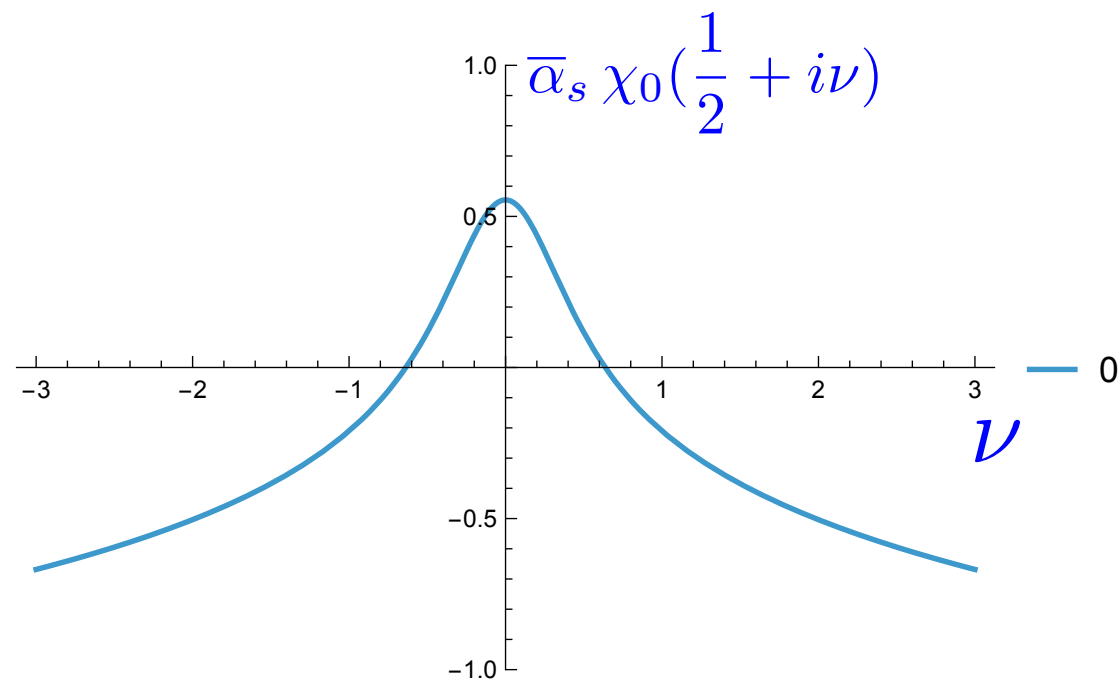
# LL kernel in Mellin space

Recall LL kernel

$$\chi_0(\gamma) = 2\psi(1) - \psi(\gamma) - \psi(1 - \gamma)$$

$$\bar{\alpha}_s = 0.2$$

Plotting  $\bar{\alpha}_s \chi_0(\gamma)$



0: collinear pole

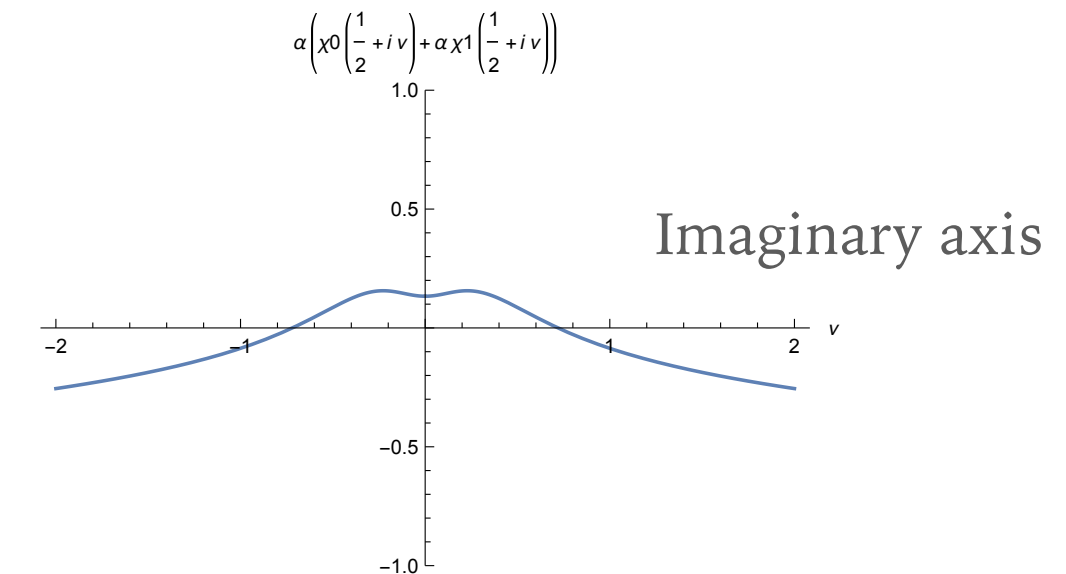
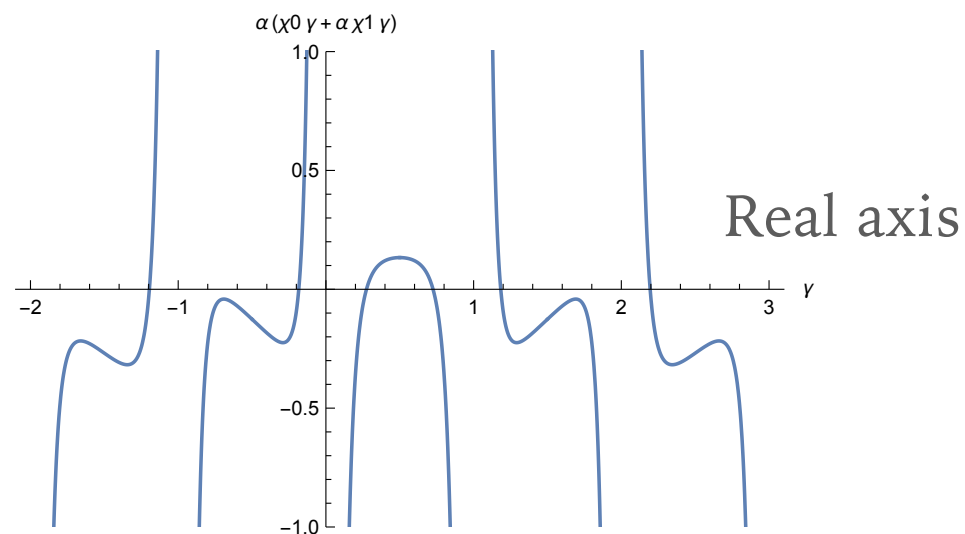
1: anti-collinear pole

single poles: 0, -1, -2, ... and 1, 2, 3, ...

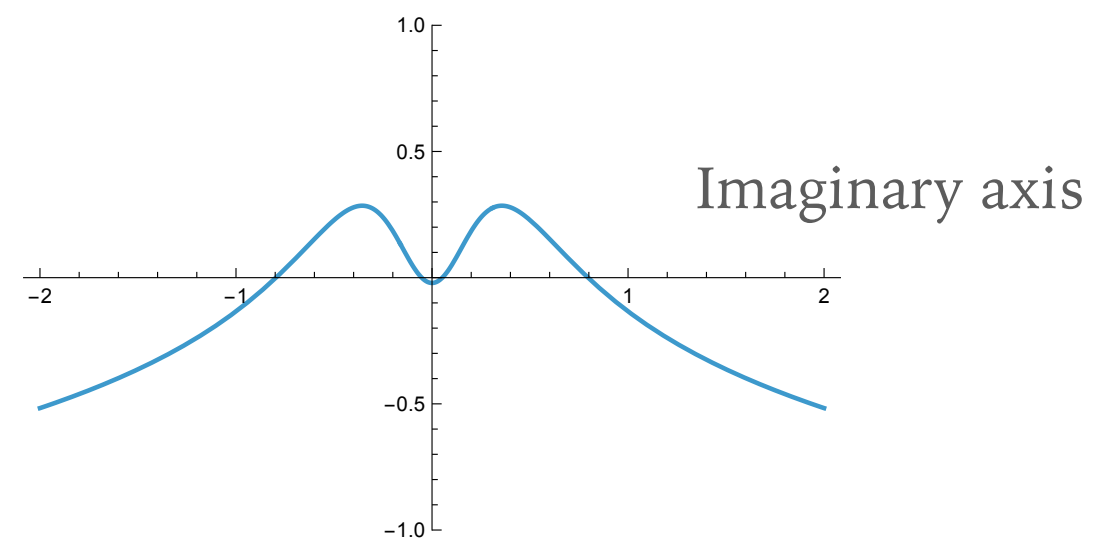
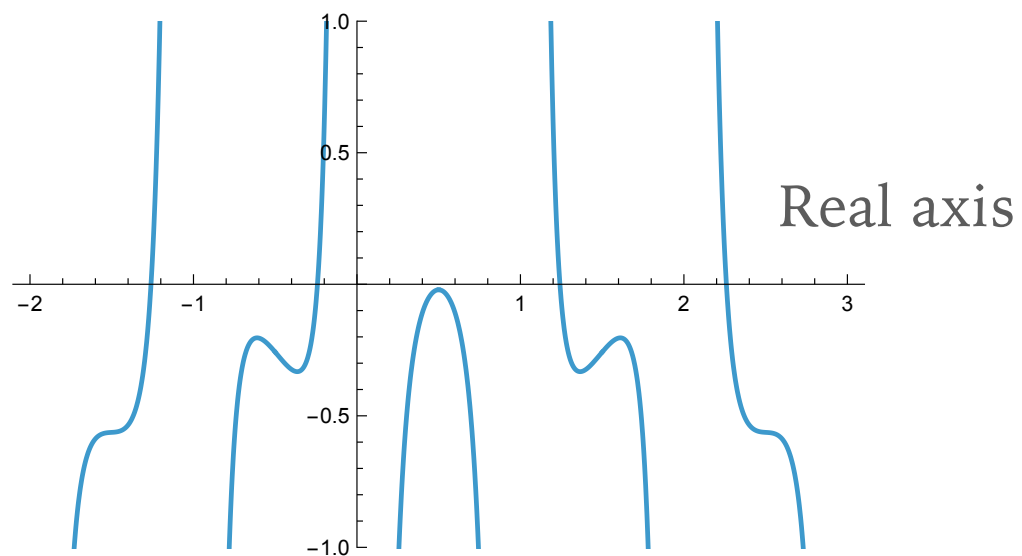
# NLL kernel in Mellin space

$$\bar{\alpha}_s = 0.1$$

(plotted for fixed coupling  $b=0$ )



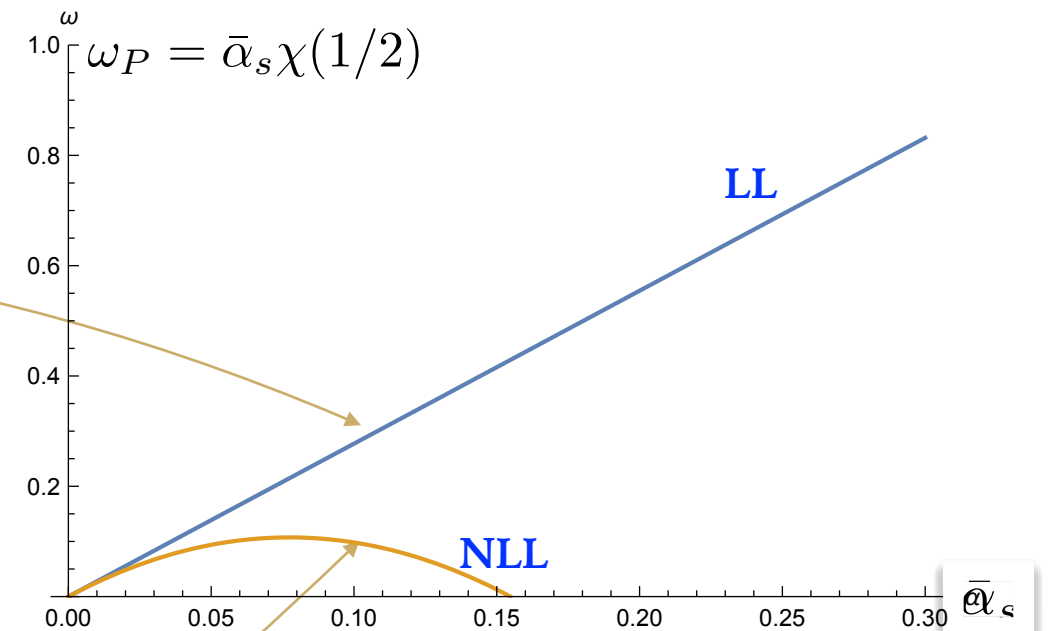
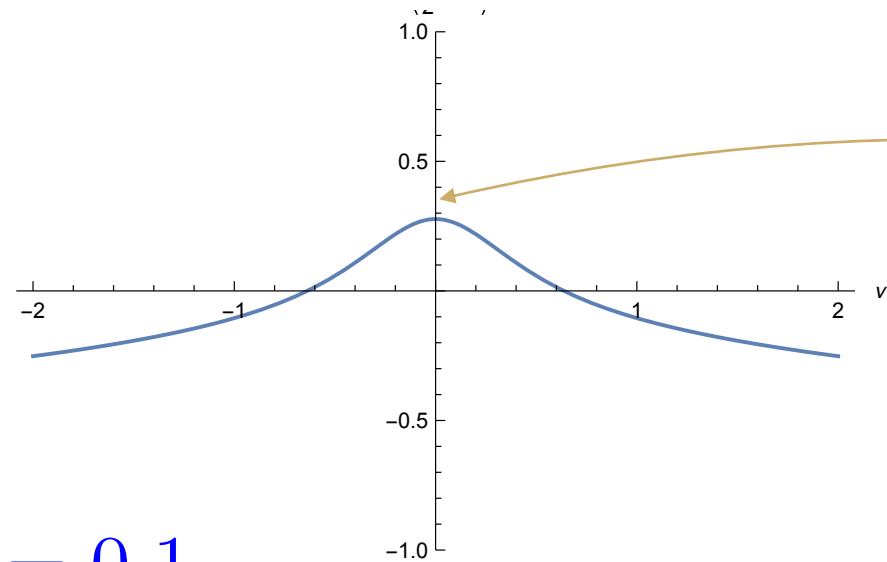
$$\bar{\alpha}_s = 0.2$$



**Large negative correction, complicated pole structure**

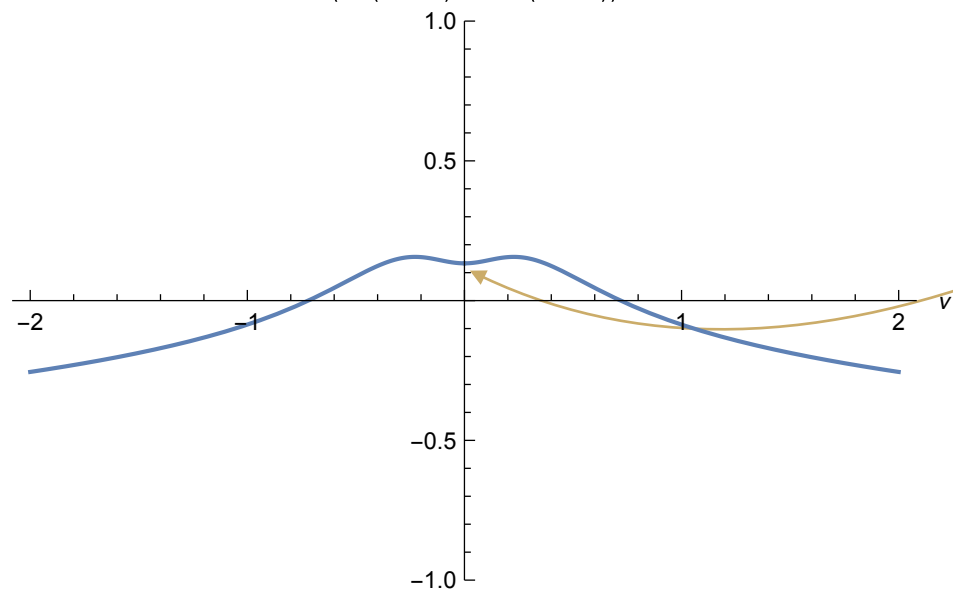
# BFKL kernel in Mellin space: LL vs NLL

$$\bar{\alpha}_s \chi_0\left(\frac{1}{2} + i\nu\right)$$



$$\bar{\alpha}_s = 0.1$$

$$\alpha \left( \chi_0\left(\frac{1}{2} + i\nu\right) + \alpha \chi_1\left(\frac{1}{2} + i\nu\right) \right)$$



Two maxima on imaginary axis  $1/2 + i\nu$  at NLLx order

# Collinear structure at NLL

$$\begin{aligned} \chi_1(\gamma) = & -\frac{b}{2}[\chi_0^2(\gamma) + \chi_0'(\gamma)] - \frac{1}{4}\chi_0''(\gamma) - \frac{1}{4} \left( \frac{\pi}{\sin \pi\gamma} \right)^2 \frac{\cos \pi\gamma}{3(1-2\gamma)} \left( 11 + \frac{\gamma(1-\gamma)}{(1+2\gamma)(3-2\gamma)} \right) \\ & + \left( \frac{67}{36} - \frac{\pi^2}{12} \right) \chi_0(\gamma) + \frac{3}{2}\zeta(3) + \frac{\pi^3}{4 \sin \pi\gamma} \\ & - \sum_{n=0}^{\infty} (-1)^n \left[ \frac{\psi(n+1+\gamma) - \psi(1)}{(n+\gamma)^2} + \frac{\psi(n+2-\gamma) - \psi(1)}{(n+1-\gamma)^2} \right] \end{aligned}$$

At LLx there are **single** poles. At NLLx there are **single**, **double** and **triple** collinear poles.

$$\chi_0^{\text{coll}} \sim \frac{1}{\gamma} + \frac{1}{1-\gamma}$$

Approximating NLL kernel by double and triple poles :

$$\chi_0'^{\text{coll}} \sim -\frac{1}{\gamma^2} + \frac{1}{(1-\gamma)^2}$$

$$\chi_1^{\text{coll}} \simeq -\frac{1}{2\gamma^3} - \frac{1}{2(1-\gamma)^3} + \frac{A_1(0)}{\gamma^2} + \frac{A_1(0) - b}{(1-\gamma)^2}$$

$$\chi_0''^{\text{coll}} \sim \frac{2}{\gamma^3} + \frac{2}{(1-\gamma)^3}$$

$$A_1(0) = -\frac{11}{12}$$

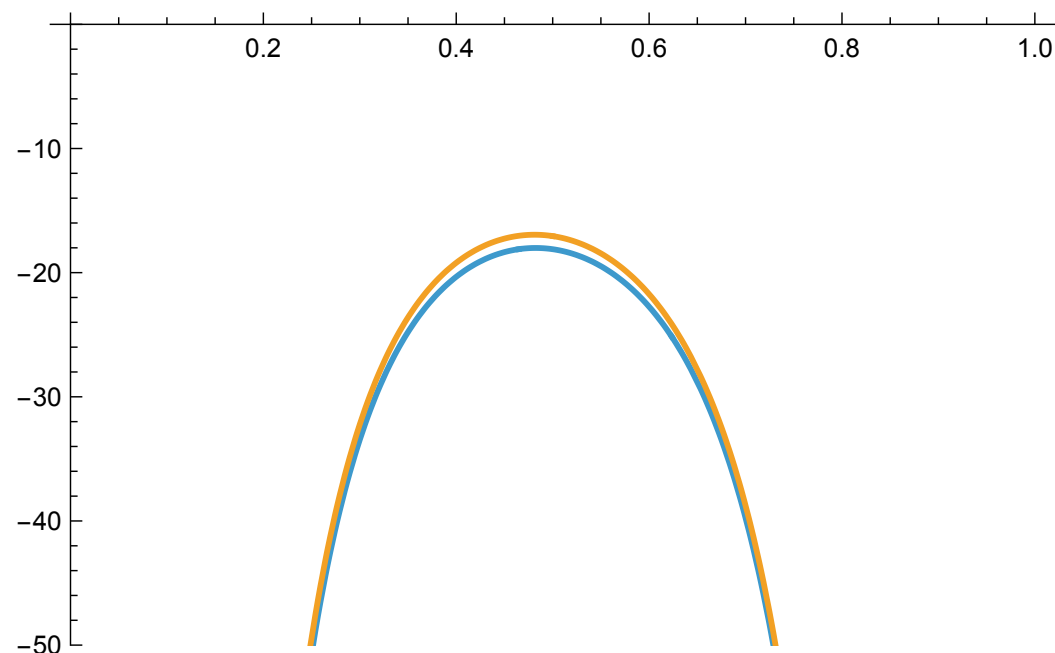
$$b = \frac{11}{12} - \frac{2n_f}{12N_c}$$

# Collinear structure of NLL

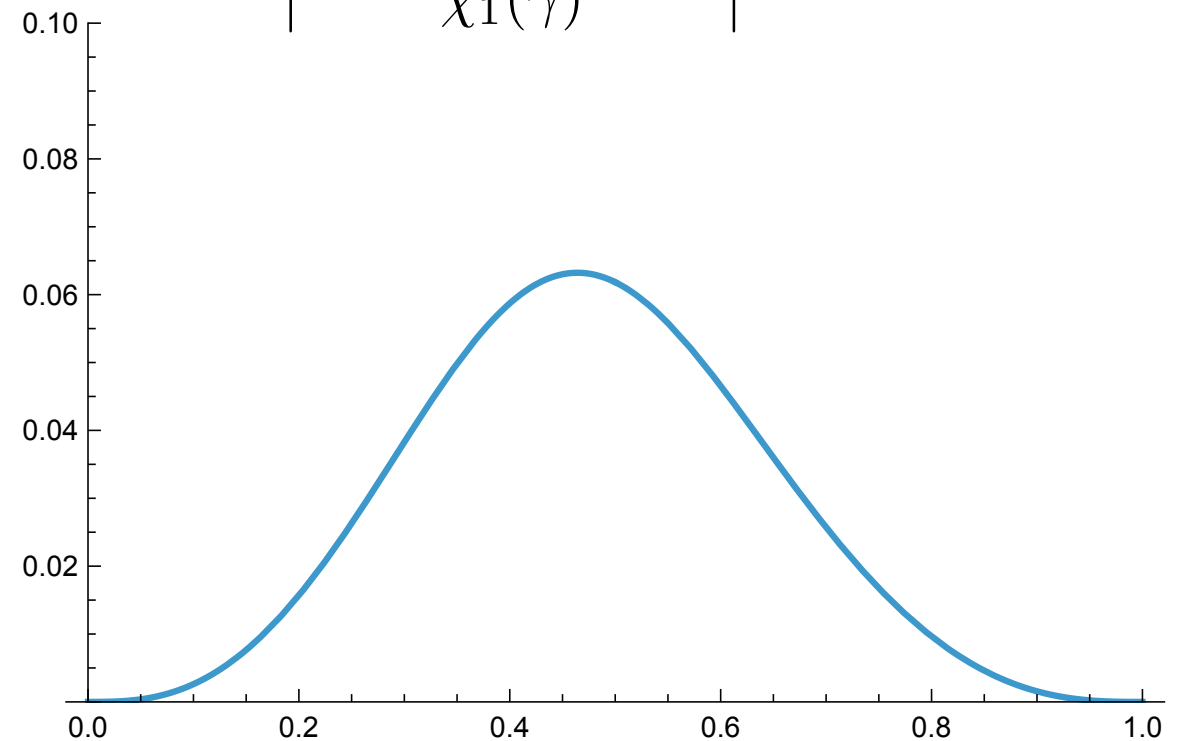
$$\chi_1^{\text{coll}} \simeq -\frac{1}{2\gamma^3} - \frac{1}{2(1-\gamma)^3} + \frac{A_1(0)}{\gamma^2} + \frac{A_1(0) - b}{(1-\gamma)^2}$$

double and triple poles of the NLL part

$\chi_1(\gamma), \chi_1^{\text{coll}}(\gamma)$



$\left| \frac{\chi_1(\gamma) - \chi_1^{\text{coll}}(\gamma)}{\chi_1(\gamma)} \right|$



Difference between exact NLL and collinear approximation of about 7% at most

# NLL contributions: running coupling

---

$$\begin{aligned} \chi_1(\gamma) = & \boxed{-\frac{b}{2}[\chi_0^2(\gamma) + \chi_0'(\gamma)]} - \frac{1}{4}\chi_0''(\gamma) - \frac{1}{4} \left( \frac{\pi}{\sin \pi\gamma} \right)^2 \frac{\cos \pi\gamma}{3(1-2\gamma)} \left( 11 + \frac{\gamma(1-\gamma)}{(1+2\gamma)(3-2\gamma)} \right) \\ & + \left( \frac{67}{36} - \frac{\pi^2}{12} \right) \chi_0(\gamma) + \frac{3}{2}\zeta(3) + \frac{\pi^3}{4 \sin \pi\gamma} \\ & - \sum_{n=0}^{\infty} (-1)^n \left[ \frac{\psi(n+1+\gamma) - \psi(1)}{(n+\gamma)^2} + \frac{\psi(n+2-\gamma) - \psi(1)}{(n+1-\gamma)^2} \right] \end{aligned}$$

$$b = \frac{11}{12} - \frac{2n_f}{12N_c}$$

The term

$$\chi^{\text{run}}(\gamma) = -\frac{b}{2}[\chi_0^2(\gamma) + \chi_0'(\gamma)]$$

corresponds to the momentum space expression

$$\mathcal{K}_0^{\text{run}} = -b \log\left(\frac{(\mathbf{k} - \mathbf{k}')^2}{\mathbf{k}^2}\right) \mathcal{K}_0(\mathbf{k}, \mathbf{k}')$$

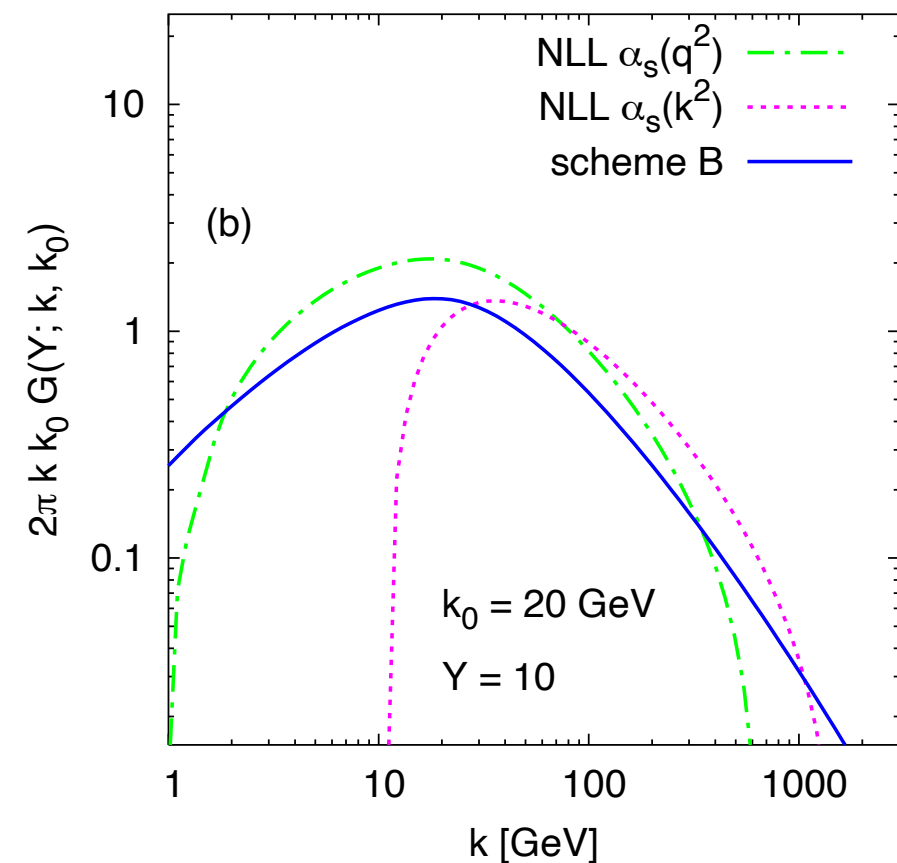
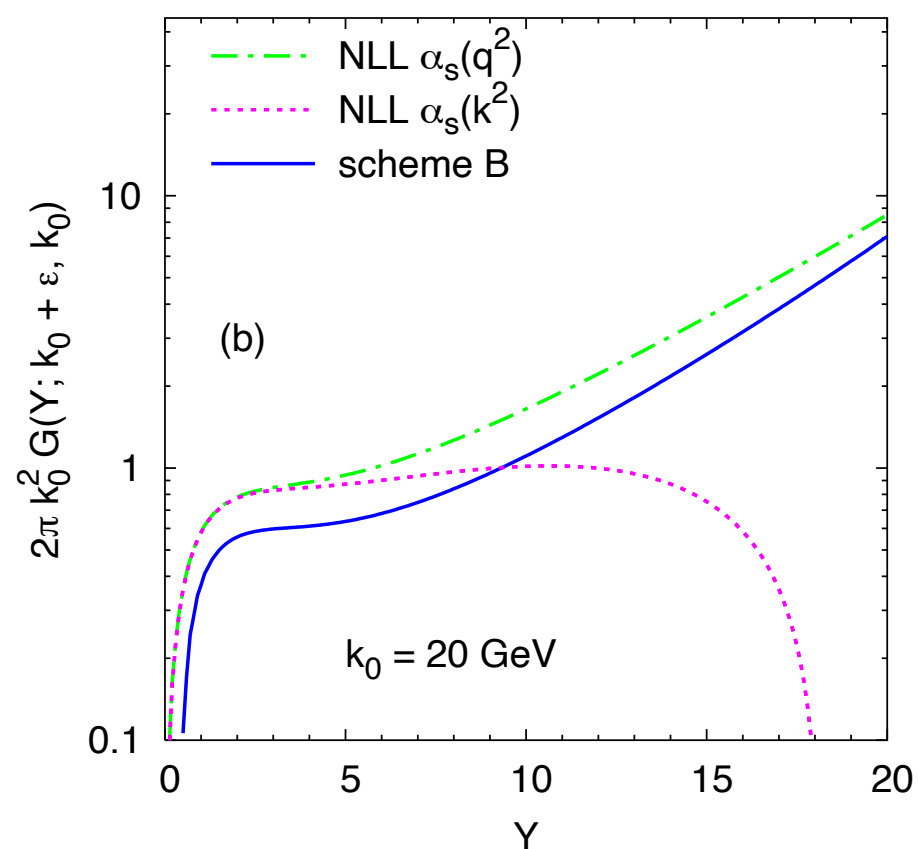
**The running coupling term in NLL part of the kernel can be completely incorporated into the leading part of the kernel if the scale is chosen to be that of emitted gluon**

# NLL contributions: running coupling

Strictly speaking up to NLL order one can choose any scale in front of the LLx kernel and then subtract the corresponding term in the NLL kernel, thanks to

$$\bar{\alpha}_s(\kappa^2) = \bar{\alpha}_s(\mu^2) - b\bar{\alpha}_s^2(\mu^2) \log\left(\frac{\kappa^2}{\mu^2}\right) = \bar{\alpha}_s(k^2) - b\bar{\alpha}_s^2(\mu^2) \log\left(\frac{\kappa^2}{k^2}\right)$$

The difference between such procedure would be of NLLx order  
In practice the difference tends to be numerically rather large



Direct solution in momentum space

# NLL contributions: DGLAP anomalous dimension

$$\begin{aligned} \chi_1(\gamma) = & -\frac{b}{2}[\chi_0^2(\gamma) + \chi_0'(\gamma)] - \frac{1}{4}\chi_0''(\gamma) - \frac{1}{4} \left( \frac{\pi}{\sin \pi\gamma} \right)^2 \frac{\cos \pi\gamma}{3(1-2\gamma)} \left( 11 + \frac{\gamma(1-\gamma)}{(1+2\gamma)(3-2\gamma)} \right) \\ & + \left( \frac{67}{36} - \frac{\pi^2}{12} \right) \chi_0(\gamma) + \frac{3}{2}\zeta(3) + \frac{\pi^3}{4 \sin \pi\gamma} \\ & - \sum_{n=0}^{\infty} (-1)^n \left[ \frac{\psi(n+1+\gamma) - \psi(1)}{(n+\gamma)^2} + \frac{\psi(n+2-\gamma) - \psi(1)}{(n+1-\gamma)^2} \right] \end{aligned}$$

Next one: **double** pole with coefficient

$$A_1(0) = -\frac{11}{12}$$

recall LO DGLAP anomalous dimension:

$$\gamma_{gg}(\omega) = \frac{\alpha_s}{2\pi} \gamma^{(0)}(\omega) = \bar{\alpha}_s \left( \frac{1}{\omega} - \frac{1}{\omega+1} + \frac{1}{\omega+2} - \frac{1}{\omega+3} - \psi(2+\omega) - \gamma_E + \frac{11}{12} - \frac{N_f}{18} \right) = \frac{\bar{\alpha}_s}{\omega} + \bar{\alpha}_s A_1(\omega)$$

Non-singular (at  $\omega = 0$ ) part of the anomalous dimension

$$A_1(\omega = 0) = -\frac{11}{12} \quad N_f = 0$$

# NLL contributions: DGLAP anomalous dimension

---

Recall LL BFKL equation in Mellin space

LL BFKL kernel in Mellin space

$$\tilde{f}(\omega, \gamma) = \tilde{f}^{(0)} + \frac{\bar{\alpha}_s}{\omega} \chi_0(\gamma) \tilde{f}(\omega, \gamma) \quad \chi_0(\gamma)$$

Consider DGLAP+ anti-DGLAP (collinear model with full LO splitting function)

$$\begin{aligned} \left( \frac{\bar{\alpha}_s}{\omega} + \bar{\alpha}_s A_1(\omega) \right) \left( \frac{1}{\gamma} + \frac{1}{1-\gamma} \right) &= \left( \frac{\bar{\alpha}_s}{\omega} + \bar{\alpha}_s A_1(0) + \dots \right) \left( \frac{1}{\gamma} + \frac{1}{1-\gamma} \right) \\ &= \frac{\bar{\alpha}_s}{\omega} \left( 1 + \omega A_1(0) + \dots \right) \left( \frac{1}{\gamma} + \frac{1}{1-\gamma} \right) \end{aligned}$$

trading  $\omega$  for  $\bar{\alpha}_s$  using BFKL solution

added term is subleading at high energy ( $\omega \rightarrow \infty$ )

$$\omega = \bar{\alpha}_s \chi_0(\gamma)$$

finally obtains

$$\left( \frac{\bar{\alpha}_s}{\omega} + \bar{\alpha}_s A_1(\omega) \right) \left( \frac{1}{\gamma} + \frac{1}{1-\gamma} \right) = \frac{\bar{\alpha}_s}{\omega} \left( \frac{1}{\gamma} + \frac{1}{1-\gamma} \right) + \bar{\alpha}_s^2 A_1(0) \left( \frac{1}{\gamma^2} + \frac{1}{(1-\gamma)^2} \right) + \dots$$

double collinear poles at NLLx order, proportional to  $A_1(0) = -11/12$  originate from the non-singular (at  $z=0$ ) part of the DGLAP splitting function

# NLL contributions: triple poles

---

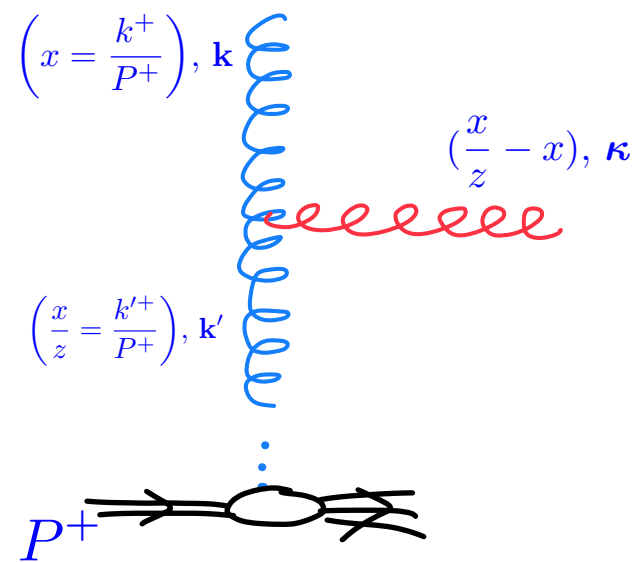
$$\begin{aligned}\chi_1(\gamma) = & -\frac{b}{2}[\chi_0^2(\gamma) + \chi_0'(\gamma)] - \frac{1}{4}\chi_0''(\gamma) - \frac{1}{4} \left( \frac{\pi}{\sin \pi\gamma} \right)^2 \frac{\cos \pi\gamma}{3(1-2\gamma)} \left( 11 + \frac{\gamma(1-\gamma)}{(1+2\gamma)(3-2\gamma)} \right) \\ & + \left( \frac{67}{36} - \frac{\pi^2}{12} \right) \chi_0(\gamma) + \frac{3}{2}\zeta(3) + \frac{\pi^3}{4 \sin \pi\gamma} \\ & - \sum_{n=0}^{\infty} (-1)^n \left[ \frac{\psi(n+1+\gamma) - \psi(1)}{(n+\gamma)^2} + \frac{\psi(n+2-\gamma) - \psi(1)}{(n+1-\gamma)^2} \right]\end{aligned}$$

Next one: **triple** pole :  $-\frac{1}{4}\chi_0''(\gamma)$

$$\chi_0''^{\text{coll}} \sim \frac{2}{\gamma^3} + \frac{2}{(1-\gamma)^3}$$

# NLL contributions: kinematical constraint

$$f(x, \mathbf{k}^2) = f^{(0)} + \bar{\alpha}_S \mathbf{k}^2 \int_x^1 \frac{dz}{z} \int \frac{d\mathbf{k}'^2}{\mathbf{k}'^2} \left\{ \frac{f(x/z, \mathbf{k}'^2) - f(x/z, \mathbf{k}^2)}{|\mathbf{k}'^2 - \mathbf{k}^2|} + \frac{f(x/z, \mathbf{k}^2)}{[4\mathbf{k}'^4 + \mathbf{k}^4]^{\frac{1}{2}}} \right\}$$



In high energy limit the integrals are **unrestricted**

$$k^\mu = (k^+, k^-, \mathbf{k}) \quad k^2 = k^+ k^- - \mathbf{k}^2$$

Virtualities dominated by transverse components

$$|k^2| \simeq \mathbf{k}^2 \quad \text{and also} \quad \mathbf{k}^2 > |k^+ k^-|$$

Using strong ordering on longitudinal momenta (-components) and condition on the on-shellness of the emitted gluon one obtains the kinematical constraint

$$\mathbf{k}'^2 < \frac{\mathbf{k}^2}{z}$$

Modification of the BFKL equation

$$f(x, \mathbf{k}^2) = f^{(0)} + \bar{\alpha}_S \mathbf{k}^2 \int_x^1 \frac{dz}{z} \int \frac{d\mathbf{k}'^2}{\mathbf{k}'^2} \left\{ \frac{f(x/z, \mathbf{k}'^2) \Theta(\mathbf{k}^2/z - \mathbf{k}'^2) - f(x/z, \mathbf{k}^2)}{|\mathbf{k}'^2 - \mathbf{k}^2|} + \frac{f(x/z, \mathbf{k}^2)}{[4\mathbf{k}'^4 + \mathbf{k}^4]^{\frac{1}{2}}} \right\}$$

Transverse integrals become **restricted**

# Kinematical constraint: shift of the poles

---

BFKL with kinematical constraint

$$f(x, \mathbf{k}^2) = f^{(0)} + \bar{\alpha}_S \mathbf{k}^2 \int_x^1 \frac{dz}{z} \int \frac{d\mathbf{k}'^2}{\mathbf{k}'^2} \left\{ \frac{f(x/z, \mathbf{k}'^2) \Theta(\mathbf{k}^2/z - \mathbf{k}'^2) - f(x/z, \mathbf{k}^2)}{|\mathbf{k}'^2 - \mathbf{k}^2|} + \frac{f(x/z, \mathbf{k}^2)}{[4\mathbf{k}'^4 + \mathbf{k}^4]^{\frac{1}{2}}} \right\}$$

Performing the two Mellin transforms leads to the kernel

$$\chi(\gamma, \omega) = 2\psi(1) - \psi(\gamma) - \psi(1 - \gamma + \omega)$$

**Leads to the shift of the poles in the kernel (asymmetric shift)  
Transverse and longitudinal momenta components no longer factorized**

# Shifts of collinear poles: energy scales

**Gluon Green's** function for BFKL

$$\mathcal{G}(s, \mathbf{k}, \mathbf{k}_0) = \frac{1}{2\pi \mathbf{k}^2} \int_{C_\omega} \frac{d\omega}{2\pi i} \left( \frac{s}{s_0} \right)^\omega \int_{C_\gamma} \frac{d\gamma}{2\pi i} \left( \frac{\mathbf{k}^2}{\mathbf{k}_0^2} \right)^\gamma G(\omega, \gamma)$$

BFKL equation in Mellin space

$$\omega G(\omega, \gamma) = 1 + \bar{\alpha}_s \chi(\gamma) G(\omega, \gamma)$$

What is energy scale  $s_0$  ?

Symmetric energy scale:  $s_0 = \mathbf{k}_0 \mathbf{k}$

This scale is symmetric, suitable for example for a process with two comparable scales (Muller-Navelet jets,  $\gamma^* \gamma^*$  scattering)

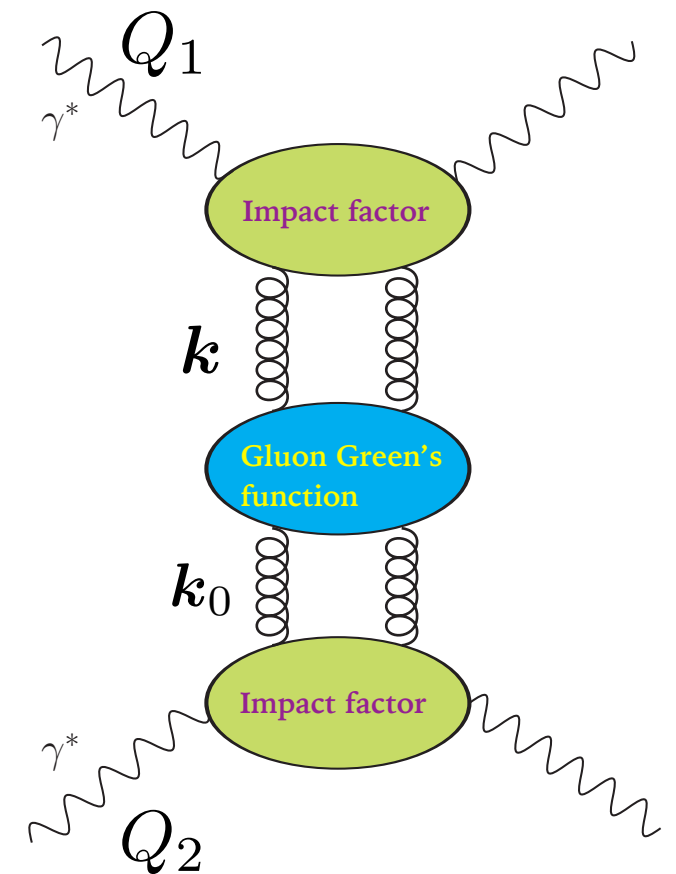
$$Q_1^2 \sim Q_2^2$$

Another scale  $s_0 = \mathbf{k}^2$

Asymmetric energy scale, suitable for DIS

$$Q_1^2 \gg Q_2^2$$

Example : virtual photon scattering



# Shifts of collinear poles: energy scales

---

$$\mathcal{G}(s, \mathbf{k}, \mathbf{k}_0) = \frac{1}{2\pi \mathbf{k}^2} \int_{C_\omega} \frac{d\omega}{2\pi i} \left(\frac{s}{s_0}\right)^\omega \int_{C_\gamma} \frac{d\gamma}{2\pi i} \left(\frac{\mathbf{k}^2}{\mathbf{k}_0^2}\right)^\gamma G(\omega, \gamma)$$

changing from one scale  $s_0 = k k_0$  to another  $s_0 = k^2$  implies

$$\left(\frac{s}{\mathbf{k} \mathbf{k}_0}\right)^\omega \left(\frac{\mathbf{k}^2}{\mathbf{k}_0^2}\right)^\gamma = \left(\frac{s}{\mathbf{k}^2}\right)^\omega \left(\frac{\mathbf{k}}{\mathbf{k}_0}\right)^\omega \left(\frac{\mathbf{k}^2}{\mathbf{k}_0^2}\right)^\gamma = \left(\frac{s}{\mathbf{k}^2}\right)^\omega \left(\frac{\mathbf{k}^2}{\mathbf{k}_0^2}\right)^{\gamma + \omega/2}$$

scale  $s_0 = k^2$

$$\mathcal{G}(s, \mathbf{k}, \mathbf{k}_0) = \frac{1}{2\pi \mathbf{k}^2} \int_{C_\omega} \frac{d\omega}{2\pi i} \left(\frac{s}{k^2}\right)^\omega \int_{C_\gamma} \frac{d\gamma}{2\pi i} \left(\frac{\mathbf{k}^2}{\mathbf{k}_0^2}\right)^{\gamma + \omega/2} G(\omega, \gamma)$$

amounts to shift in  $\gamma$

$$\mathcal{G}(s, \mathbf{k}, \mathbf{k}_0) = \frac{1}{2\pi \mathbf{k}^2} \int_{C_\omega} \frac{d\omega}{2\pi i} \left(\frac{s}{k^2}\right)^\omega \int_{C_\gamma} \frac{d\gamma}{2\pi i} \left(\frac{\mathbf{k}^2}{\mathbf{k}_0^2}\right)^\gamma G(\omega, \gamma - \omega/2)$$

This can be accommodated if including shift in the kernel eigenvalue

$$s_0 = k k_0 \quad \chi(\gamma) = 2\psi(1) - \psi(\gamma + \omega/2) - \psi(1 - \gamma + \omega/2)$$

$$s_0 = k^2 \quad \chi(\gamma) = 2\psi(1) - \psi(\gamma) - \psi(1 - \gamma + \omega)$$

# Triple poles from the shift

---

Therefore gluon Green's function and the kernel obtain  $\omega$  dependence : shift of poles in kernel

$$\chi(\gamma, \omega) = 2\psi(1) - \psi(\gamma + \omega/2) - \psi(1 - \gamma + \omega/2)$$

Expanding to first order in  $\omega$

$$\chi(\gamma, \omega) \simeq \chi_0(\gamma) + \frac{\omega}{2} (-\psi^{(1)}(\gamma) - \psi^{(1)}(1 - \gamma))$$

Using solution to BFKL at lowest order in the coupling

$$\omega = \bar{\alpha}_s \chi_0(\gamma)$$

$$-\psi^{(1)}(\gamma) - \psi^{(1)}(1 - \gamma) \sim -\frac{1}{\gamma^2} - \frac{1}{(1 - \gamma)^2}$$

Generate the triple collinear poles:

$$\chi_0(\gamma) \left[ \frac{\bar{\alpha}_s}{2\gamma^3} - \frac{\bar{\alpha}_s}{2(1 - \gamma)^3} \right]$$

# Cubic poles in NLL

---

$$\begin{aligned} \chi_1(\gamma) = & -\frac{b}{2}[\chi_0^2(\gamma) + \chi_0'(\gamma)] - \frac{1}{4}\chi_0''(\gamma) - \frac{1}{4} \left( \frac{\pi}{\sin \pi\gamma} \right)^2 \frac{\cos \pi\gamma}{3(1-2\gamma)} \left( 11 + \frac{\gamma(1-\gamma)}{(1+2\gamma)(3-2\gamma)} \right) \\ & + \left( \frac{67}{36} - \frac{\pi^2}{12} \right) \chi_0(\gamma) + \frac{3}{2}\zeta(3) + \frac{\pi^3}{4 \sin \pi\gamma} \\ & - \sum_{n=0}^{\infty} (-1)^n \left[ \frac{\psi(n+1+\gamma) - \psi(1)}{(n+\gamma)^2} + \frac{\psi(n+2-\gamma) - \psi(1)}{(n+1-\gamma)^2} \right] \end{aligned}$$

Cubic poles:

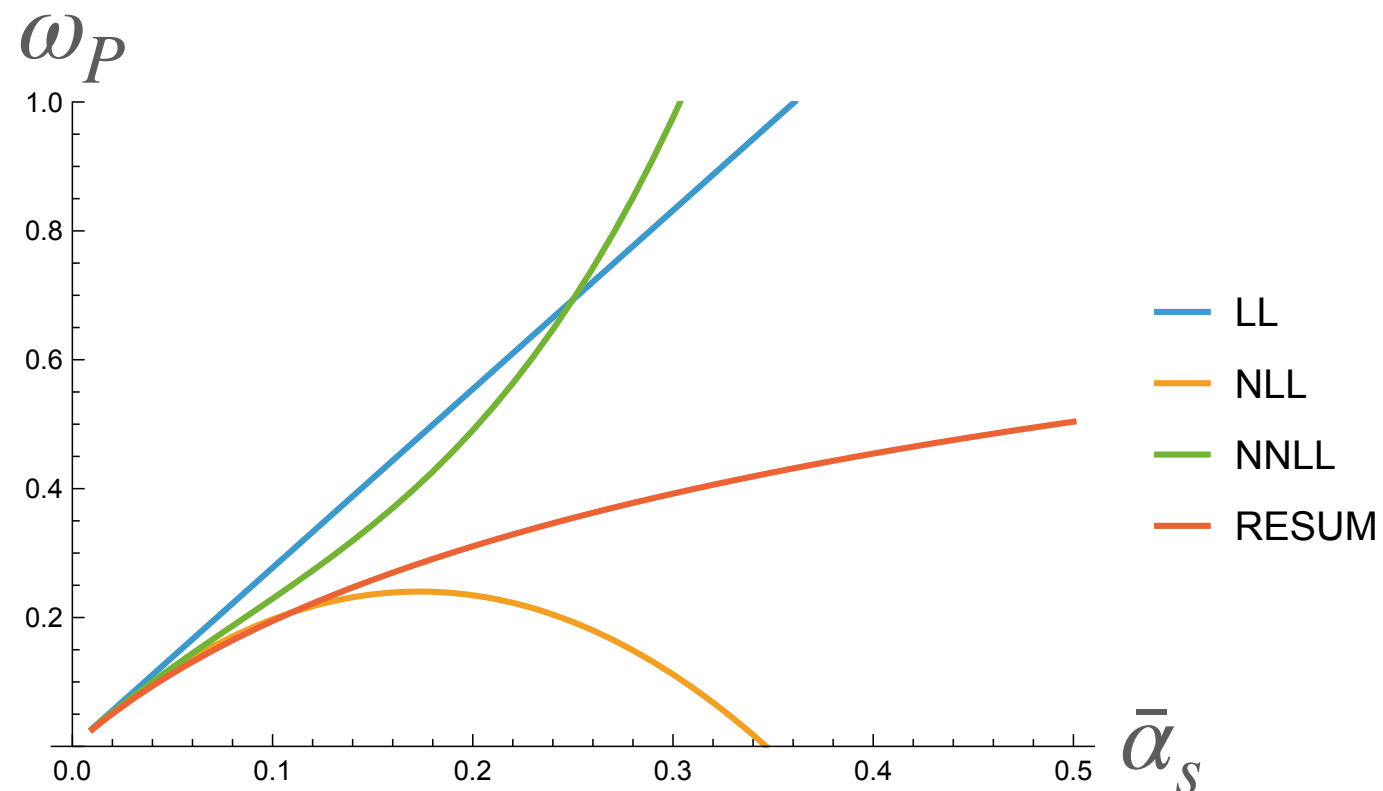
$$-\frac{1}{4}\chi_0''(\gamma) \sim -\frac{\bar{\alpha}_s}{2\gamma^3} - \frac{\bar{\alpha}_s}{2(1-\gamma)^3}$$

Exactly the same as from the symmetric shift

# Shifted kernel: resummation and truncation

Shifted,  $\omega$  dependent kernel provides with resummation to all orders in coupling

$$\chi(\gamma, \omega) = 2\psi(1) - \psi(\gamma + \omega/2) - \psi(1 - \gamma + \omega/2)$$



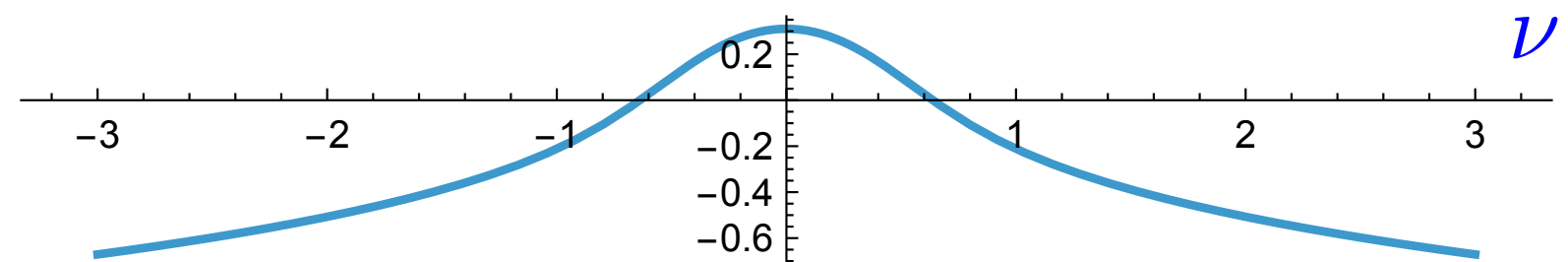
Fixed order case:

$$\omega_P = \bar{\alpha}_s \chi(1/2) = \sum_{n=0} \bar{\alpha}_s^{n+1} \chi_n(\gamma = 1/2)$$

Resummed case:

$$\omega_P = \chi_{\text{eff}}(\gamma = 1/2, \bar{\alpha}_s) \rightarrow \omega = \bar{\alpha}_s \chi(\gamma = 1/2, \omega)$$

$$\chi_{\text{eff}}(1/2 + I\nu, \bar{\alpha}_s = 0.2)$$



# Resummation setup

$$\tilde{\mathcal{K}}_\omega = \bar{\alpha}_s(\mathbf{q}^2) K_0^\omega + \omega \bar{\alpha}_s(k_{>}^2) K_c^\omega + \bar{\alpha}_s^2(k_{>}^2) \tilde{K}_1^\omega$$

*Ciafaloni, Colferai, Salam, AS*

*LL with shifts*

*non-singular DGLAP*

*NLL with subtractions*

symmetric scale

$$\chi_0^\omega = 2\psi(1) - \psi\left(\gamma + \frac{\omega}{2}\right) - \psi\left(1 - \gamma + \frac{\omega}{2}\right)$$

$$\chi_c^\omega(\gamma) = \frac{A_1(\omega)}{\gamma + \frac{\omega}{2}} + \frac{A_1(\omega)}{1 - \gamma + \frac{\omega}{2}},$$

Resummed kernel

$$\begin{aligned} \tilde{\chi}_1(\gamma) &= \chi_1(\gamma) - \chi_0^0(\gamma)[\chi_0^1(\gamma) + \chi_c^0(\gamma)] - \chi_0^{\text{run}}(\gamma) \\ &= \chi_1(\gamma) + \frac{1}{2}\chi_0^0(\gamma)\frac{\pi^2}{\sin^2(\pi\gamma)} - \chi_0^0(\gamma)\frac{A_1(0)}{\gamma(1-\gamma)} + \frac{b}{2}(\chi_0' + \chi_0^2) \end{aligned}$$

Additional subtraction needed to satisfy the momentum sum rule.

Solution to the evolution equation done in momentum space

# CCSS evolution

Ciafaloni, Colferai, Salam, AS

## Formulated in momentum space: solving integral equation

Form of the convolution: three main parts

$$\mathcal{K}_0^{\text{kc}}(z; \mathbf{k}, \mathbf{k}') \otimes_{z, \mathbf{q}} f\left(\frac{x}{z}, k'\right) + \mathcal{K}_0^{\text{coll}}(z; k, k') \otimes_{z, k'} f\left(\frac{x}{z}, k'\right) + \mathcal{K}_1^{\text{subtr}}(z; k, k') \otimes_{z, k'} f\left(\frac{x}{z}, k'\right)$$

### LLx with kinematical constraint

$$\begin{aligned} \mathcal{K}_0^{\text{kc}}(z; \mathbf{k}, \mathbf{k}') \otimes_{z, \mathbf{q}} f\left(\frac{x}{z}, k'\right) \\ = \int_x^1 \frac{dz}{z} \int \frac{d^2 \mathbf{q}}{\pi \mathbf{q}^2} \bar{\alpha}_s(\mathbf{q}^2) \left[ f\left(\frac{x}{z}, |\mathbf{k} + \mathbf{q}|\right) \Theta\left(\frac{k^2}{z} - k'^2\right) - \Theta(k - q) f\left(\frac{x}{z}, k\right) \right] \end{aligned}$$

### DGLAP evolution with non-singular part of the splitting function

$$\tilde{P}_{gg}^{(0)} = P_{gg}^{(0)} - \frac{1}{z}$$

$$\begin{aligned} \mathcal{K}_0^{\text{coll}}(z; k, k') \otimes_{z, k'} f\left(\frac{x}{z}, k'\right) &= \int_x^1 \frac{dz}{z} \int_0^{k^2} \frac{dk'^2}{k^2} \bar{\alpha}_s(k^2) z \tilde{P}_{gg}(z) f\left(\frac{x}{z}, k'\right) \\ &+ \int_x^1 \frac{dz}{z} \int_{k^2}^{k^2/z} \frac{dk'^2}{k'^2} \bar{\alpha}_s(k'^2) z \frac{k'^2}{k^2} \tilde{P}_{gg}\left(z \frac{k'^2}{k^2}\right) f\left(\frac{x}{z}, k'\right) \end{aligned}$$

asymmetric scale

# CCSS evolution: ctd.

## NLLx BFKL with subtractions included

$$\begin{aligned}
 \int_x^1 \frac{dz}{z} \int dk'^2 \bar{\alpha}_s^2(k_{>}^2) \tilde{K}_1(k, k') f\left(\frac{x}{z}, k'\right) &= \frac{1}{4} \int_x^1 \frac{dz}{z} \int dk'^2 \bar{\alpha}_s^2(k_{>}^2) \left\{ \right. \\
 &\left( \frac{67}{9} - \frac{\pi^2}{3} \right) \frac{1}{|k'^2 - k^2|} \left[ f\left(\frac{x}{z}, k'^2\right) - \frac{2k_{<}^2}{(k'^2 + k^2)} f\left(\frac{x}{z}, k^2\right) \right] + \\
 &\left[ -\frac{1}{32} \left( \frac{2}{k'^2} + \frac{2}{k^2} + \left( \frac{1}{k'^2} - \frac{1}{k^2} \right) \log \left( \frac{k^2}{k'^2} \right) \right) + \frac{4\text{Li}_2(1 - k_{<}^2/k_{>}^2)}{|k'^2 - k^2|} \right. \\
 &\left. -4A_1(0) \text{sgn}(k^2 - k'^2) \left( \frac{1}{k^2} \log \frac{|k'^2 - k^2|}{k'^2} - \frac{1}{k'^2} \log \frac{|k'^2 - k^2|}{k^2} \right) \right. \\
 &\left. - \left( 3 + \left( \frac{3}{4} - \frac{(k'^2 + k^2)^2}{32k'^2 k^2} \right) \int_0^\infty \frac{dy}{k^2 + y^2 k'^2} \log \left| \frac{1+y}{1-y} \right| \right. \right. \\
 &\left. \left. + \frac{1}{k'^2 + k^2} \left( \frac{\pi^2}{3} + 4\text{Li}_2\left(\frac{k_{<}^2}{k_{>}^2}\right) \right) \right] f\left(\frac{x}{z}, k'\right) \right\} \\
 &+ \frac{1}{4} 6\zeta(3) \int_x^1 \frac{dz}{z} \bar{\alpha}_s^2(k^2) f\left(\frac{x}{z}, k\right) .
 \end{aligned}$$

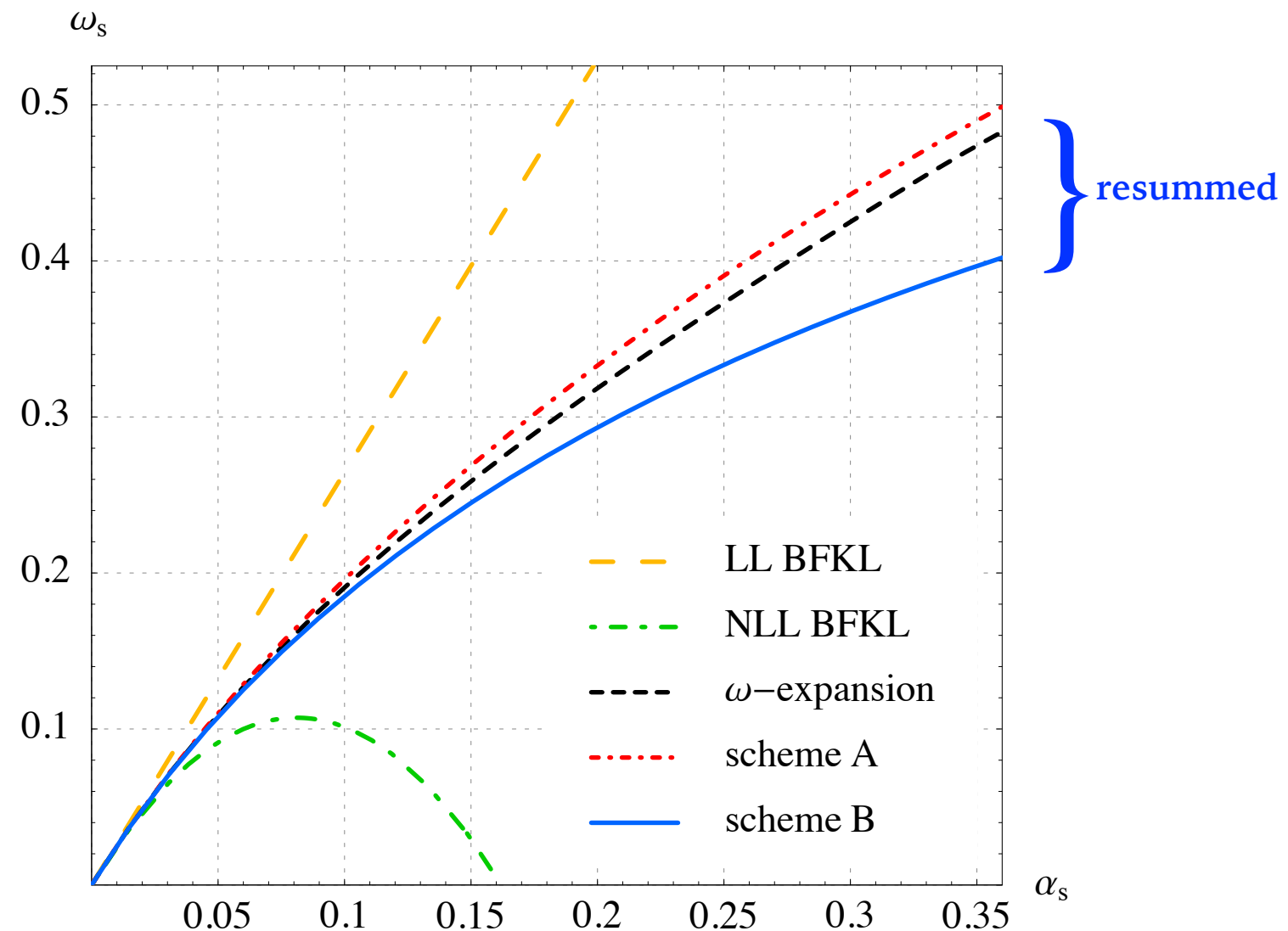
subtractions

+ additional subtractions to guarantee consistency with NLO DGLAP and momentum sum rule

# Resummation at small x

Ciafaloni, Colferai, Salam, AS

- Include **kinematical constraint: limits on transverse momenta**
- Include DGLAP **splitting function** and **running coupling** in the leading part
- Subtractions to avoid double counting, guarantee **momentum sum** rule
- The **integro-differential** equation becomes double integral equation
- **Transverse** and **longitudinal** momenta no longer factorized

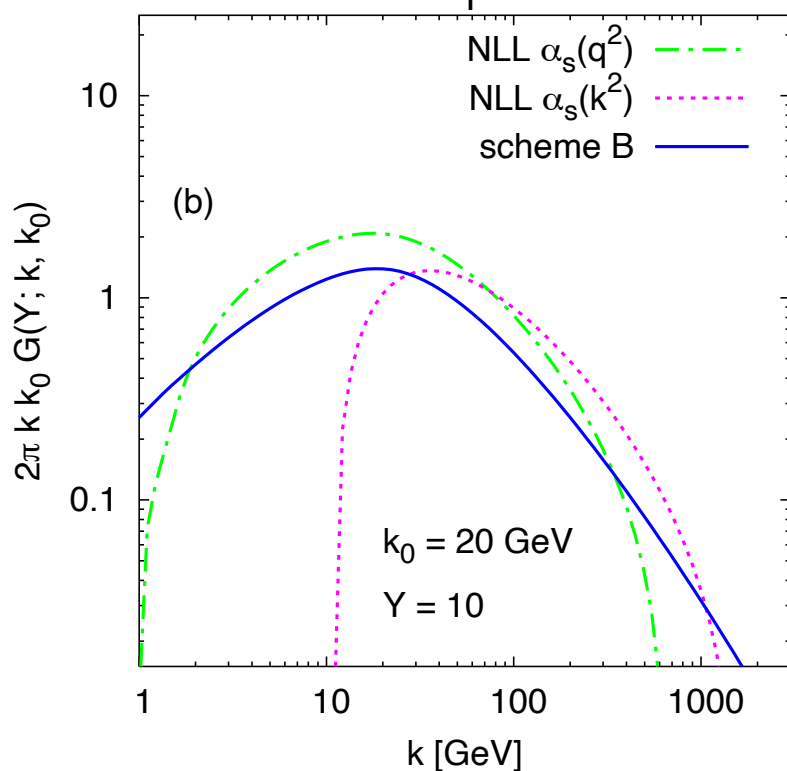
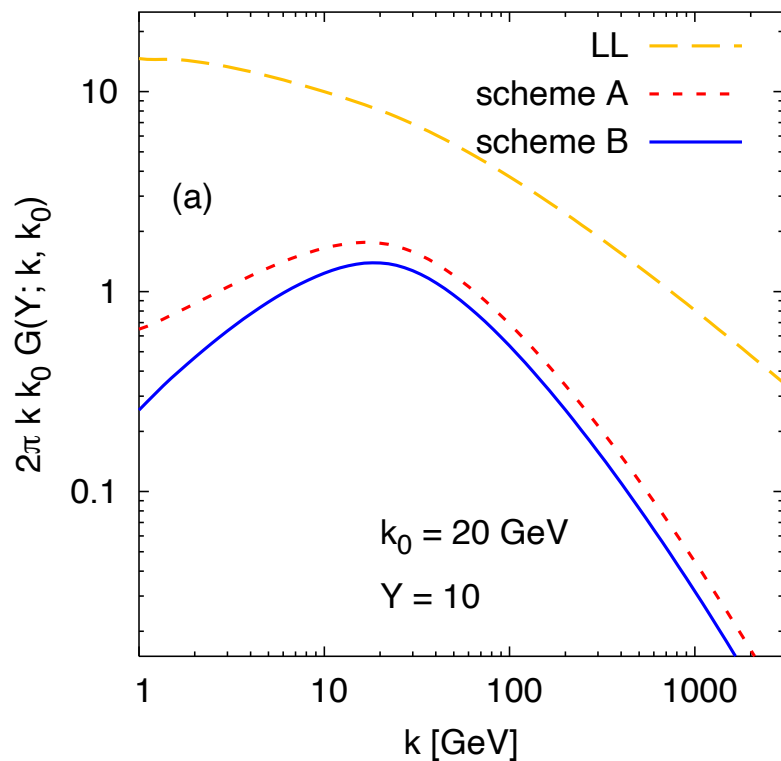
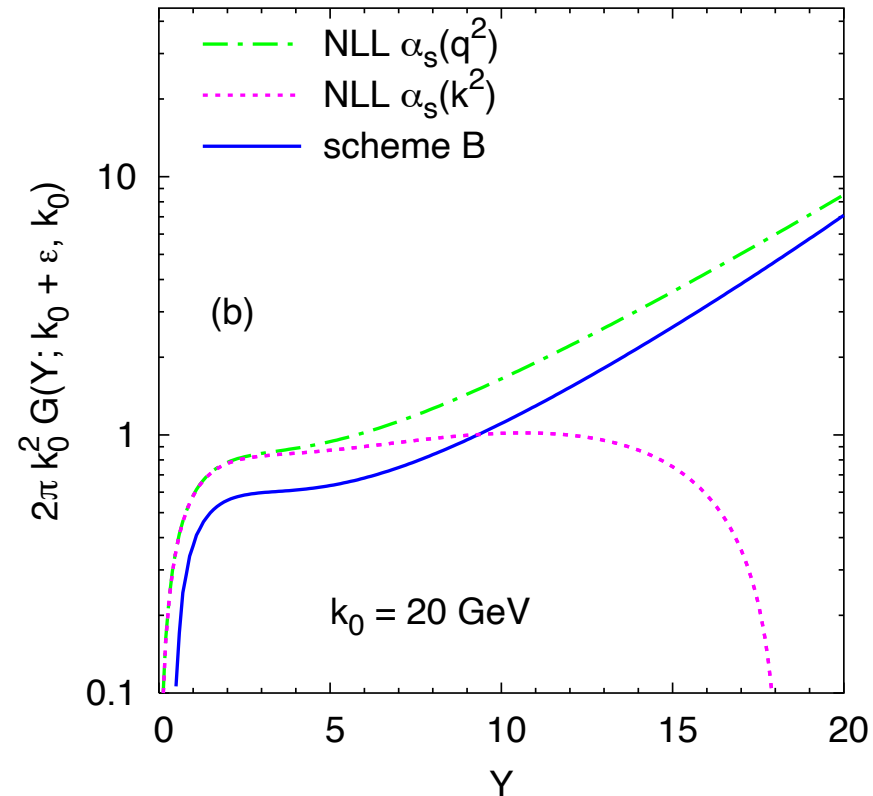
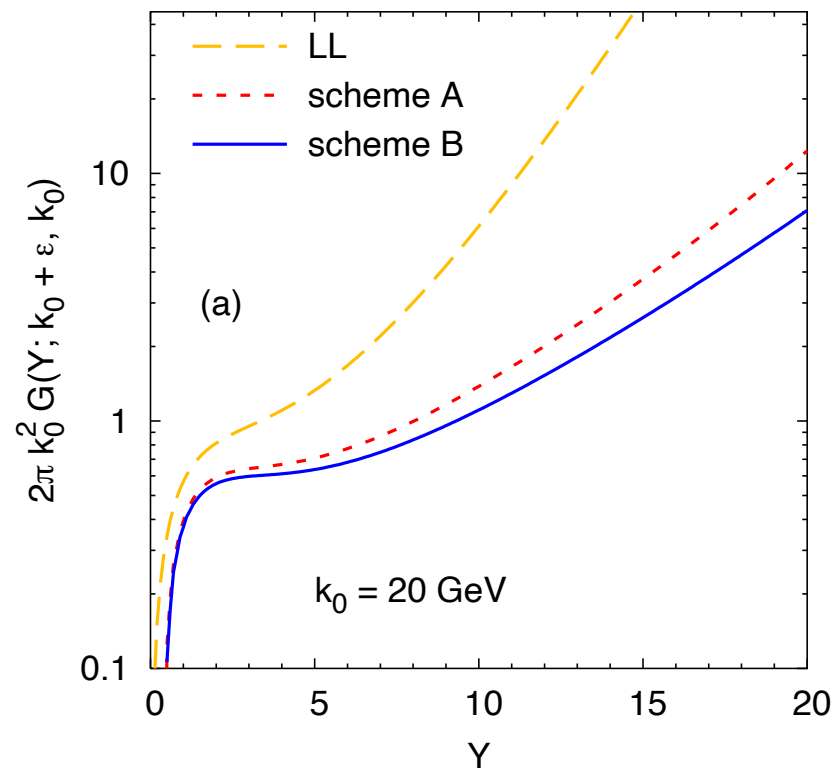


Resummation stabilizes the BFKL expansion

Intercept, and therefore the resulting growth with  $1/x$  is slowed down

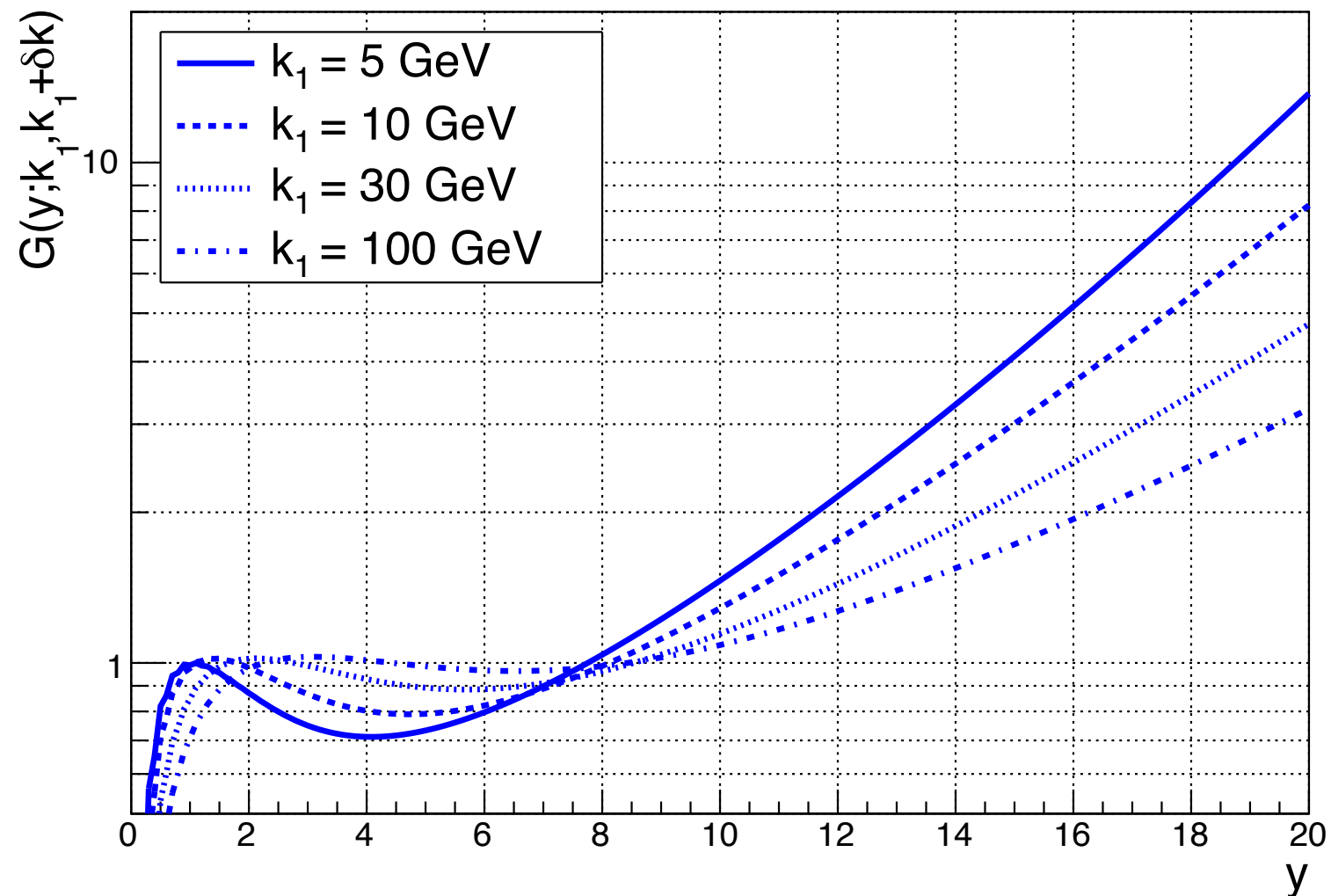
More consistent with phenomenology

# Features of resummed gluon Green's function



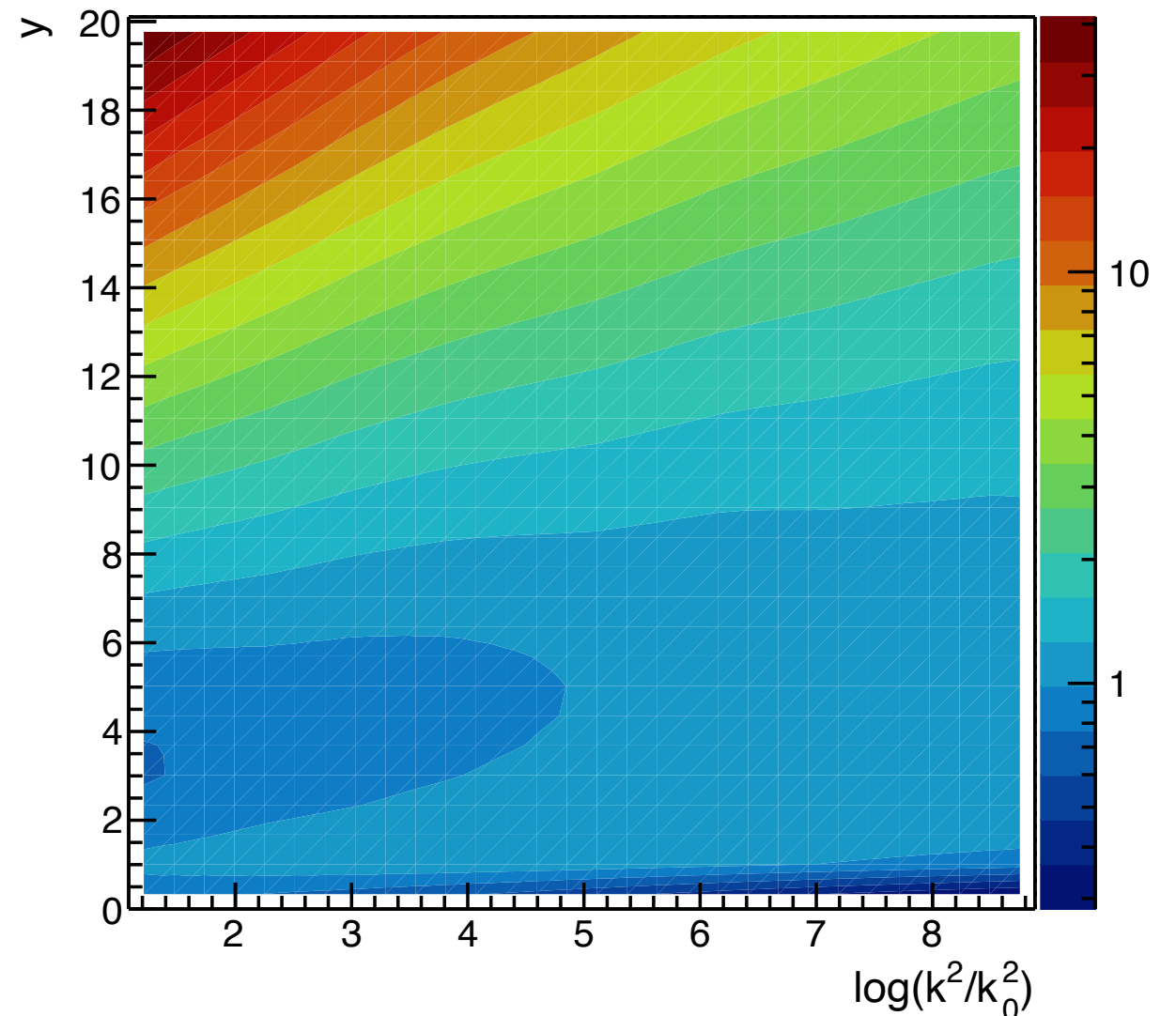
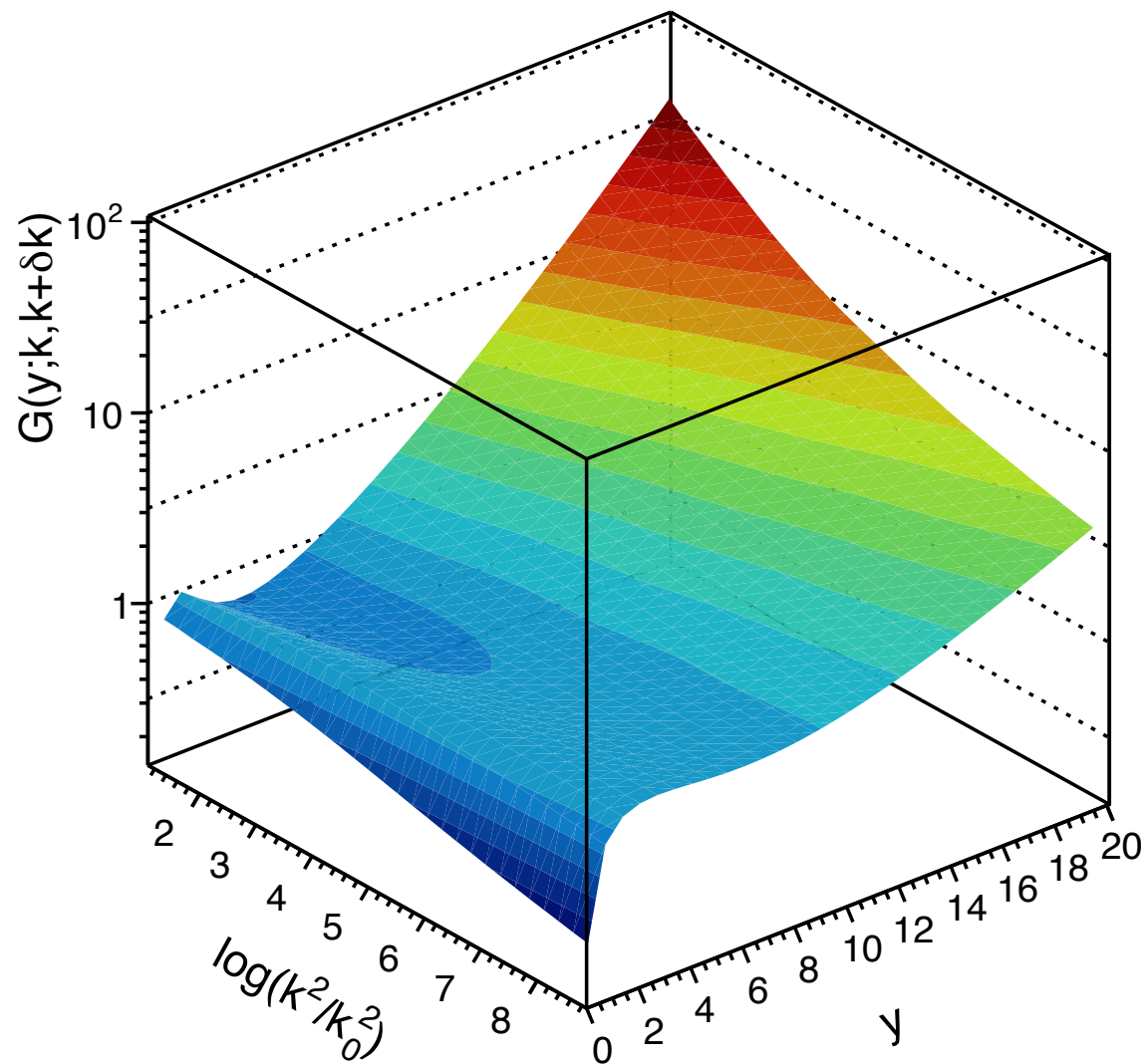
- Resummed GGF compared with pure NLL and LL (with running coupling)
- Significant reduction of the high energy growth with respect to LL
- Large preasymptotic effects: growth is delayed to higher rapidities
- Large  $k$  behavior substantially steeper in resummed calculation than in the LL one
- This is an effect of the reduced diffusion (smaller  $\chi''_{\text{eff}}$ )
- Resummed result more stable than NLL

# Features of resummed gluon Green's function



Effects of resummation: Lowering effective power  
Onset of small  $x$  rise delayed  
Dip or plateau

# Gluon Green's function



Strong preasymptotic effects, which delay the onset of growth towards small  $x$  / large  $y$   
Plateau in rapidity

# Resummed splitting function

---

- Deconvolution of the integral equation.
- Calculate the integrated density:  $xg(x, Q^2) = \int^{Q^2} dk_T^2 G^{(s_0=k_T^2)}(x; k_T, k_{0T})$
- Solve numerically for the splitting function:

$$\frac{dg(x, Q^2)}{d \log Q^2} = \int \frac{dz}{z} P_{\text{eff}}(z, Q^2) g\left(\frac{x}{z}, Q^2\right)$$

At large values of  $Q^2$  the results should be independent of the regularization of the coupling and the choice of  $k_0$ .

**Factorization in  $Q^2$  of the non-perturbative and perturbative contributions.**

# Spitting function

---

Recall: gluon-gluon splitting function has logarithmic enhancements at small  $x$

$$xP_{gg}(x) = \underbrace{\sum_{n=1} a_n \alpha_s^n \ln^{n-1} \frac{1}{x}}_{\text{LLx}} + \underbrace{\sum_{n=2} b_n \alpha_s^n \ln^{n-2} \frac{1}{x}}_{\text{NLLx}} + \dots$$

First small  $x$  logarithmic term which belongs to LLx hierarchy should appear at N<sup>3</sup>LO

DGLAP

$$\bar{\gamma} = \frac{\bar{\alpha}_s}{\omega} + 2\zeta(3) \left(\frac{\bar{\alpha}_s}{\omega}\right)^4 + 2\zeta(5) \left(\frac{\bar{\alpha}_s}{\omega}\right)^6 + \dots$$

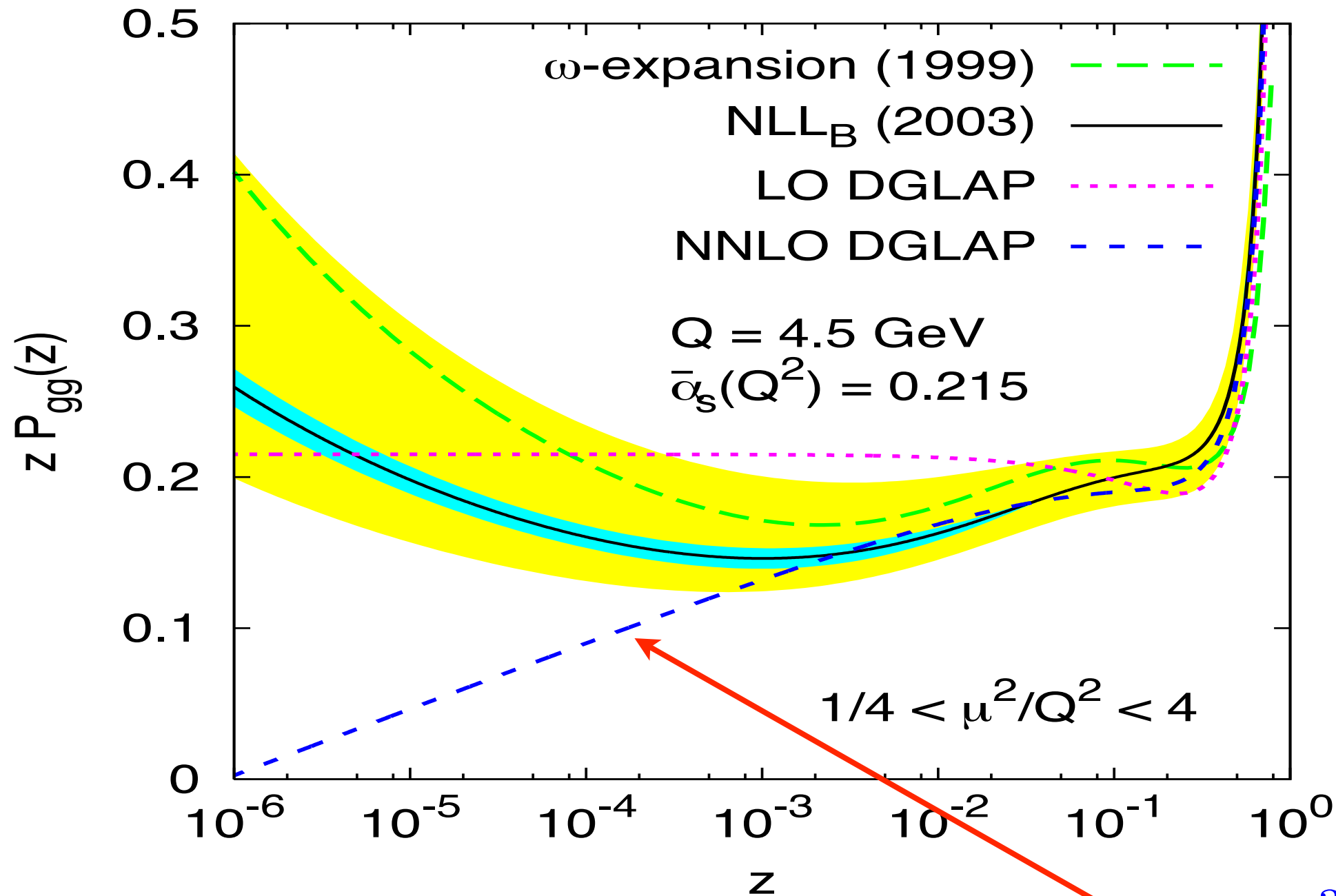
$$\frac{1}{2\pi i} \int_C d\omega x^{-\omega-1} \bar{\gamma}(\omega) = \frac{1}{2\pi i} \int_C d\omega x^{-\omega-1} \sum_{k=1}^{\infty} a_k \left(\frac{\bar{\alpha}_s}{\omega}\right)^k = \sum_{k=1}^{\infty} \frac{a_k}{(k-1)!} \frac{\bar{\alpha}_s}{x} (\bar{\alpha}_s \ln 1/x)^{k-1}$$

$$0.4\bar{\alpha}_s^4 \ln^3 1/x$$

First small  $x$  logarithmic term which belongs to NLLx hierarchy recovered at NNLO DGLAP

$$-1.54\bar{\alpha}_s^3 \ln 1/x$$

# Resummed splitting function



Dip in the resummed splitting function

Is this a universal feature ?

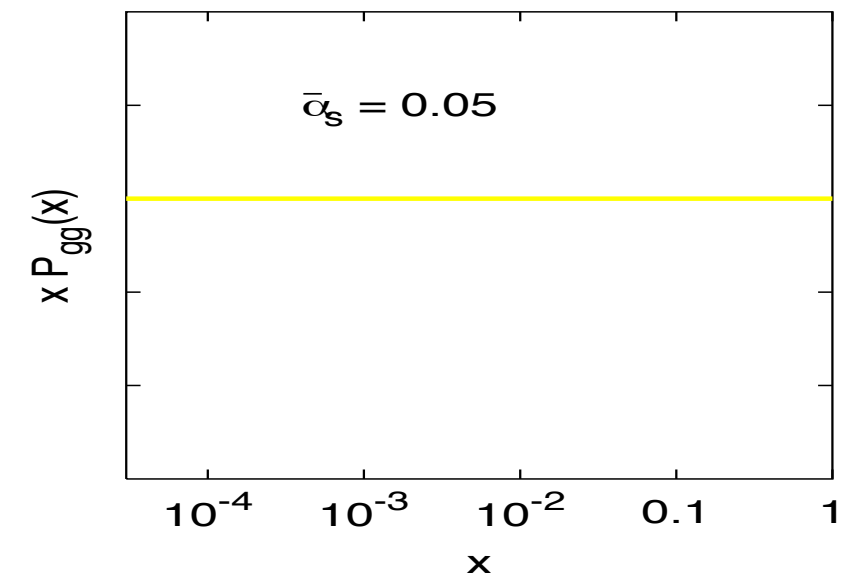
$$-1.54 \bar{\alpha}_s^3 \ln 1/x$$

Initial decrease is consistent with the small x NNLO term.

# Understanding the features of the splitting function

Perturbative terms in the splitting function

	LL <sub>x</sub>	NLL <sub>x</sub>	NNLL <sub>x</sub>	...
$\alpha_s$	x	-	-	
$\alpha_s^2$	0	$n_f$	-	
$\alpha_s^3$	0	x	x	
$\alpha_s^4$	x	x	x	const.
$\alpha_s^5$	0	x	x	$\ln 1/x$
$\vdots$				$\ln^2 1/x$
$\vdots$				$\ln^3 1/x$



$$-1.54\bar{\alpha}_s^3 \ln 1/x + 0.401\bar{\alpha}_s^4 \ln^3 1/x$$

There is a minimum when

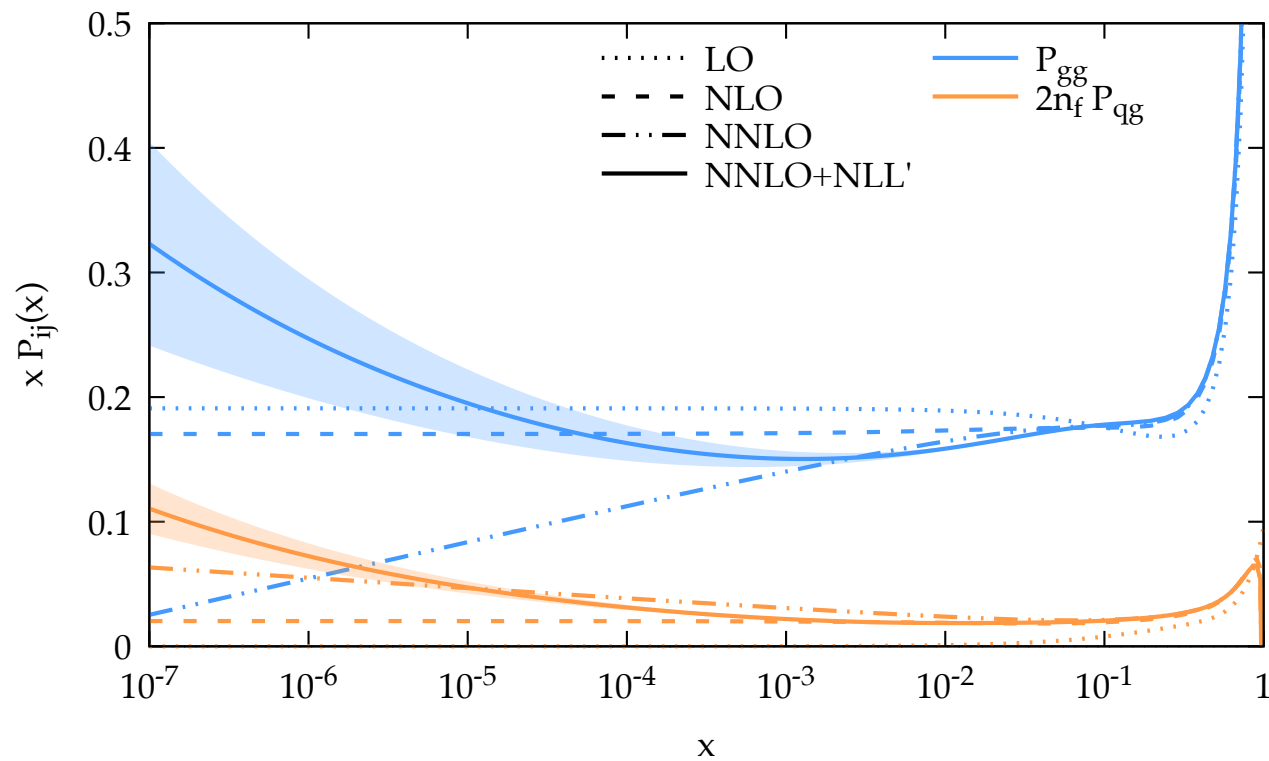
$$\alpha_s \ln^2 \frac{1}{x} \sim 1 \longrightarrow \ln \frac{1}{x} \sim \frac{1}{\sqrt{\alpha_s}}$$

In general: dip comes from the interplay between NNLO and the resummation.

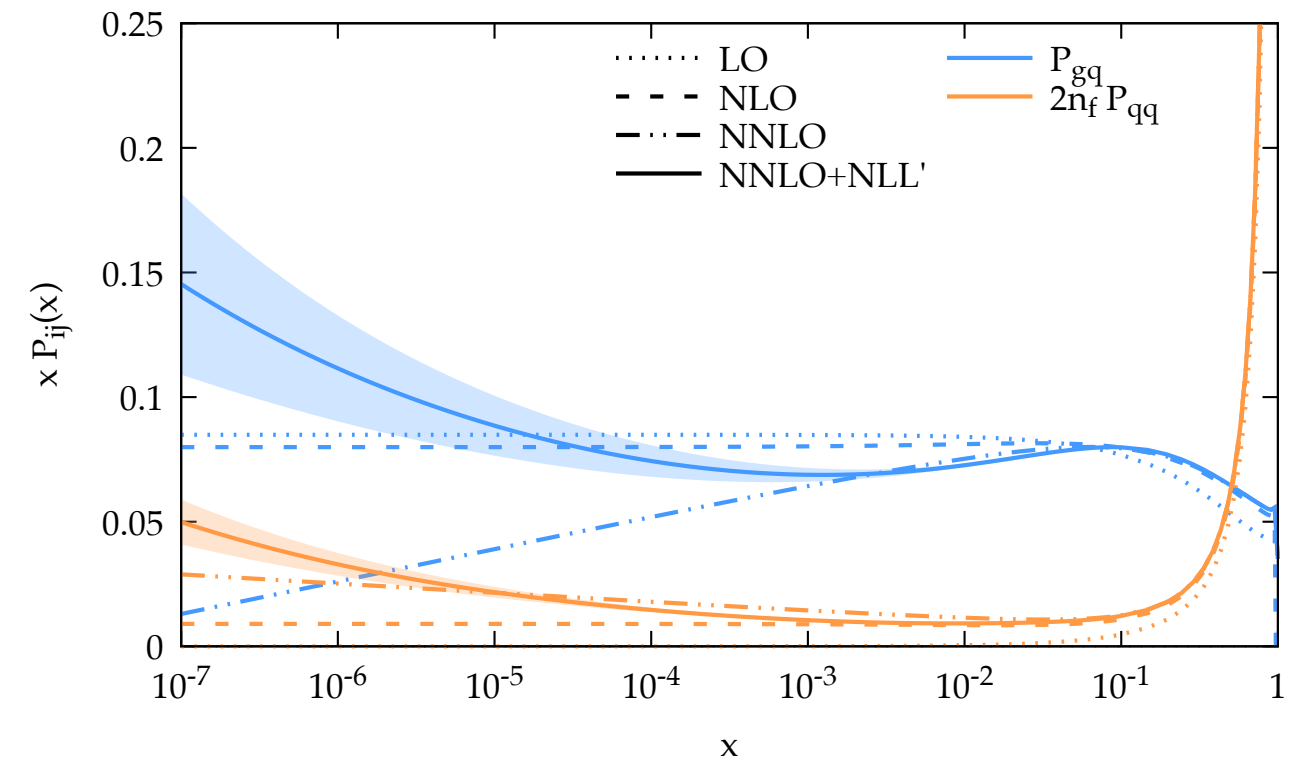
# Resummation: latest results on the splitting function

Bonvini, Frixione, Stagnitto

$\alpha_s = 0.20, n_f = 3, Q_0 \overline{\text{MS}}$



$\alpha_s = 0.20, n_f = 3, Q_0 \overline{\text{MS}}$



Dip in the splitting function visible in other resummation approaches

# Phenomenology: Structure function

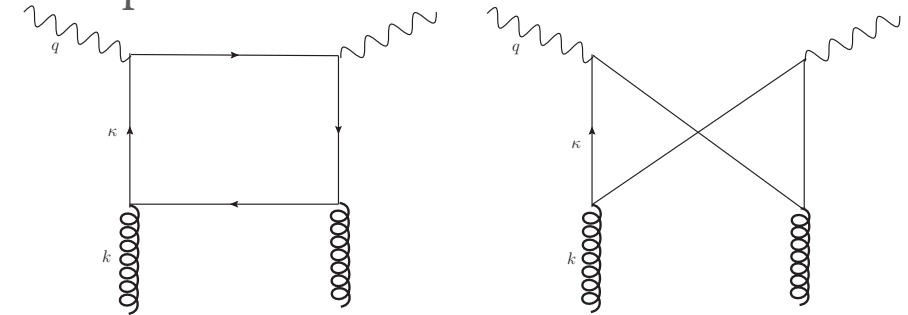
Evaluate structure function from  $k_T$  factorization

$$F_2(x, Q^2) = \sum e_q^2 S_q(x, Q^2)$$

$$S_q(x, Q^2) = \int_x^1 \frac{dz}{z} \int \frac{dk^2}{k^2} S_{\text{box}}^q(z, m_q^2, k^2, Q^2) f\left(\frac{x}{z}, k^2\right)$$

Photon-gluon impact factor

Graphs at LO



Explicit expression

$$S_q(x, Q^2) = \frac{Q^2}{4\pi^2} \int \frac{dk^2}{k^4} \int_0^1 d\beta \int dk' \alpha_s \left\{ [\beta^2 + (1 - \beta^2)] \left( \frac{\kappa}{D_{1q}} - \frac{\kappa - \mathbf{k}}{D_{2q}} \right)^2 + [m_q^2 + 4Q^2 \beta^2 (1 - \beta)^2] \left( \frac{1}{D_{1q}} - \frac{1}{D_{2q}} \right)^2 \right\} f\left(\frac{x}{z}, k^2\right) \Theta\left(1 - \frac{x}{z}\right)$$

Denominators

$$D_{1q} = \kappa^2 + \beta(1 - \beta)Q^2 + m_q^2, \quad D_{2q} = (\kappa - \mathbf{k})^2 + \beta(1 - \beta)Q^2 + m_q^2$$

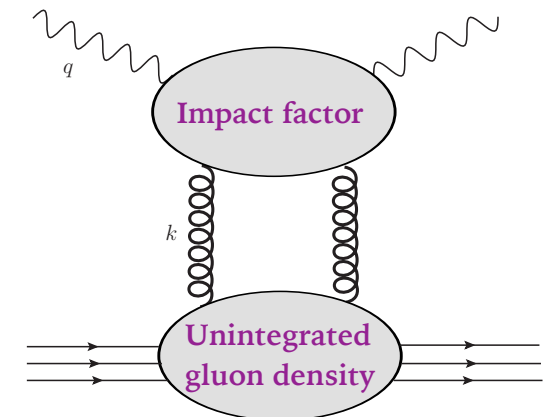
$\kappa, \mathbf{k}$  quark and gluon transverse momenta

Argument of the gluon density incorporating **exact** kinematics

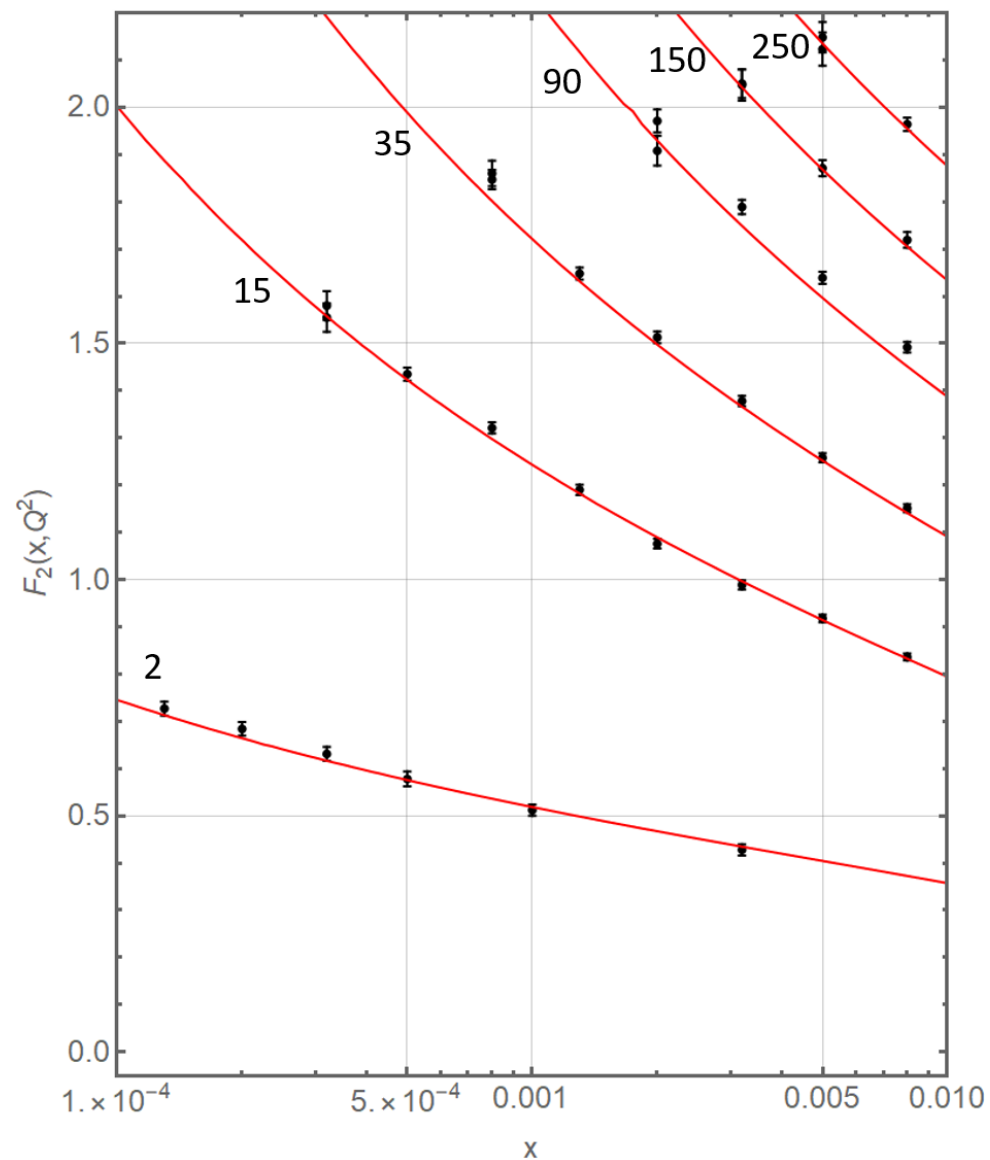
$$z = \left[ 1 + \frac{\kappa'^2 + m_q^2}{\beta(1 - \beta)Q^2} + \frac{k^2}{Q^2} \right]^{-1}$$

Higher order terms in impact factor

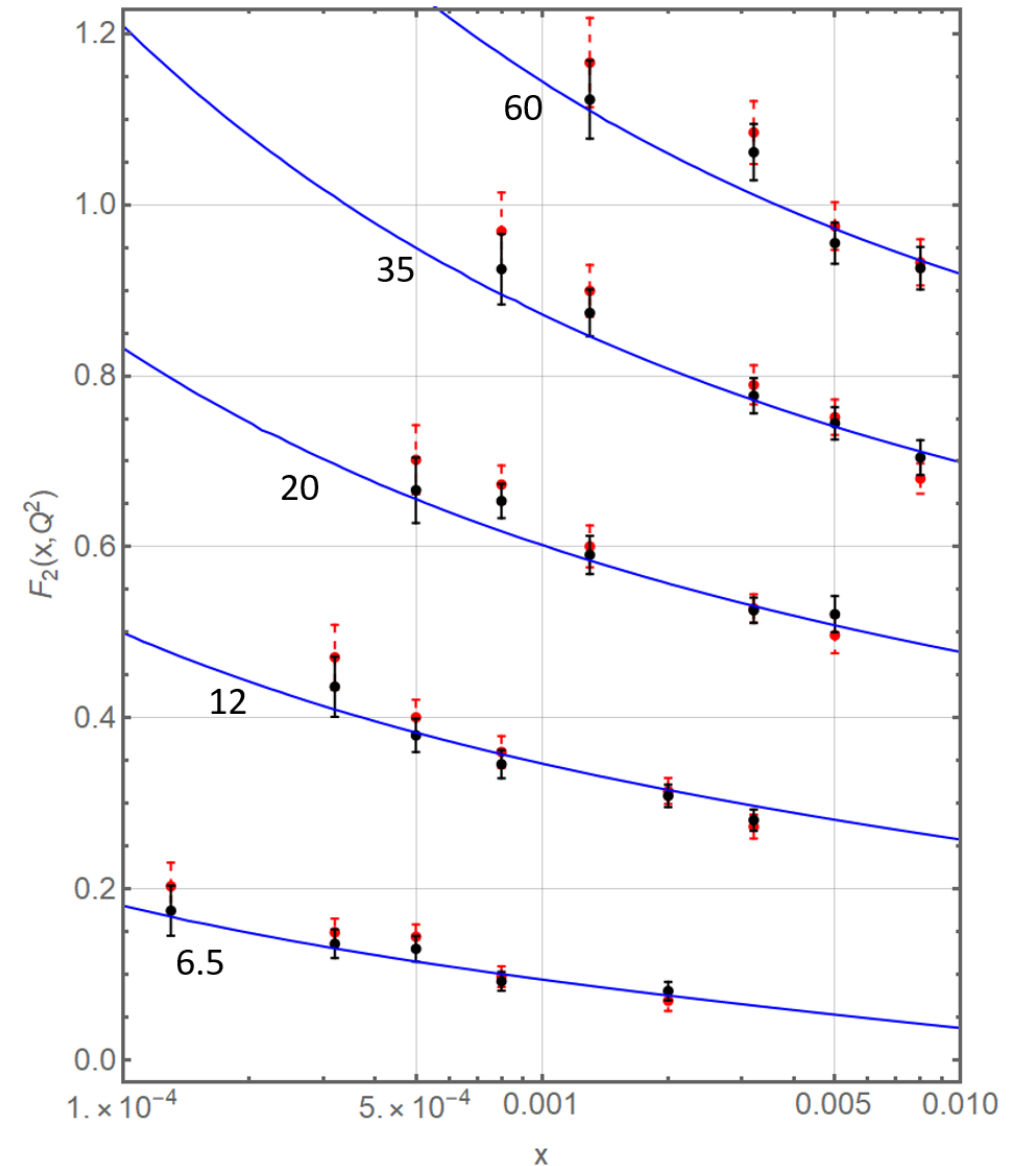
*Bialas, Peschanski, Navelet*



# Results: $F_2$ and $F_{2c}$



*Inclusive*



*Charm structure function*

*Li, AS*

Excellent description of the data on structure functions  $F_2$  and  $F_{2c}$

# Phenomenology: resummation in $P_{gg}$ and $P_{qg}$

BFKL anomalous dimension at LO

$$\bar{\gamma} = \frac{\bar{\alpha}_S}{\omega} + 2\zeta(3) \left(\frac{\bar{\alpha}_S}{\omega}\right)^4 + 2\zeta(5) \left(\frac{\bar{\alpha}_S}{\omega}\right)^6 + \dots$$

Resummed splitting function at LL and beyond

$$xP_{gg}(x) = \sum_{k=1}^{\infty} \frac{a_k^{(0)}}{(k-1)!} \bar{\alpha}_s (\bar{\alpha}_s \ln 1/x)^{k-1} + \sum_{k=1}^{\infty} \frac{a_k^{(1)}}{k!} \bar{\alpha}_s (\bar{\alpha}_s^2 \ln 1/x)^k + \dots$$

Recall relation of kT factorization to collinear

$$Q^2 \frac{\partial \bar{F}_2(\omega, Q^2)}{\partial Q^2} = \hat{F}_2(\omega, \bar{\gamma}) R \bar{\gamma}^2 \tilde{f}^{(0)}(\omega, \bar{\gamma}) (Q^2)^{\bar{\gamma}}$$

small x resummed version of the collinear formula

$$Q^2 \frac{\partial \bar{F}_2(\omega, Q^2)}{\partial Q^2} = \sum_q 2e_q^2 P_{qg}(\omega, \bar{\gamma}) g(\omega, Q^2)$$

with resummed  $P_{qg}$  function

$$xP_{qg}(x) = xP_{qg}^{(0)}(x) + \sum_{k=1}^{\infty} \frac{b_k}{(k-1)!} \bar{\alpha}_s (\bar{\alpha}_s \ln 1/x)^{k-1} + \dots$$

where  $xP_{qg}^{(0)} \rightarrow 0$  when  $x \rightarrow 0$

Small x terms both in  $P_{gg}$  and in  $P_{qg}$

Turns out numerically very important in  $P_{qg}$

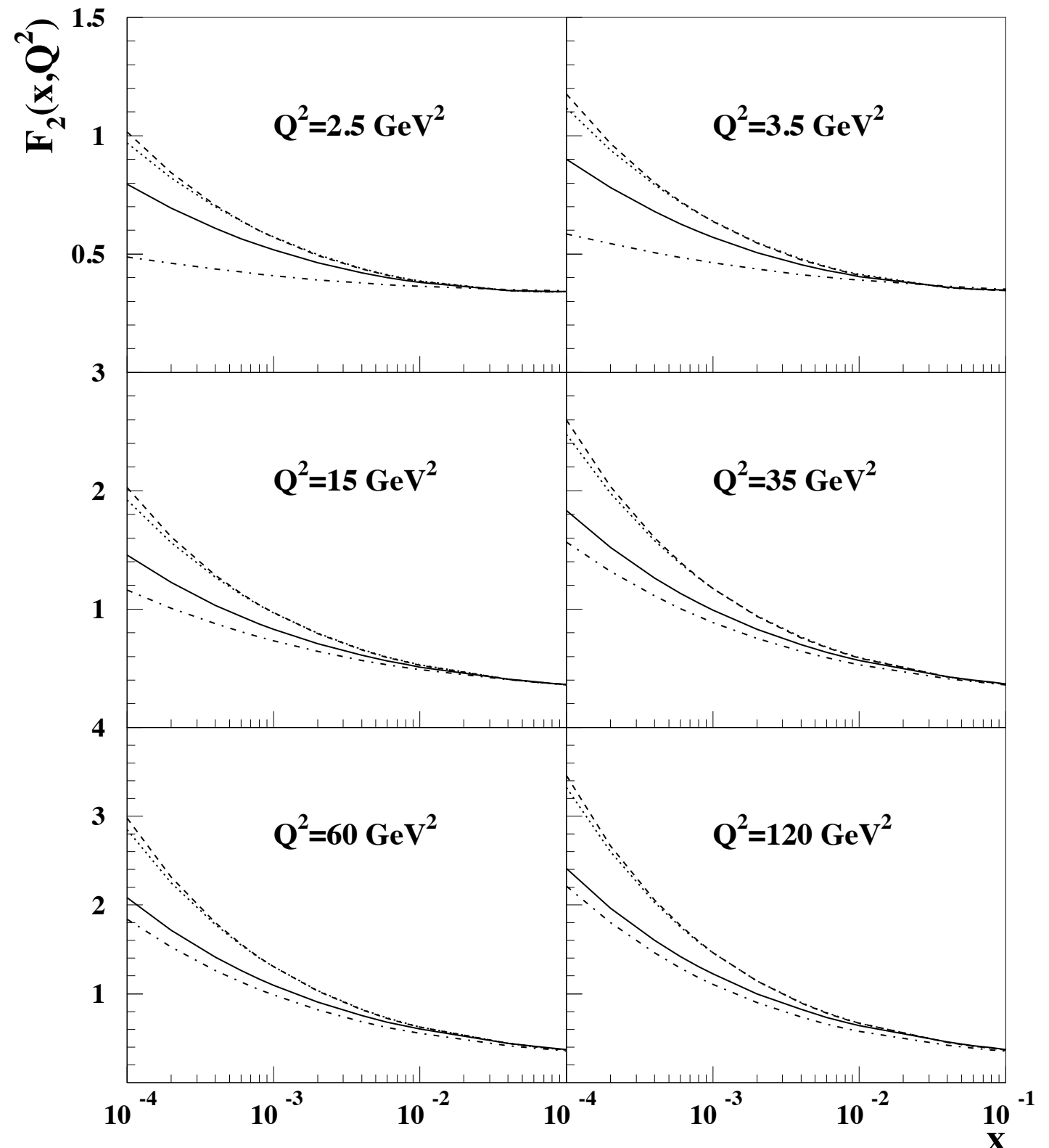
# Phenomenology: small x resummation in $P_{gg}$ and $P_{qg}$

Four scenarios (same input distributions):

- Resummed BFKL in the gluon sector (includes non-singular part of LO DGLAP splitting function and kinematical constraint) + and  $k_T$  factorization (**solid**)
- BFKL in the gluon sector (includes LO DGLAP splitting function but **no kinematical constraint**) + and  $k_T$  factorization (**dashed**)
- Pure DGLAP in the gluon sector and  $k_T$  factorization (**dotted**)
- LO DGLAP evolution in the gluon and quark sector (**dotted-dashed**)

Large effects from kinematical constraint : terms beyond  $LLx$  important.

Also Shows that resummation in the  $P_{qg}$  function is very important

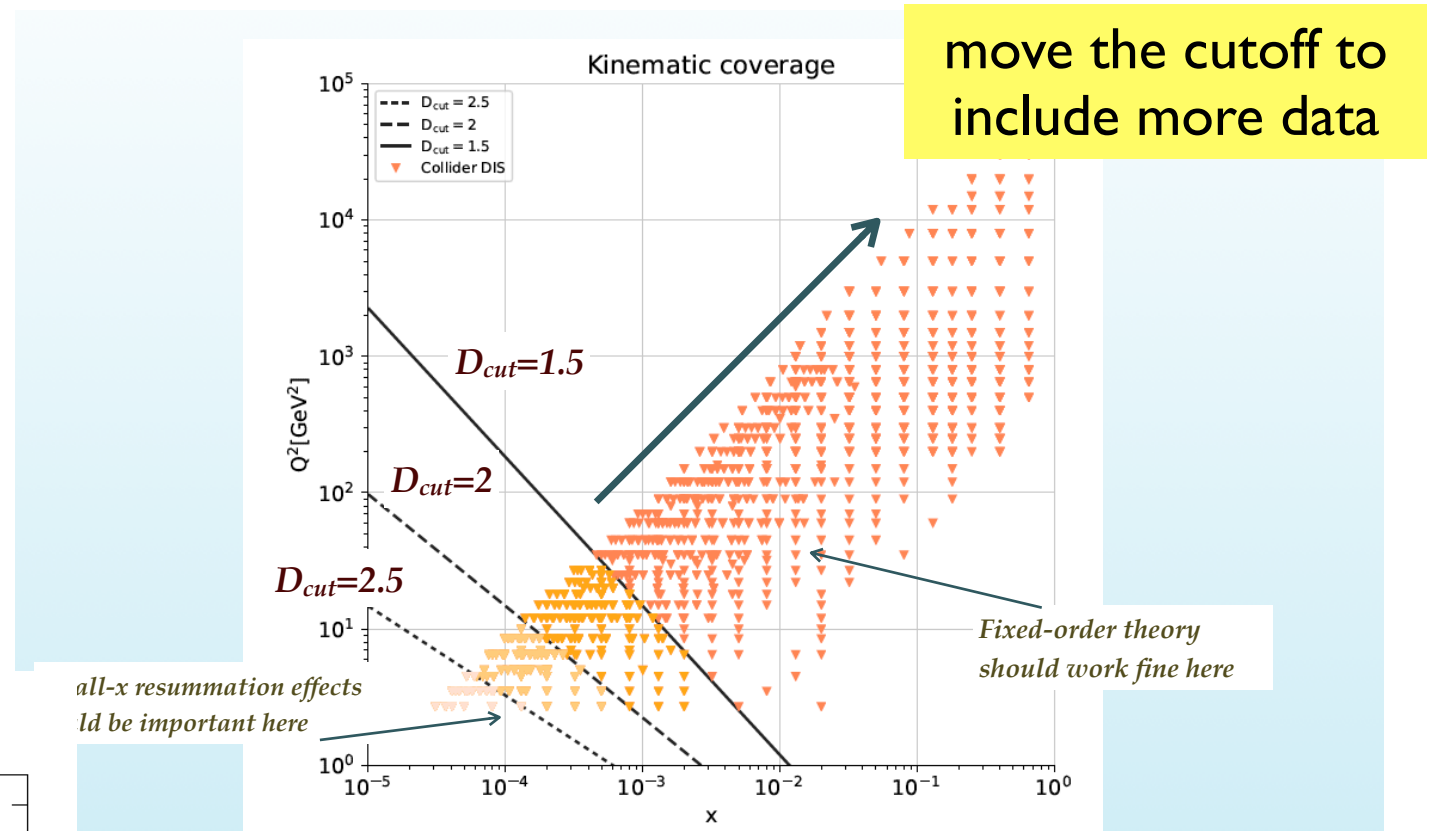
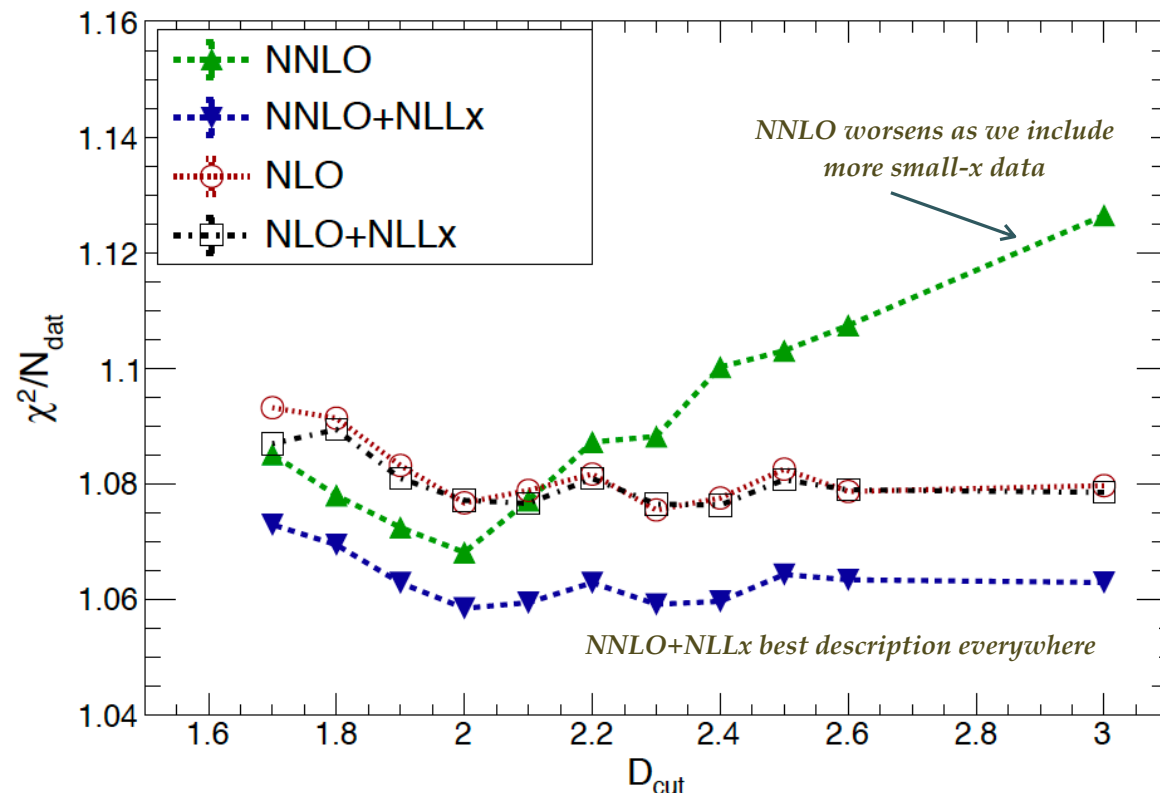


# Small x resummation and HERA data

*Ball, Bertoni, Bonvini, Marzani, Rojo, Rottoli*

- Perform fits to data with the cut on small  $x$ /small  $Q^2$  region
- Observe the variation or lack of variation in  $\chi^2$

NNPDF3.1sx, HERA NC inclusive data

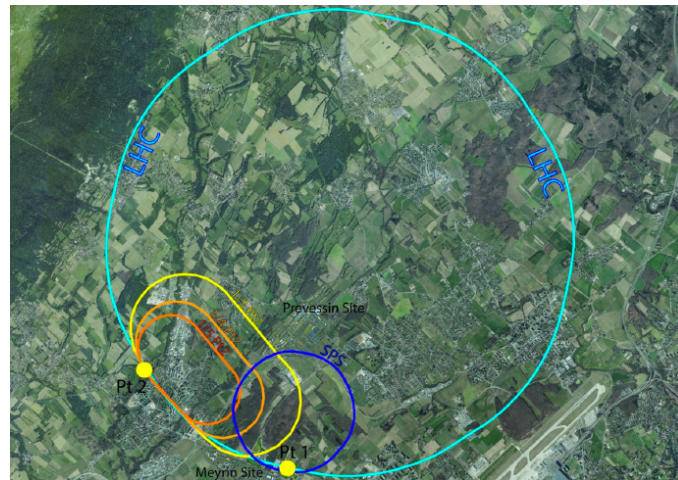


- $\chi^2$  changes for DGLAP at NNLO when more small  $x$  data are included
- NNLO+NNLLx gives best description
- Interestingly NLO and NLO+NLLx do not differ by a lot (flat splitting function at NLO?)

# Impact of resummation at higher energies: future colliders

Future colliders like FCC-hh or LHeC have the potential to open up new kinematic regime of small  $x$ .

Example: LHeC and FCC-eh



50 x 7000 GeV<sup>2</sup>: 1.2 TeV ep collider

Operation: 2035+, Cost: O(1) BCHF

CDR: 1206.2913 J.Phys.G (550 citations)

Upgrade to 10<sup>34</sup> cm<sup>-2</sup>s<sup>-1</sup>, for Higgs, BSM

CERN-ACC-Note-2018-0084 (ESSP)

[arXiv:2007.14491](https://arxiv.org/abs/2007.14491), subm J.Phys.G

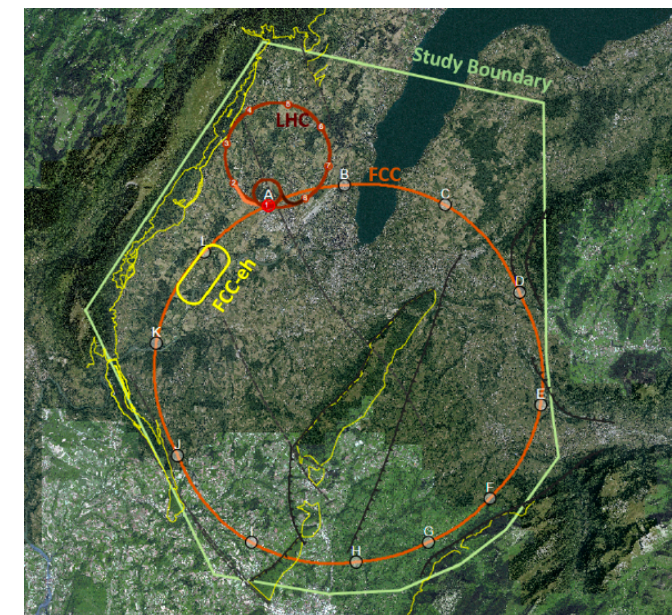
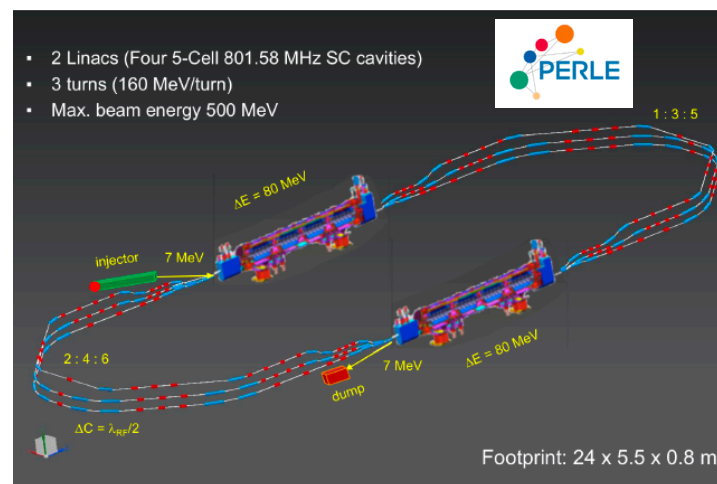
## LHeC, PERLE and FCC-eh

Powerful ERL for Experiments @ Orsay  
 CDR: 1705.08783 J.Phys.G  
 CERN-ACC-Note-2018-0086 (ESSP)

Operation: 2025+, Cost: O(20) MEuro

LHeC ERL Parameters and Configuration  
 $I_e=20\text{mA}$ , 802 MHz SRF, 3 turns  $\rightarrow$   
 $E_e=500\text{ MeV} \rightarrow$  first 10 MW ERL facility

BINP, CERN, Daresbury, Jlab, Liverpool, Orsay (IJC), +



60 x 50000 GeV<sup>2</sup>: 3.5 TeV ep collider

Operation: 2050+, Cost (of ep) O(1-2) BCHF

Concurrent Operation with FCC-hh

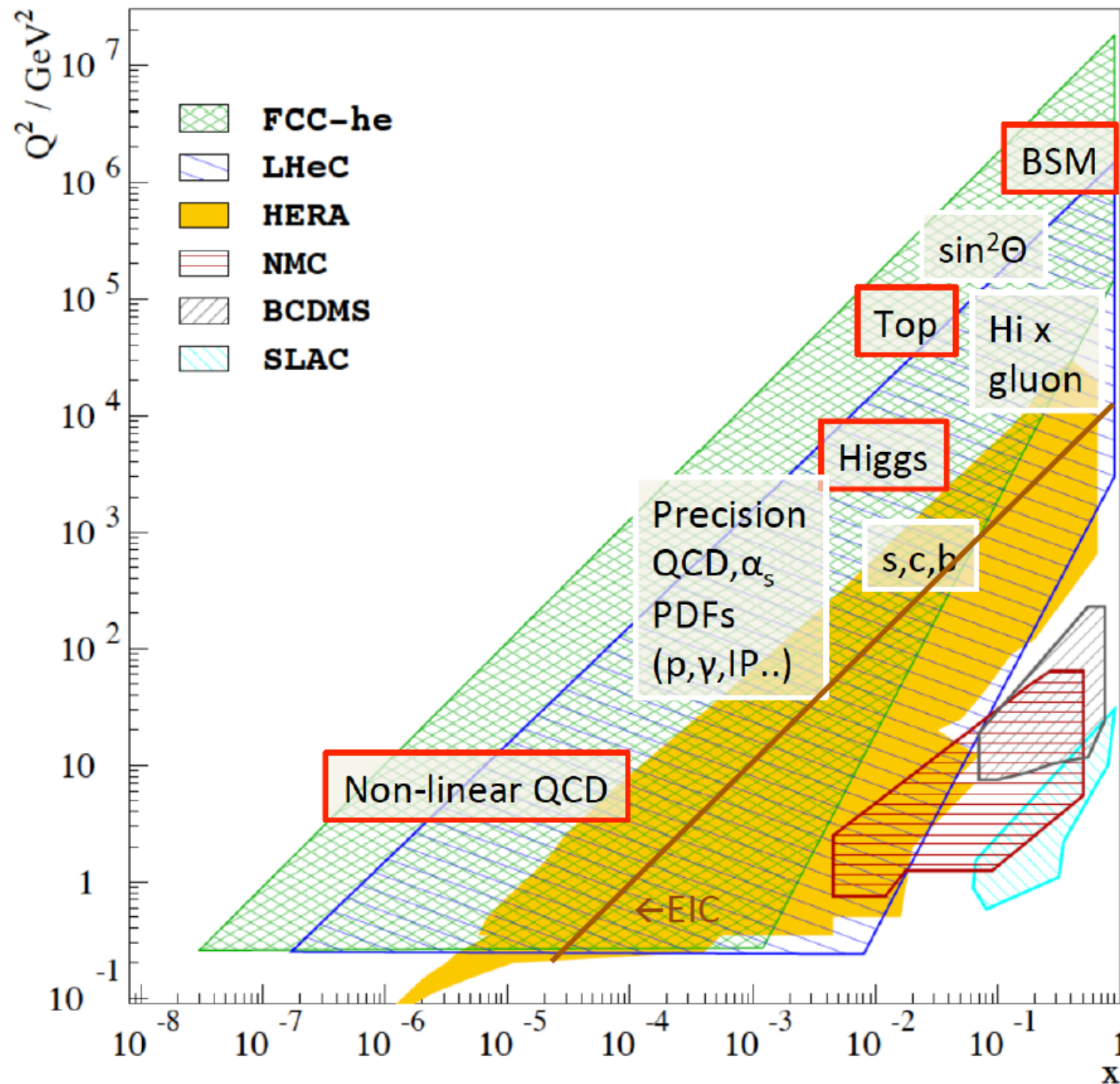
FCC CDR:

*Eur.Phys.J.ST* 228 (2019) 6, 474 Physics

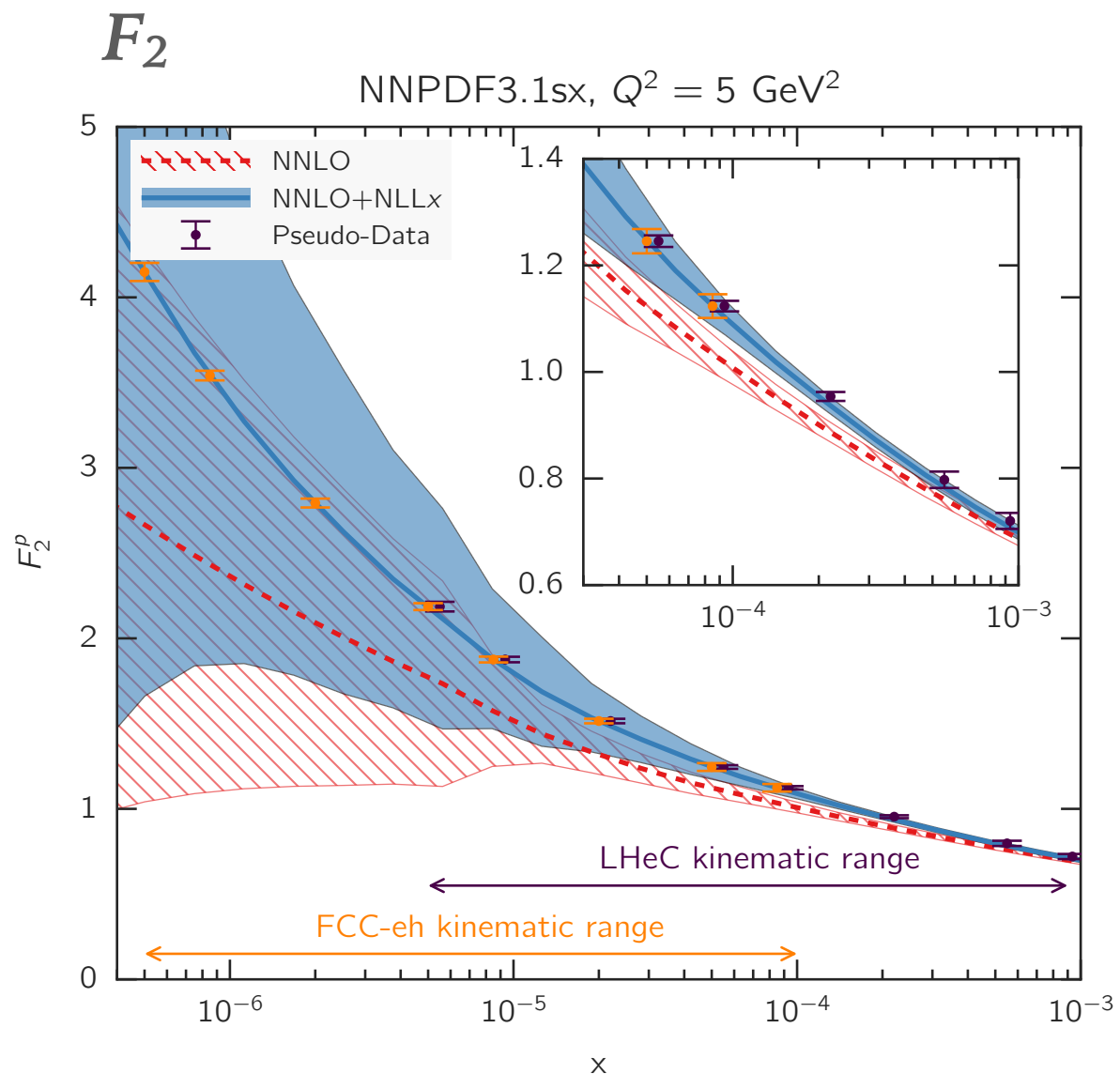
*Eur.Phys.J.ST* 228 (2019) 4, 755 FCC-hh/eh

Future CERN Colliders: 1810.13022 Bordry+

# Kinematic range for LHeC and FCC-eh



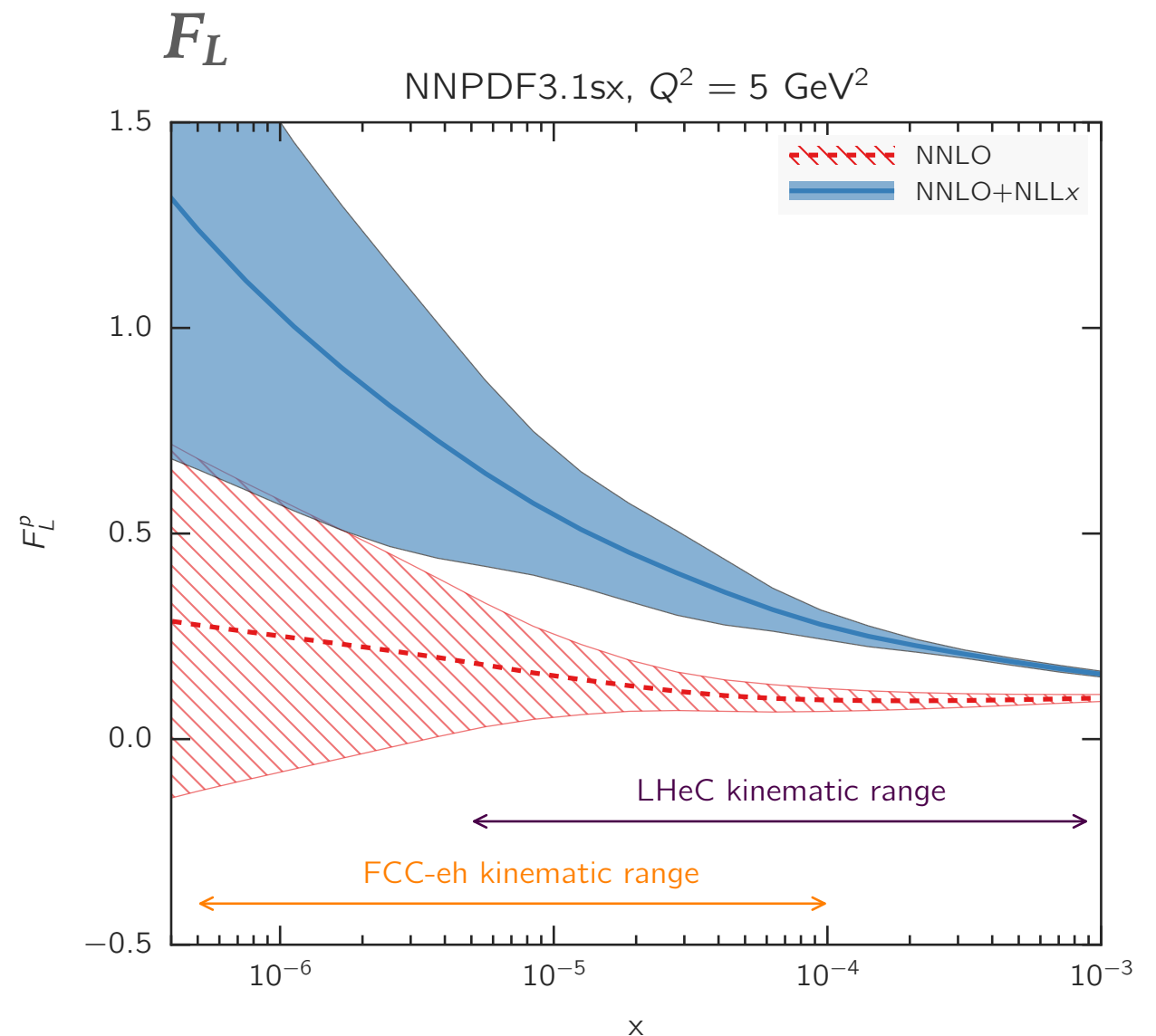
# Novel dynamics at small $x$ : resummation



Important consequences for LHeC and FCC-eh

20-40% difference of central values for  $F_2$

Factor 2 to 4 for  $F_L$



DGLAP fit will likely fail at the LHeC/FCC range

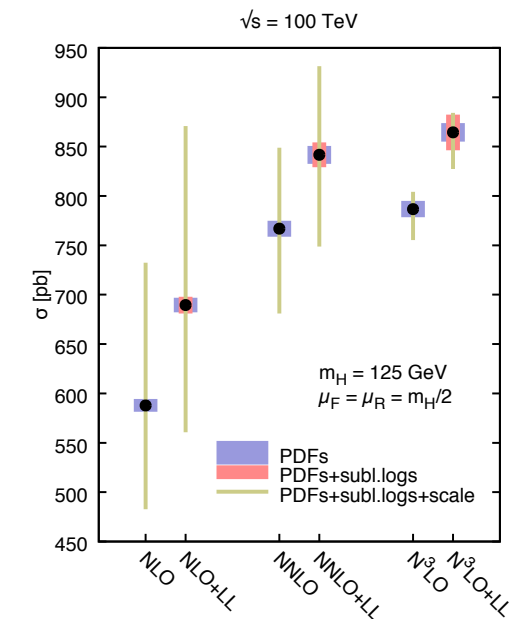
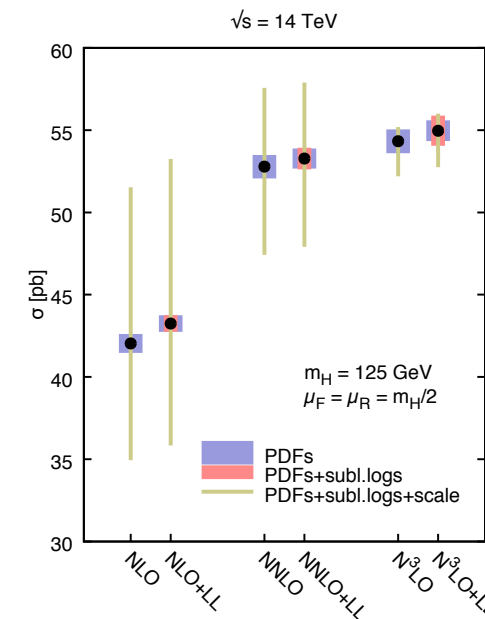
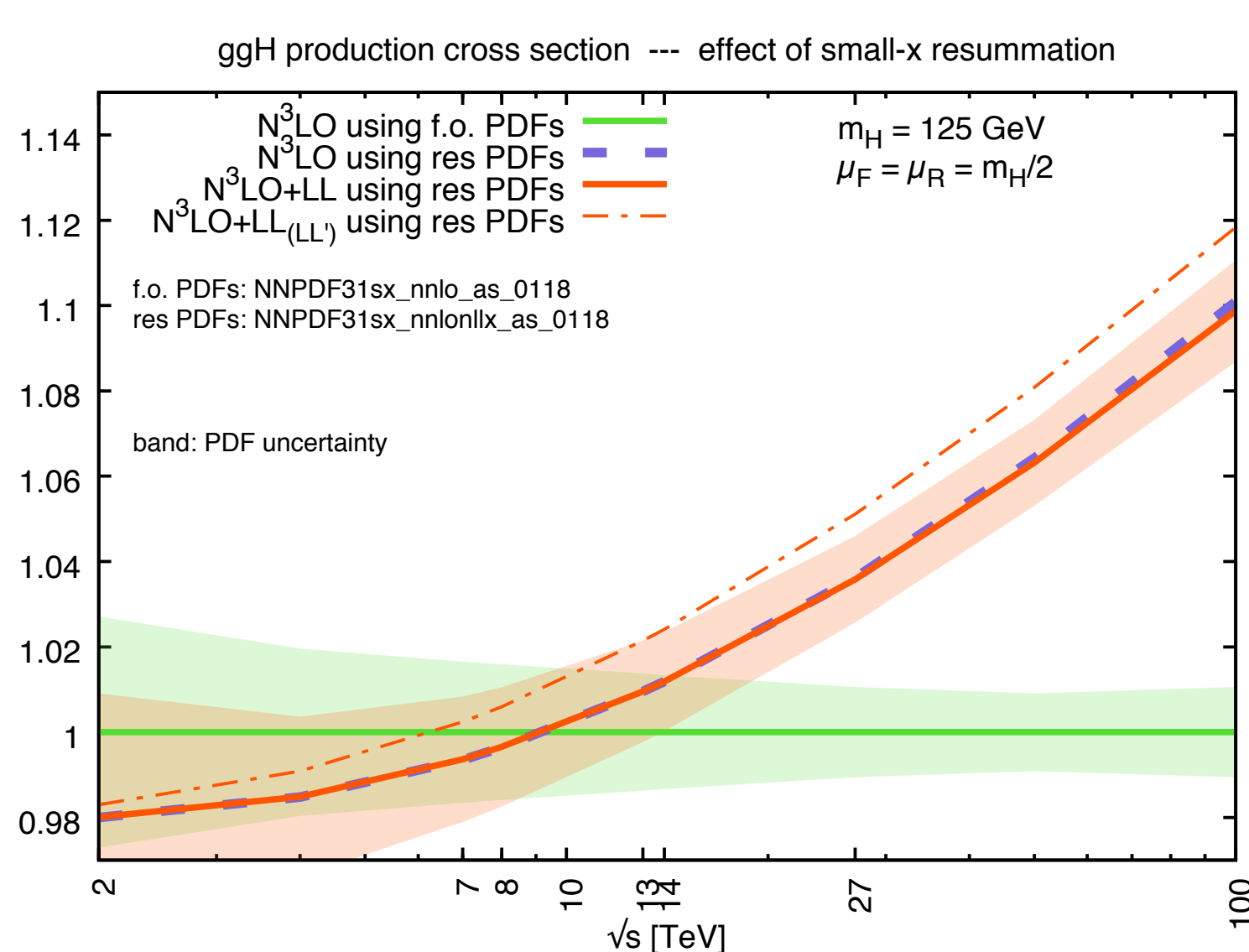
**Resummation mandatory for LHeC and FCC-eh**

# Impact on Higgs production at hadron colliders

Small x resummation will have an impact on the many observables at hadron colliders at high energy

Example: Higgs production cross section in pp as a function of energy

Ratio of resummed to fixed order N<sup>3</sup>LO



Size of different uncertainties: PDFs, scale, resummation at different energies

At FCC-hh the resummation will play important role

Bonvini

# Example: application of LL BFKL to $\gamma^*\gamma^*$ scattering

CERN-EP/2001-075  
October 31, 2001

CERN-EP-2001-064  
31 August 2001

## Measurement of the Hadronic Cross-Section for the Scattering of Two Virtual Photons at LEP

The OPAL Collaboration

### Abstract

The interaction of virtual photons is investigated using the reaction  $e^+e^- \rightarrow e^+e^- \text{ hadrons}$  based on data taken by the OPAL experiment at  $e^+e^-$  centre-of-mass energies  $\sqrt{s_{ee}} = 189 - 209$  GeV, for  $W > 5$  GeV and at an average  $Q^2$  of  $17.9$  GeV<sup>2</sup>. The measured cross-sections are compared to predictions of the Quark Parton Model (QPM), to the Leading Order QCD Monte Carlo model PHOJET to the NLO prediction for the reaction  $e^+e^- \rightarrow e^+e^- q\bar{q}$ , and to BFKL calculations. PHOJET, NLO  $e^+e^- \rightarrow e^+e^- q\bar{q}$ , and QPM describe the data reasonably well, whereas the cross-section predicted by a Leading Order BFKL calculation is too large.

## Double-Tag Events in Two-Photon Collisions at LEP

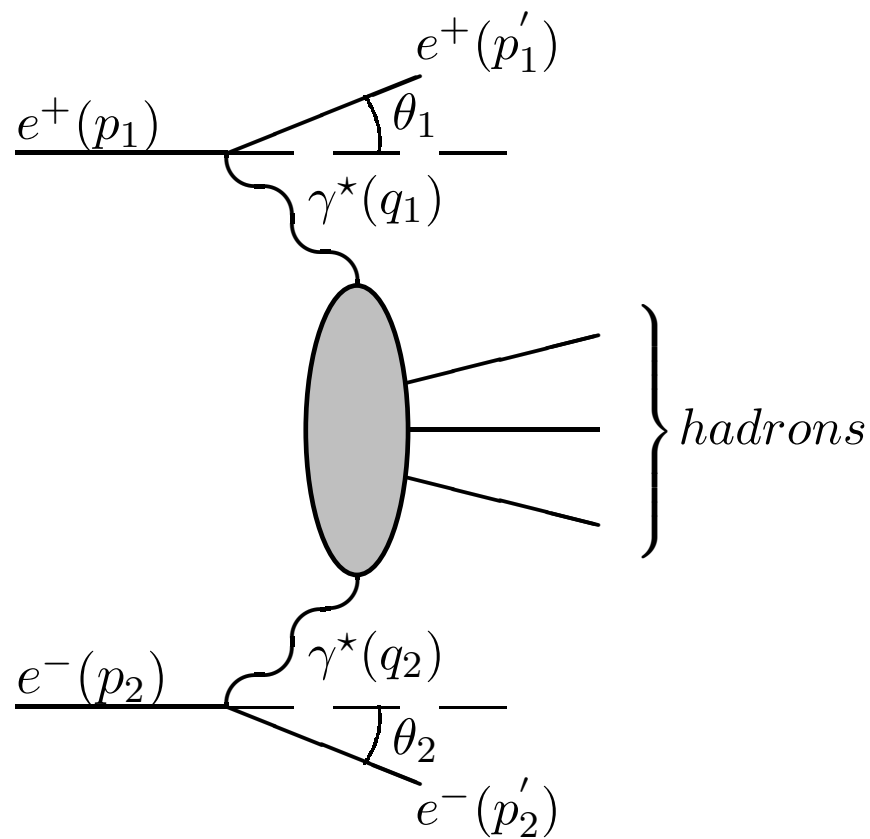
The L3 Collaboration

### Abstract

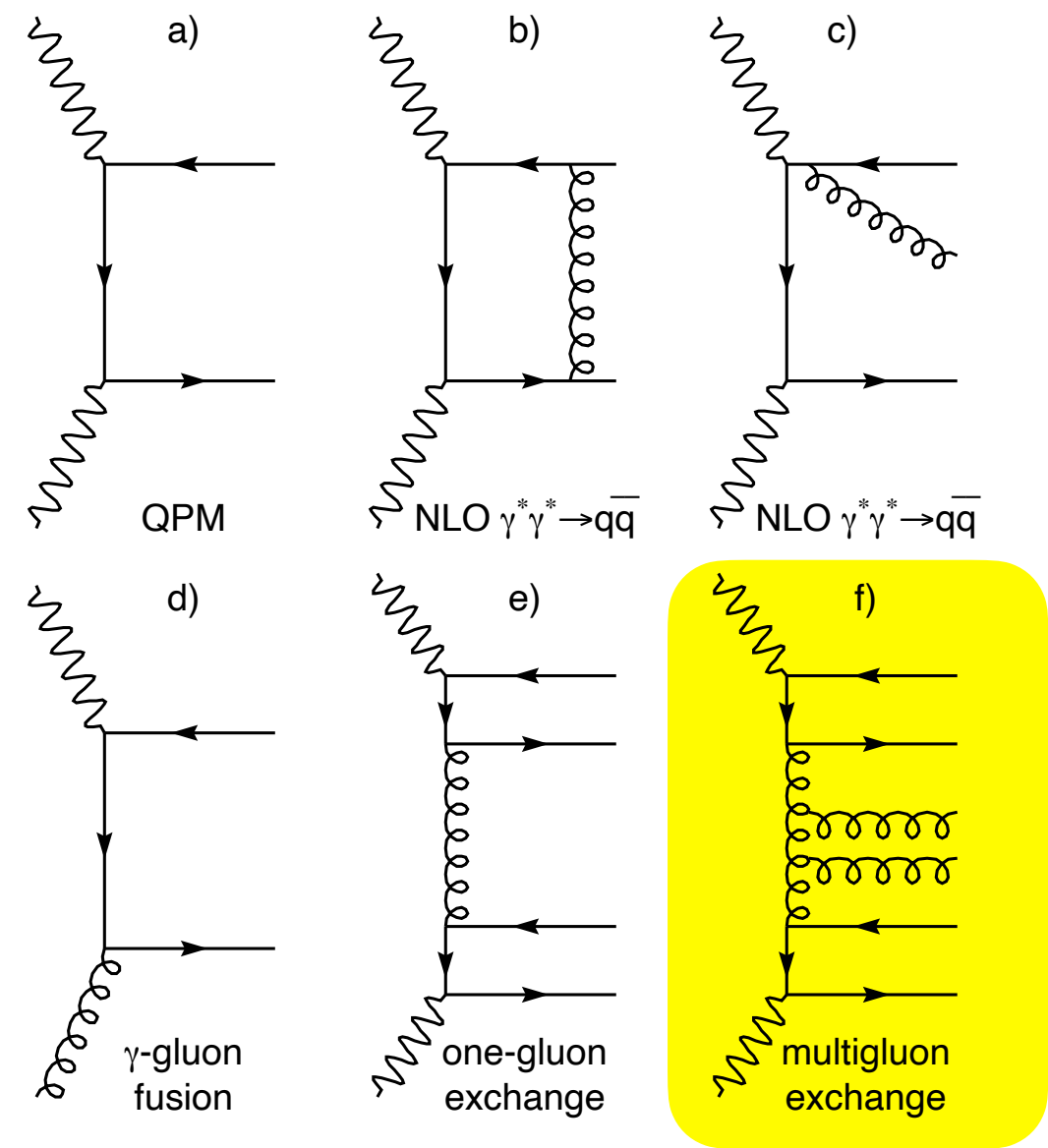
Double-tag events in two-photon collisions are studied using the L3 detector at LEP centre-of-mass energies from  $\sqrt{s} = 189$  GeV to 209 GeV. The cross sections of the  $e^+e^- \rightarrow e^+e^- \text{ hadrons}$  and  $\gamma^*\gamma^* \rightarrow \text{hadrons}$  processes are measured as a function of the product of the photon virtualities,  $Q^2 = \sqrt{Q_1^2 Q_2^2}$ , of the two-photon mass,  $W_{\gamma\gamma}$ , and of the variable  $Y = \ln(W_{\gamma\gamma}^2/Q^2)$ . The average photon virtuality is  $\langle Q_1^2 \rangle = \langle Q_2^2 \rangle = 16$  GeV<sup>2</sup>. The results are in agreement with next-to-leading order calculations for the process  $\gamma^*\gamma^* \rightarrow q\bar{q}$  in the interval  $2 \leq Y \leq 5$ . An excess is observed in the interval  $5 < Y \leq 7$ , corresponding to  $W_{\gamma\gamma}$  greater than 40 GeV. This may be interpreted as a contribution of resolved photon QCD processes or the onset of BFKL phenomena.

# Example: application of LL BFKL to $\gamma^*\gamma^*$ scattering

Process:  $e^+e^- \longrightarrow e^+e^- + \text{hadrons}$   
 doubly-tagged events

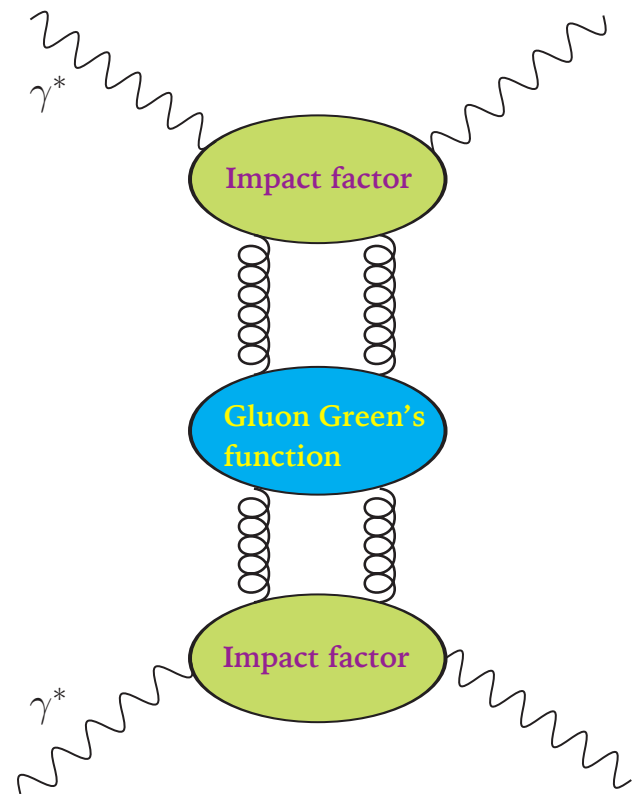


Sample diagrams which contribute



Dominant at large energy (rapidity)

# Example: application of LL BFKL to $\gamma^*\gamma^*$ scattering



High-energy factorization

Two virtual photons provide large perturbative scales:  $Q_1^2, Q_2^2$

rapidity  $Y = \ln \frac{W_{\gamma\gamma}^2}{\sqrt{Q_1^2 Q_2^2}}$

$$s = W_{\gamma\gamma}^2$$

$$\sigma^{(jk)}(s, Q_1, Q_2) = \frac{1}{2\pi Q_1 Q_2} \int \frac{d\omega}{2\pi i} \left(\frac{s}{s_0}\right)^\omega \int \frac{d\gamma}{2\pi i} \left(\frac{Q_1^2}{Q_2^2}\right)^{\gamma - \frac{1}{2}} \phi^{(j)}(\gamma) G(\omega, \gamma) \phi^{(k)}(1 - \gamma)$$

$Q_1^2 = -q_1^2, Q_2^2 = -q_2^2$  are negative photon virtualities

$\phi^{(j,k)}$  impact factors: known up to NLO  
*Balitsky, Chirilli*

$s = (q_1 + q_2)^2$  for the  $\gamma^*\gamma^*$  process

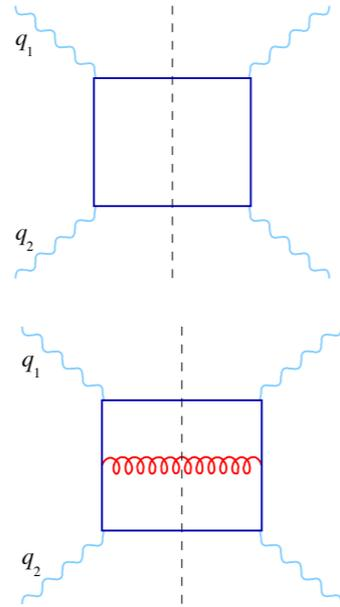
$G(\omega, \gamma)$  BFKL gluon Green's function

$j, k$  photon polarizations

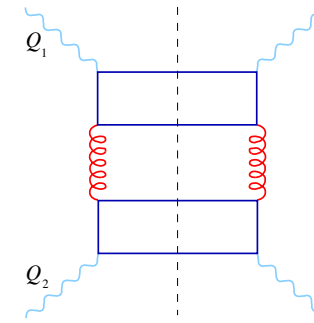
$$G(\omega, \gamma) = \frac{1}{\omega - \bar{\alpha}_s \chi(\gamma)}$$

# Example: application of LL BFKL to $\gamma^*\gamma^*$ scattering

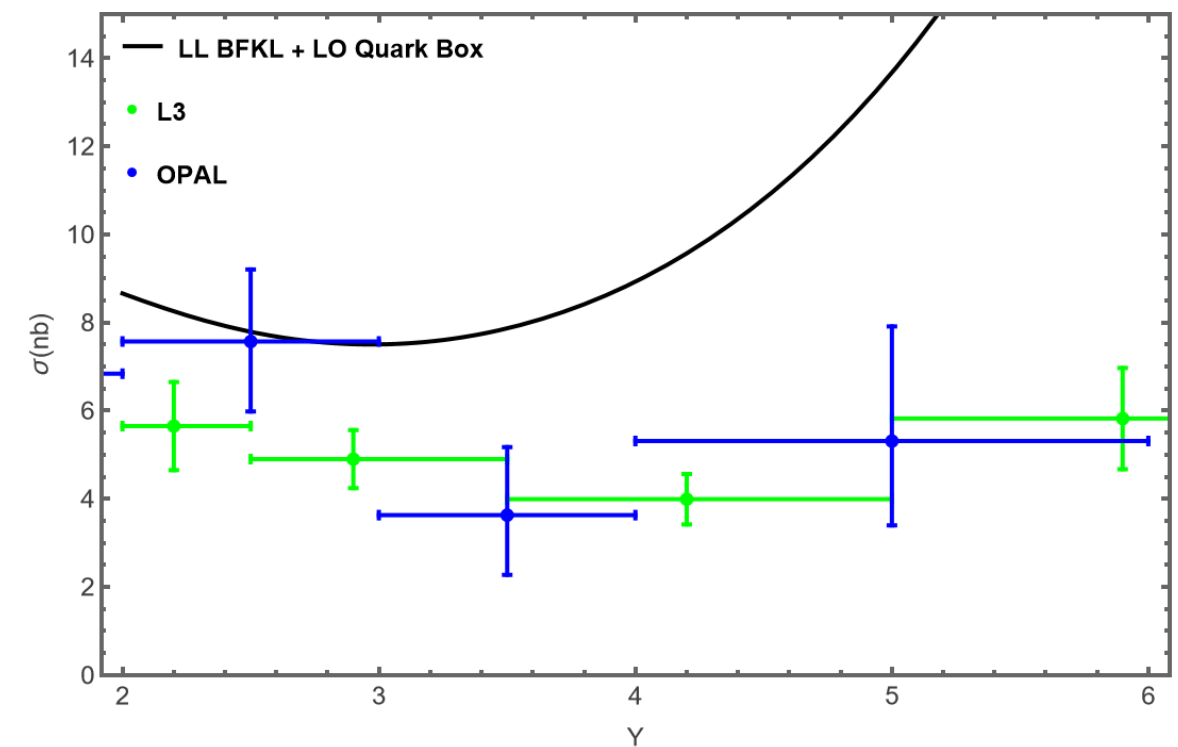
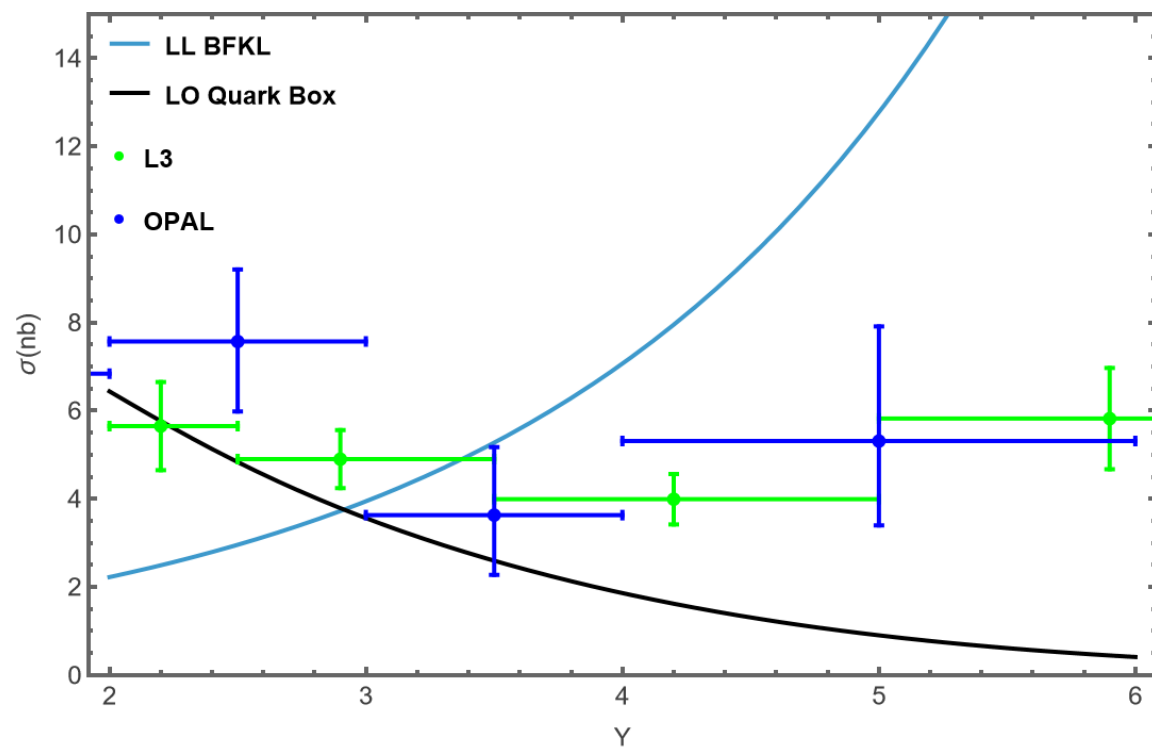
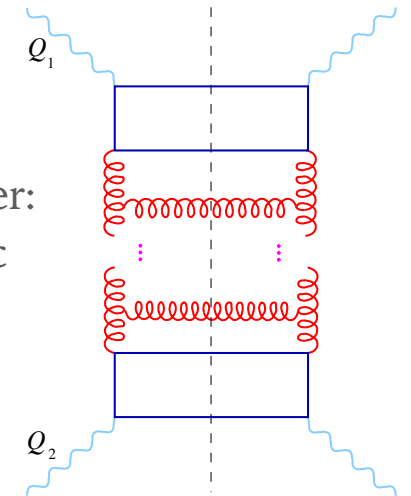
- lowest order process
- quark box (+crossed)
- spin  $j=1/2$  exchange
- falling cross section with  $s$
- Perturbative log corrections



- constant cross section: exchange of gluon in t channel

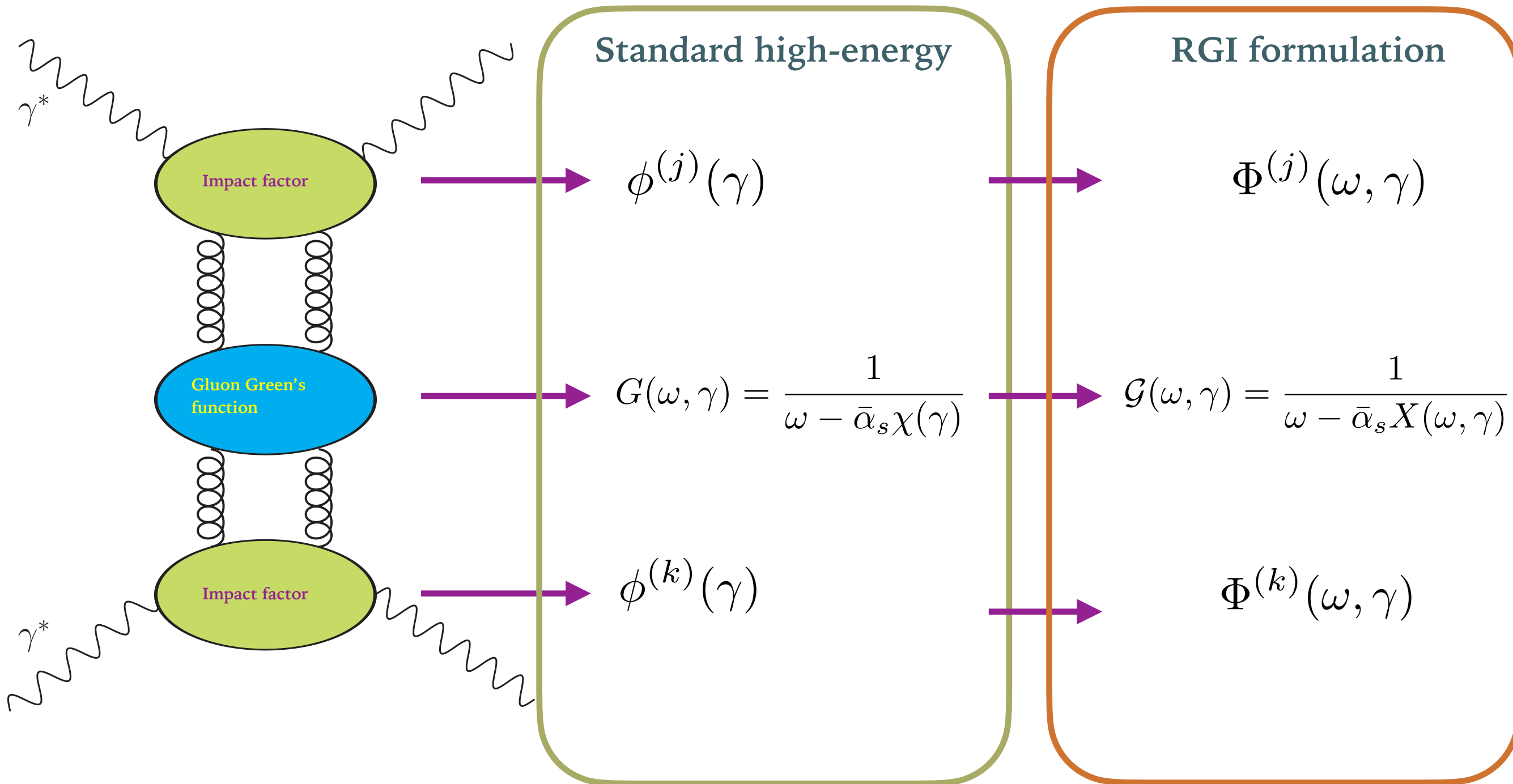


BFKL ladder:  
logarithmic  
corrections



BFKL at LLx order overestimates the data and gives too steep growth of the cross section

# Resummation with impact factors

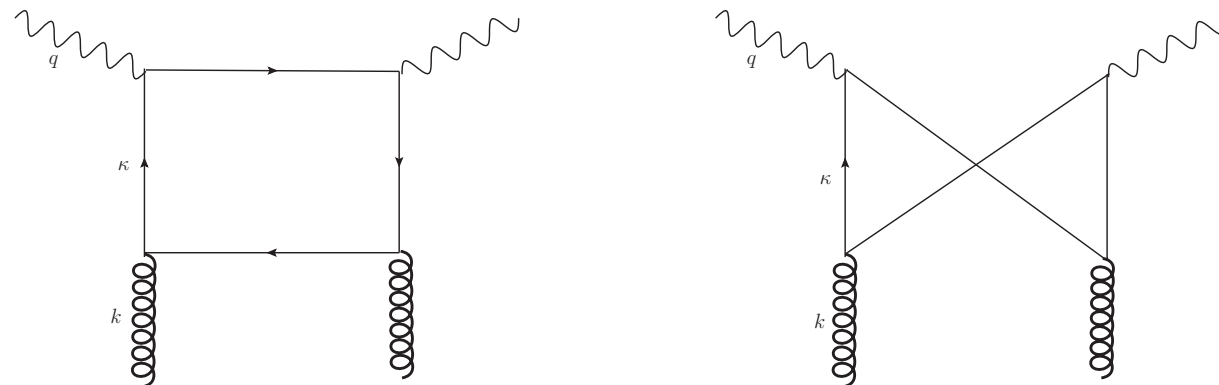


# HE formula with exact kinematics: argument of the gluon density

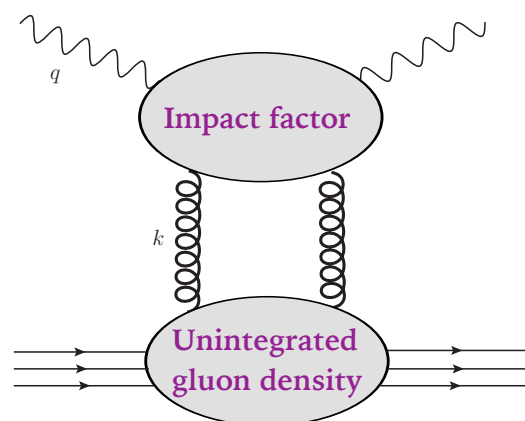
How to get correct  $\omega$  dependence of the impact factors ?

$$\phi^{(k)}(\gamma) \longrightarrow \Phi^{(k)}(\omega, \gamma)$$

Graphs at LO



Consider structure function in DIS in high-energy factorization (momentum space)



Impact factor (in mom.space)

$$F_{2,L}(x, Q^2) = \hat{F}_0(Q^2, \mathbf{k}, \boldsymbol{\kappa}, z) \otimes f(x_g, \mathbf{k}^2)$$

unintegrated gluon density

In the high-energy limit at LO (or in dipole model) :

$$x_g = x_{Bj}$$

Exact kinematics:

$$x_g = x_{Bj} \left( 1 + \frac{\mathbf{k}^2}{Q^2} + z(1-z) \frac{\boldsymbol{\kappa}^2 + m^2}{Q^2} \right)$$

# LO impact factor with exact kinematics: shift of poles

$$F_{2,L}(x, Q^2) = \hat{F}_0(Q^2, \mathbf{k}, \boldsymbol{\kappa}, z) \otimes f(x_g, \mathbf{k}^2)$$



Mellin space

$$\Phi(\omega, \gamma) \quad \omega \text{ dependent impact factor}$$

Transverse

$$\Phi^{(T)}(\omega, \gamma) \sim \frac{1}{\gamma^2} + \frac{1}{(1 - \gamma + \omega)^2}$$

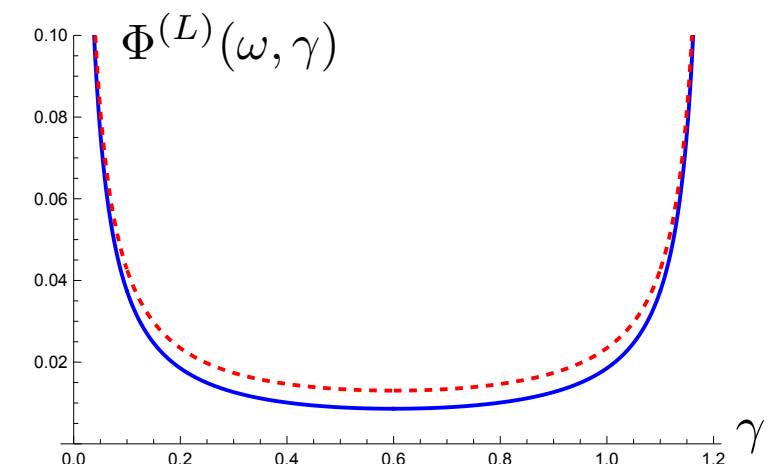
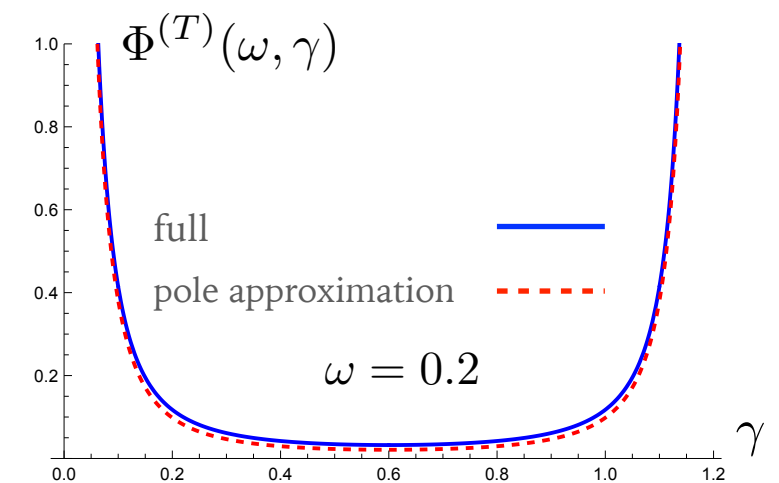
Longitudinal

$$\Phi^{(L)}(\omega, \gamma) \sim \frac{1}{\gamma} + \frac{1}{1 - \gamma + \omega}$$

Reduce to  $\phi_0^{(T,L)}(\gamma)$  when  $\omega \rightarrow 0$

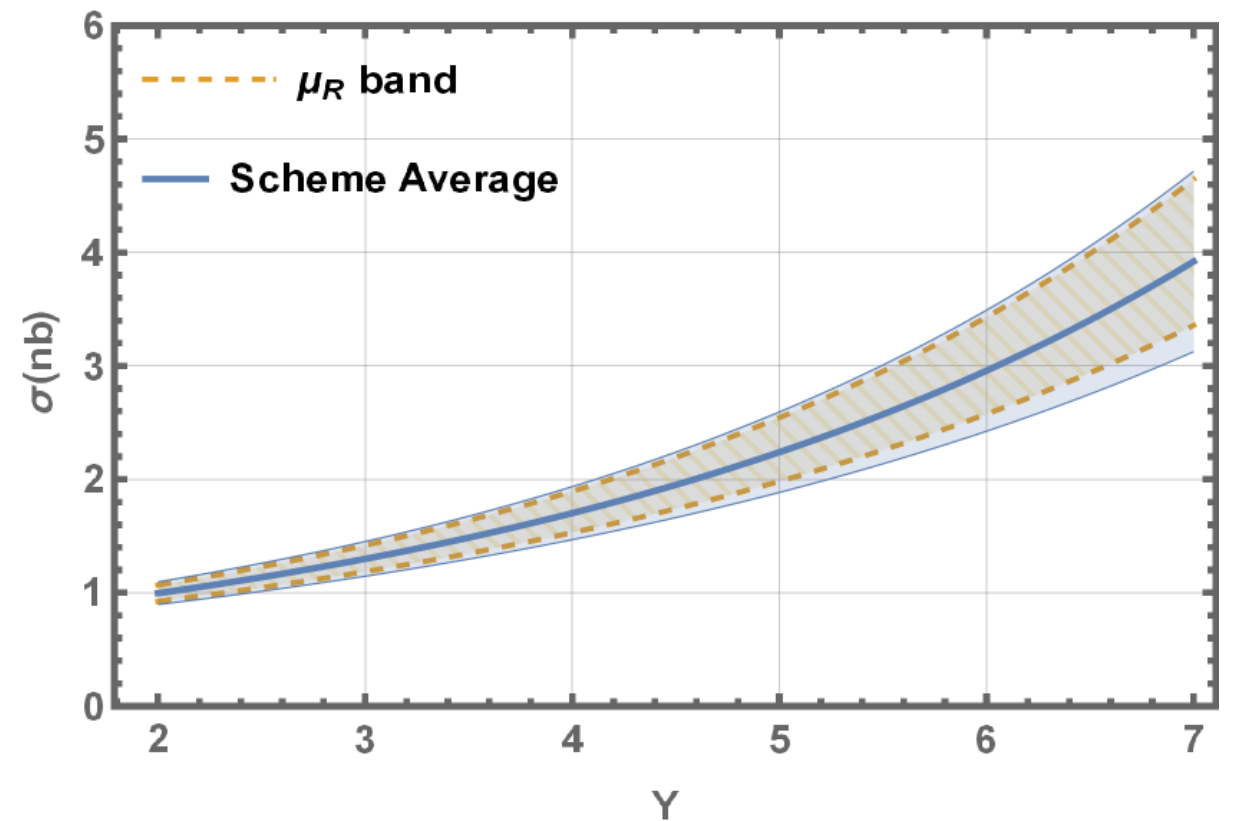
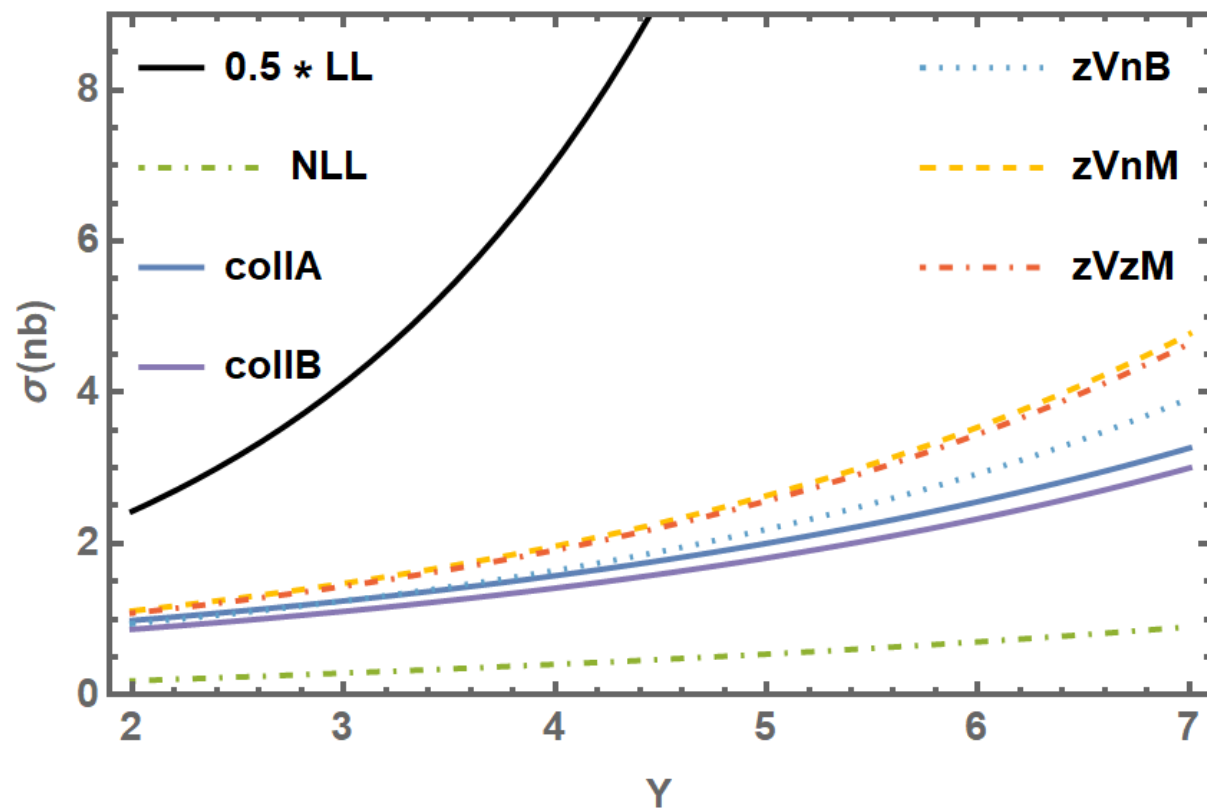
Similar  $\omega$  shifts of poles as in GGF

*Bialas, Navelet, Peschanski*



# BFKL contribution to $\gamma^*\gamma^*$ cross section

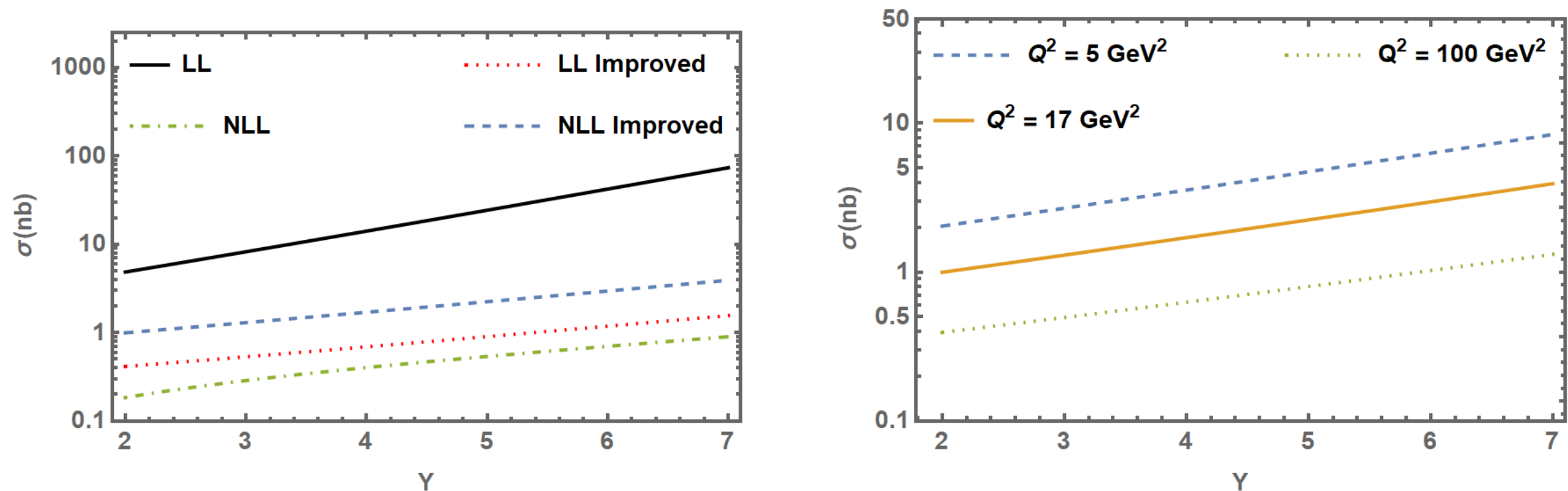
$$Q_1^2 = Q_2^2 = 17 \text{ GeV}^2$$



- Resummed calculation between LL and NLL result (LL result scaled by 0.5 for visibility)
- Pure NLL calculation give very small contribution
- Resummed calculation leads to growth in between LL and NLL
- differences between different resummation schemes are comparable to the renormalization scale dependence ( $0.5\mu_0^2 < \mu_R^2 < 2\mu_0^2$ ,  $\mu_0^2 = Q_1Q_2$ )

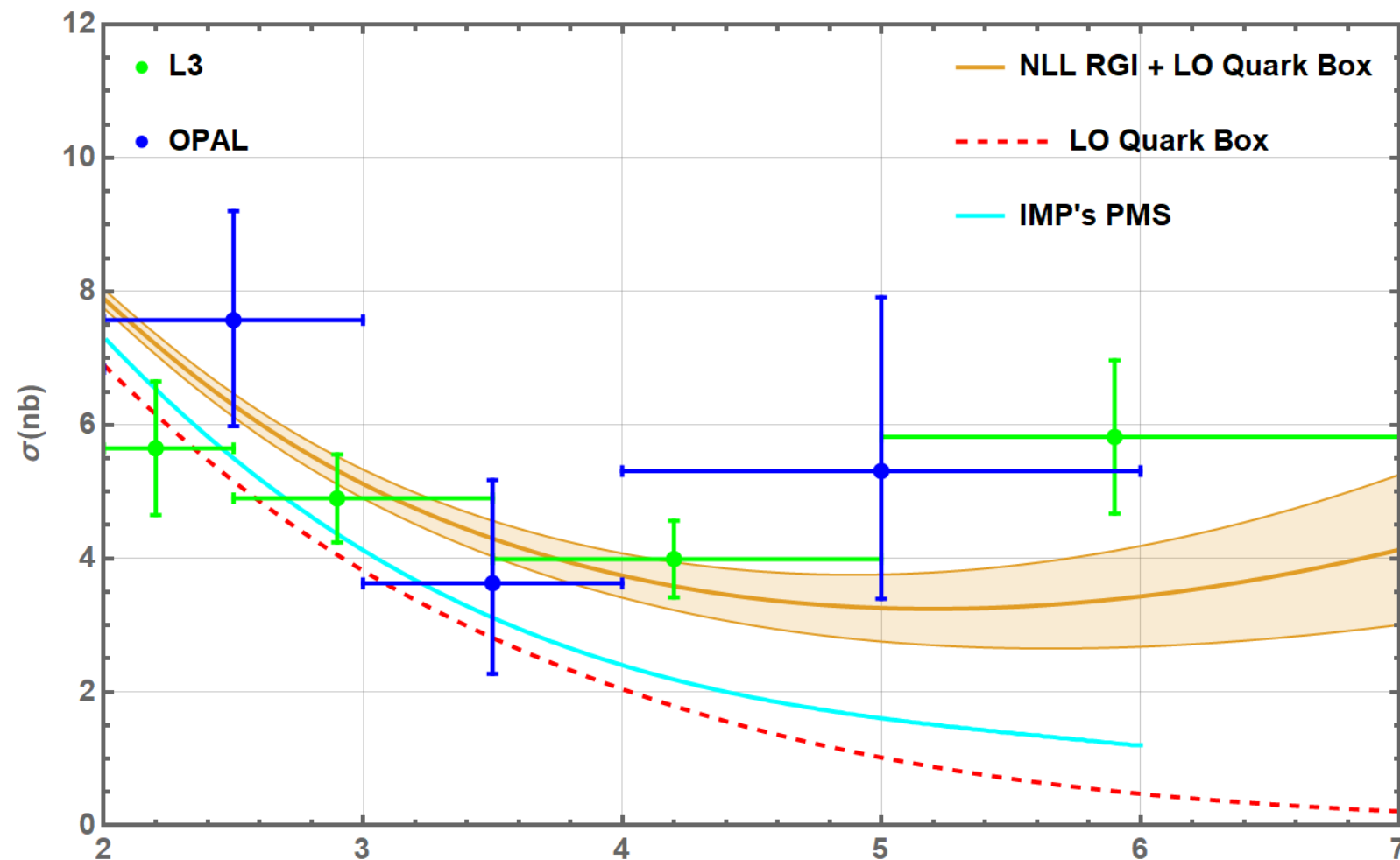
# BFKL contribution to $\gamma^*\gamma^*$ cross section

Logarithmic vertical scale



- Change in slope with respect to the LL is clearly visible
- Already LL improved: which is shifted eigenfunction and impact factors, brings down the curves significantly with respect to pure LL
- NLL improved above LL improved due to the positive corrections in the impact factors
- Strong dependence of the cross section on scale  $Q^2$
- Change in slope due to the smaller value of the coupling which affects the value of the leading exponent in the gluon Green's function

# Results for $\gamma^*\gamma^*$ cross section: comparison with data



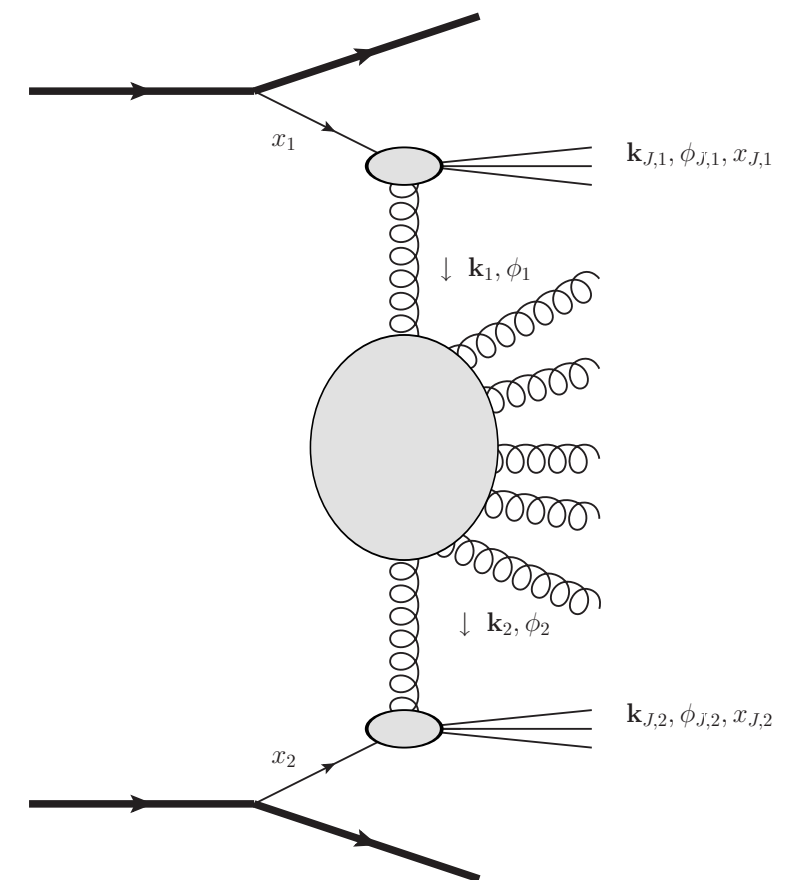
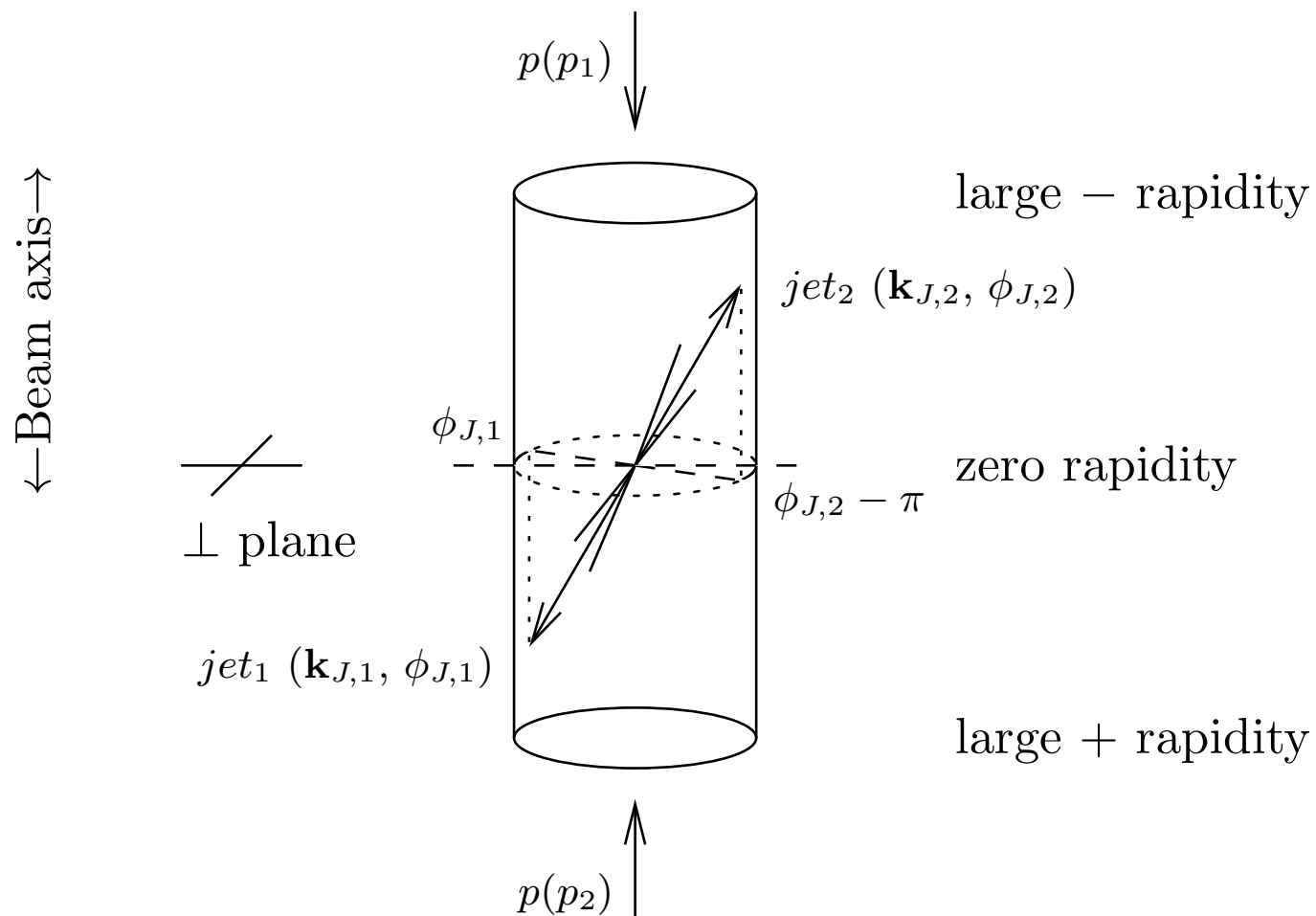
- Comparison with L3 and OPAL data from LEP  $Y$
- BFKL contribution is added to the quark box contribution which dominates at low rapidities (energies)
- The resulting cross section is a combination of two terms: one decreasing with rapidity and one increasing with rapidity
- Overall, good description of the experimental data, within the errors
- Results are larger than the pure NLL results (*Ivanov, Murdaca, Papa*)

# BFKL tests: Mueller–Navelet jets

Mueller-Navelet jets: two jets separated by the large rapidity interval

Can be a good test of the BFKL dynamics

Plots from *Colferai, Schwenssen, Szymanowski, Wallon*

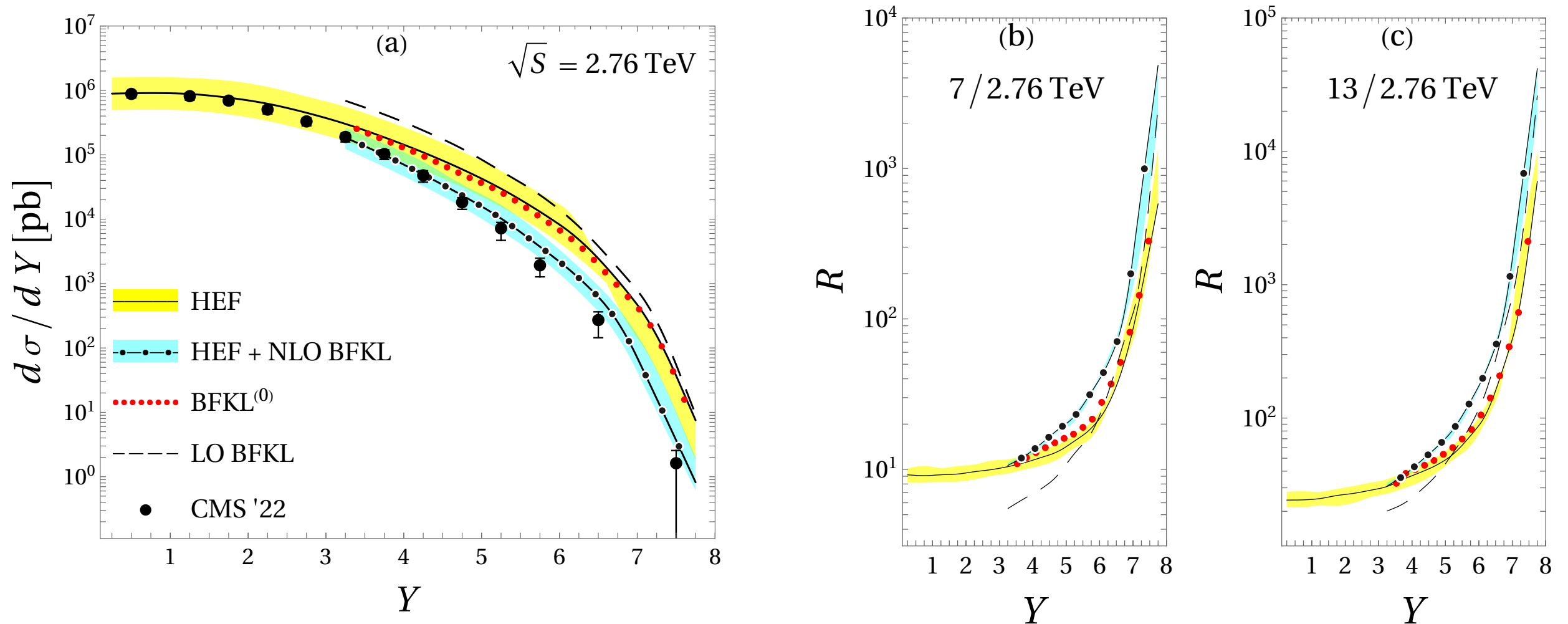


$$\frac{d\sigma}{d|\mathbf{k}_{J,1}| d|\mathbf{k}_{J,2}| dy_{J,1} dy_{J,2}} = \int d\phi_{J,1} d\phi_{J,2} \int d^2\mathbf{k}_1 d^2\mathbf{k}_2 \Phi(\mathbf{k}_{J,1}, x_{J,1}, -\mathbf{k}_1) G(\mathbf{k}_1, \mathbf{k}_2, \hat{s}) \Phi(\mathbf{k}_{J,2}, x_{J,2}, \mathbf{k}_2),$$

# Mueller–Navelet jets from BFKL

Chernyshev, Nefedov, Saleev

$$\frac{d\sigma}{d|\mathbf{k}_{J,1}| d|\mathbf{k}_{J,2}| dy_{J,1} dy_{J,2}} = \int d\phi_{J,1} d\phi_{J,2} \int d^2\mathbf{k}_1 d^2\mathbf{k}_2 \Phi(\mathbf{k}_{J,1}, x_{J,1}, -\mathbf{k}_1) G(\mathbf{k}_1, \mathbf{k}_2, \hat{s}) \Phi(\mathbf{k}_{J,2}, x_{J,2}, \mathbf{k}_2),$$

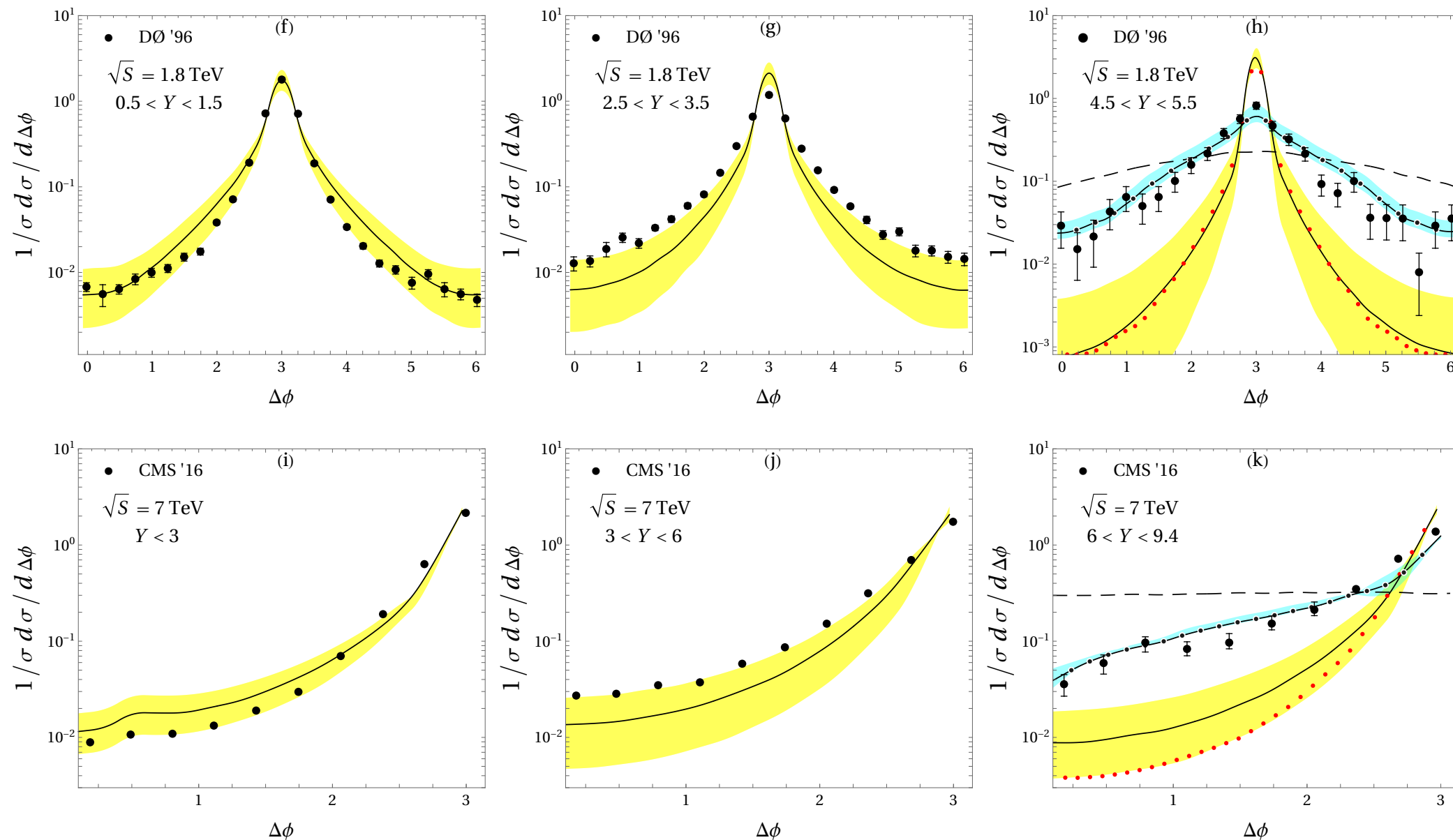


Cross section as a function of rapidity between jets

Ratio of cross sections at different energies: BFKL grows significantly faster

# Mueller–Navelet jets: azimuthal decorrelations

Chernyshev, Nefedov, Saleev



CMS cuts  
 $p_{T1,2} > 35$  GeV

D0 cuts  
 $p_{T1} > 50$  GeV  
 $p_{T2} > 20$  GeV

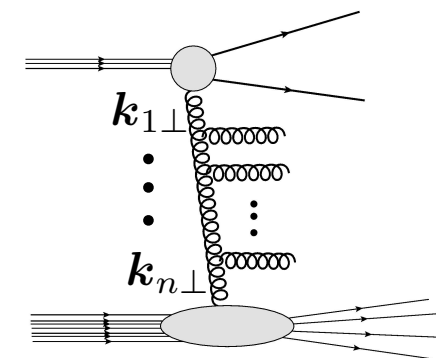
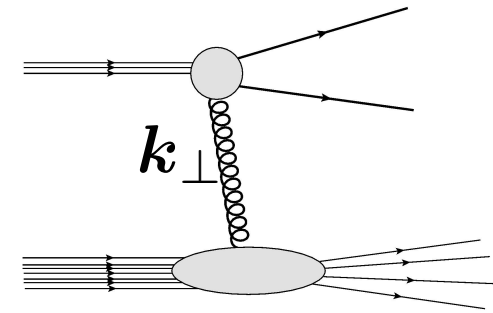
Azimuthal (de)correlations of jets: a good test of the BFKL dynamics between the jets

Jets become more decorrelated with wider rapidity separation: good description with collinearly improved NLL BFKL

# Azimuthal decorrelations: tests of small x dynamics

---

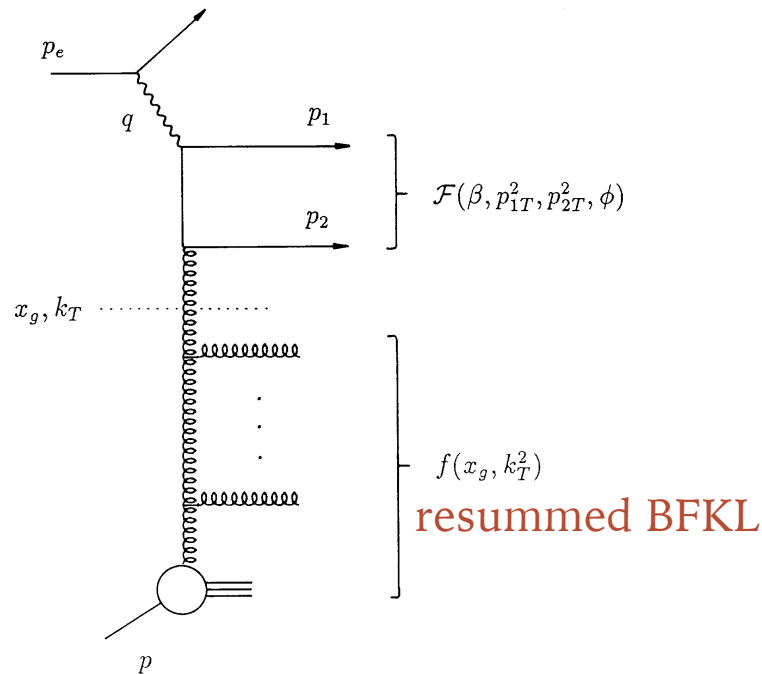
- **Transverse momentum** from the target can lead to the modification of **angular correlation** between the two produced hadrons/jets (at forward rapidities)
- **Broadening** of angular correlation should be present even in linear BFKL due to the **diffusion** of the transverse momenta at low x



Note: In the dense regime potential source of **decorrelation** due to multiple scatterings and the **saturation scale** being dependent on x and A : saturation (lecture 4)

# Dijets in DIS

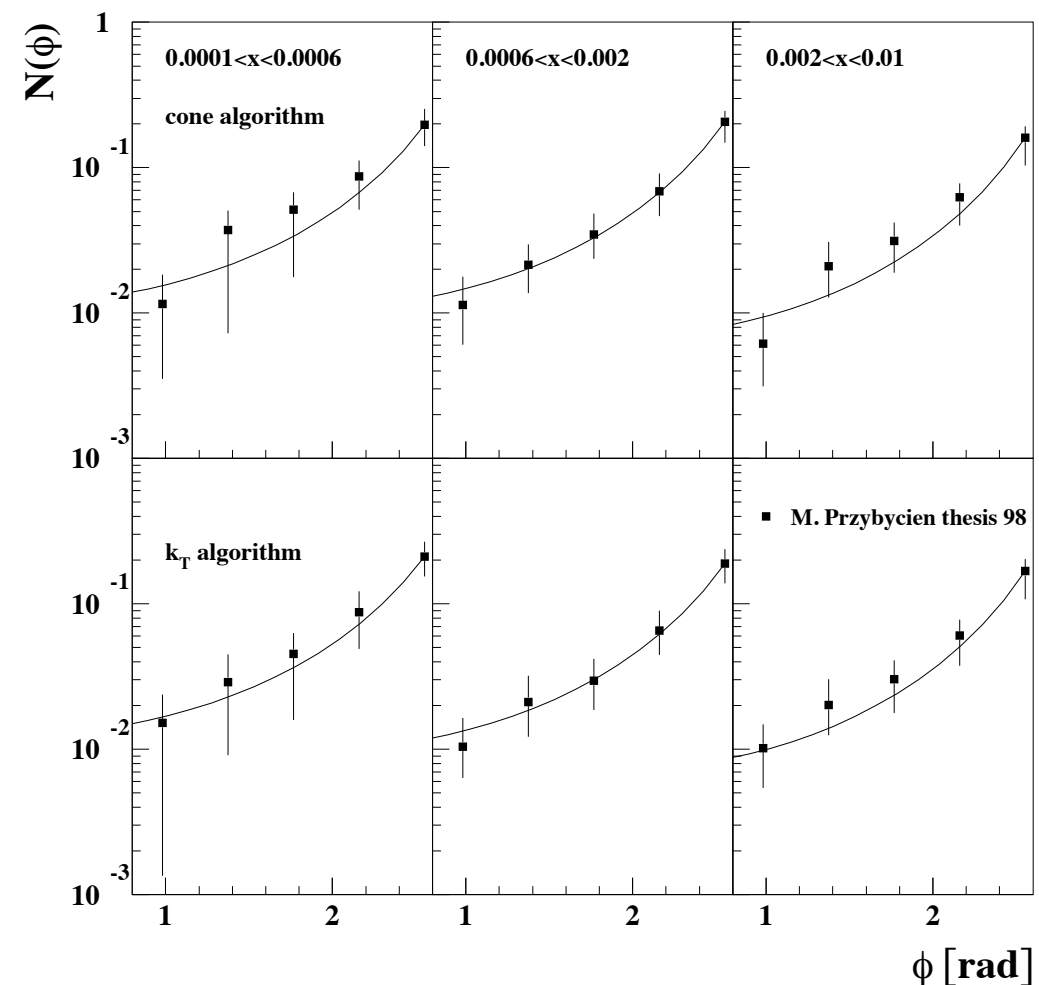
- **Azimuthal distributions** between two jets at HERA computed using the linear BFKL/DGLAP evolution ('resummed BFKL').
- **Transverse momentum** due to BFKL **diffusion** should lead to broadening of the distribution.
- Good description (parameter free).
- However, the kinematics is not very small x, **non-BFKL calculations described data** too.



$$\frac{d\sigma}{dx dQ^2 d\phi dp_{1T}^2 dp_{2T}^2} = \frac{4\pi\alpha^2}{xQ^2} \left[ \left(1 - y - \frac{y^2}{2}\right) \frac{dF_T}{d\phi dp_{1T}^2 dp_{2T}^2} + (1 - y) \frac{dF_L}{d\phi dp_{1T}^2 dp_{2T}^2} \right]$$

$$\frac{dF_i}{d\phi dp_{1T}^2 dp_{2T}^2} = \sum_q \int_0^1 d\beta \mathcal{F}_i^q(\beta, p_{1T}^2, p_{2T}^2, \phi, Q^2) \frac{f(x_g, k_T^2)}{k_T^4}$$

$$k_T^2 = p_{1T}^2 + p_{2T}^2 + 2p_{1T}p_{2T} \cos \phi$$

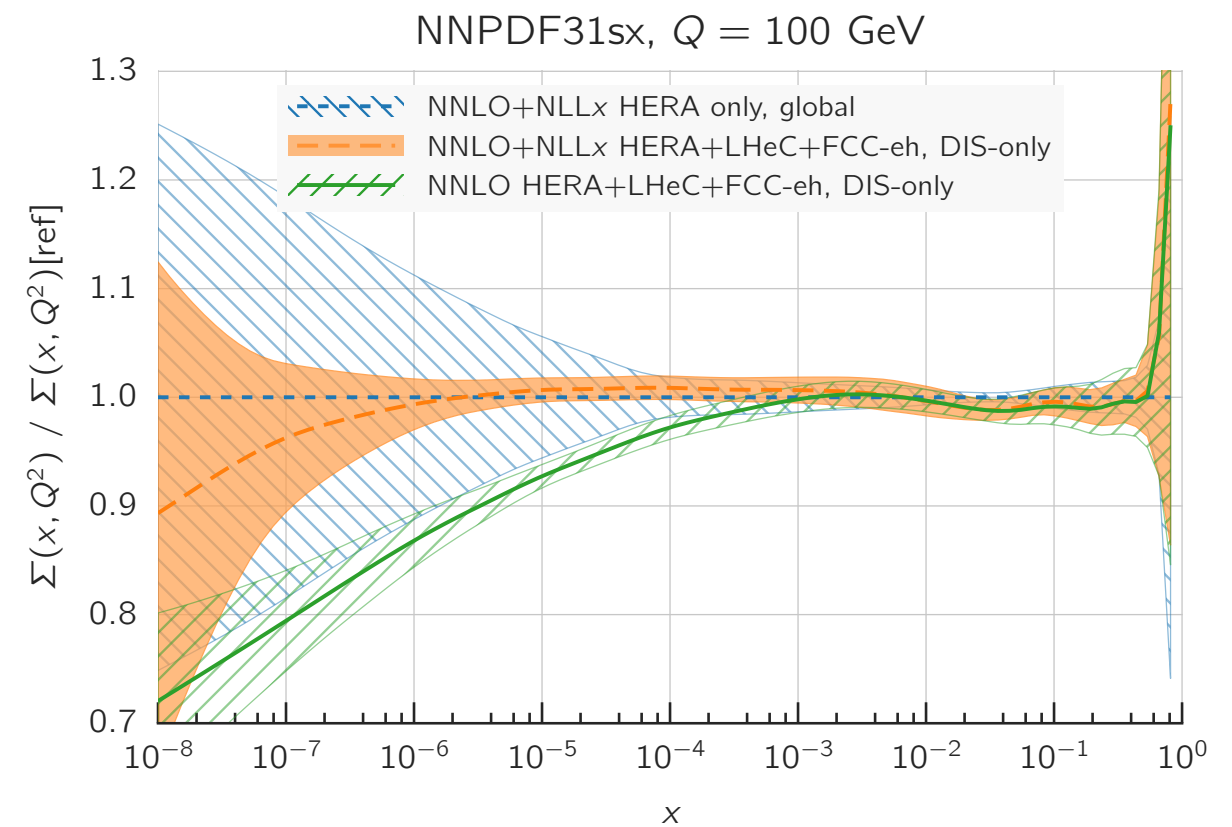
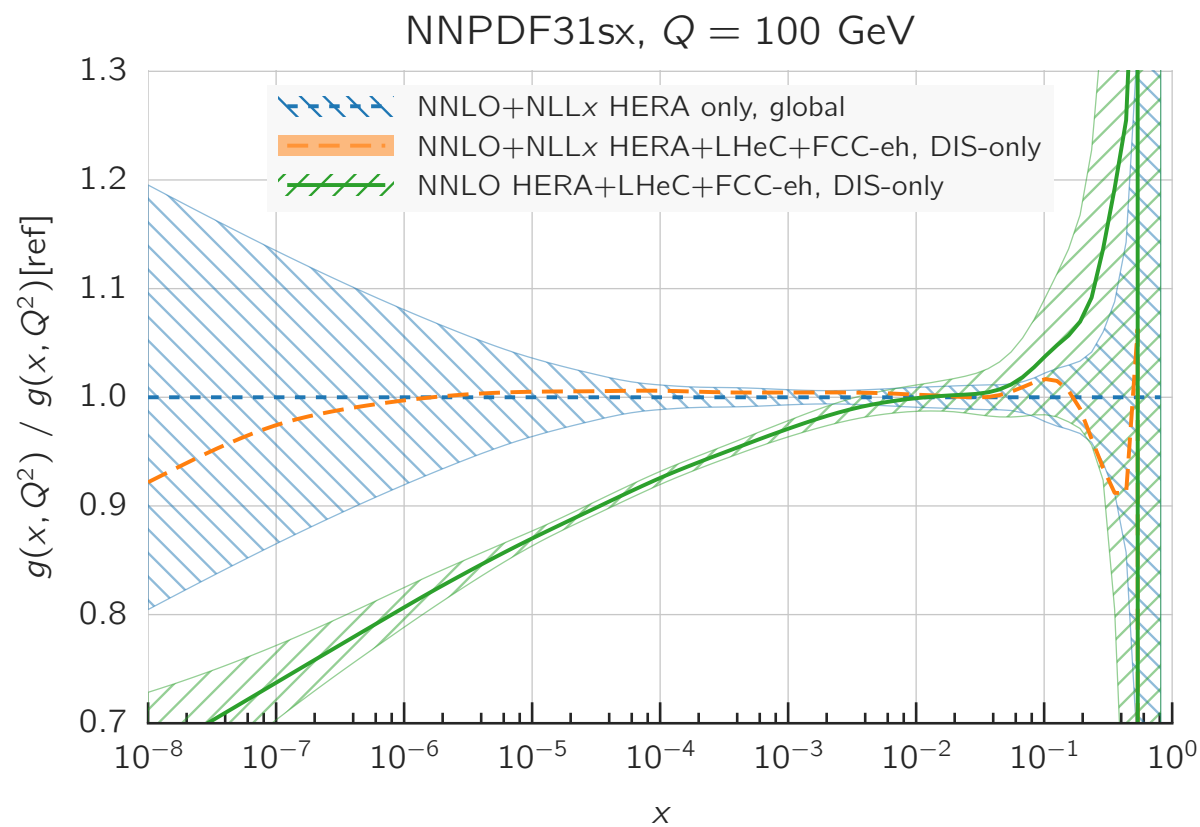


# backup

---

# Novel dynamics at small x : resummation

*Ball, Bertone, Bonvini, Marzani, Rojo, Rottoli*



Large differences in the parton density at low  $x$ .

Essential for LHeC and FCC-eh